

ENTROPY PRODUCTION IN  
TICKING CLOCKS

MASTER THESIS SUBMITTED BY

JULIAN ARNOLD



# Entropy production in ticking clocks

Master thesis

submitted by

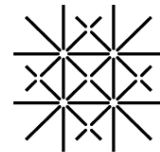
Julian Arnold

Institute for Theoretical Physics, ETH Zurich, 8093 Zürich

Department of Physics, University of Basel, Klingelbergstrasse 82, 4056 Basel

Zürich, 2021

**ETH** zürich



University  
of Basel

---

Supervisors: Dr. Mischa Prebin Woods  
Prof. Dr. Christoph Bruder  
Prof. Dr. Renato Renner

# Contents

<b>Introduction</b>	<b>1</b>
<b>I Ticking clock model</b>	<b>3</b>
I.1 Examples of ticking clocks . . . . .	13
I.1.1 Ladder ticking clock . . . . .	13
I.1.2 Quasi-ideal ticking clock . . . . .	15
I.2 Accuracy of ticking clocks . . . . .	15
I.3 Classical ticking clocks . . . . .	18
<b>II Entropy production per tick of a ticking clock</b>	<b>23</b>
II.1 Entropy production of thermodynamic ticking clocks . . . . .	25
II.2 Entropy production in open quantum systems . . . . .	32
II.2.1 Entropy production as correlation between system and environment . .	32
II.2.1.a Connection to Landauer's erasure principle . . . . .	38
II.3 Observer-dependent clockwork states . . . . .	39
II.4 Modelling a ticking clock's environment . . . . .	48
II.4.1 Dilation of quantum states . . . . .	49
II.4.2 Dilation of quantum channels . . . . .	50
II.4.2.a Information leakage of noisy quantum channel . . . . .	54
II.5 Measures of entropy production per tick of a ticking clock . . . . .	55
II.5.1 Based on dilation of clockwork states . . . . .	55
II.5.2 Based on dilation of ticking channels . . . . .	61
II.5.2.a Alternative ticking channels . . . . .	64
II.5.3 Based on the second law of thermodynamics . . . . .	67
II.5.4 Summary . . . . .	70
II.6 Re-analysis of thermodynamic ticking clock . . . . .	70
<b>III Relationship between accuracy and entropy production of ticking clocks</b>	<b>77</b>
III.1 Quantum ticking clocks . . . . .	78
III.1.1 Zero temporal information at vanishing entropy production per tick . .	78
III.1.2 Infinite temporal information at vanishing entropy production . . . .	80
III.2 Classical ticking clocks . . . . .	84
III.2.1 Analysis of first tick . . . . .	85
III.2.1.a Qubit clockwork . . . . .	87
III.2.1.b Clockworks of dimension $d > 2$ . . . . .	93
III.2.2 Implications for later ticks of arbitrary classical ticking clocks . . . .	101

<b>Conclusion and outlook</b>	<b>109</b>
<b>A Quantum information and entropy</b>	<b>115</b>
<b>B Additional proofs</b>	<b>117</b>
B.1 Delay functions and accuracy of ticking clocks . . . . .	117
B.2 Entropy production as correlation between system and environment . . . . .	119
B.3 Distinct approaches to calculate observer-dependent clockwork states . . . . .	121
B.4 Kraus operator representation of ticking channels . . . . .	125
B.5 Observer-dependent clockwork states for ticking clocks with vanishing no-tick operators . . . . .	126
B.6 Accuracy of classical ticking clocks with a diagonal no-tick generator . . . . .	127
B.7 Observer-dependent clockwork states for classical ticking clocks . . . . .	128
B.8 Accuracy and entropy production of ladder ticking clock . . . . .	129

# Introduction

Clocks keep track of the passage of time by counting recurring physical events, such as the revolutions of Earth or the swings of a pendulum [1]. Using atomic transitions as frequency references, current state-of-the-art optical atomic clocks are capable of measuring time at an uncertainty of a fraction of a second over the entire age of the universe [2, 3]. This exceeds the precision with which we can determine any other physical quantity [1]. As such, these devices allow for significant advancements at other frontiers of science, such as in the search for variations in fundamental constants [4], or in the detection of gravitational waves [5].

The transition frequencies at the heart of atomic clocks are governed solely by quantum theory, which makes them ideal frequency references. Despite this, the role of time itself in quantum theory is still not well understood. Whereas other physical quantities, such as position and momentum, can be assigned a Hermitian operator, it is not possible to rigorously define an analogous observable for time [6, 7]. Consequently, time remains a parameter that appears in dynamical equations of motions that needs to be measured indirectly. As alluded to above, the act of observing and quantifying the passage of time is fundamentally linked to the usage of clocks as reference systems. Thus, fundamental questions about time and the act of timekeeping can be addressed through the study of quantum systems that serve as clocks. By keeping track of measurable quantities during the evolution of such systems, which is governed by a time parameter  $t$ , allows for the latter to be estimated [8–11].

Ticking clocks provide information about the flow of time in the form of discrete “ticking” events [12–17]. Importantly, ticking clocks emit their ticks to the outside world – its environment – such that they are accessible to a potential observer. This necessitates that any quantum system which models a ticking clock must be open and interact with its environment because the unitary dynamics of a closed quantum system would not allow for a uni-directional flow of information that breaks time-reversal symmetry. As such, any ticking clock must be an open quantum system that displays irreversible dynamics. From a thermodynamic point of view, this provides a connection between the task of timekeeping and the second law of thermodynamics, which associates a net production of (irreversible) entropy with irreversible processes. In the 18th century, the question of the maximal efficiency with which one can con-

vert heat to work arose. Similarly, one can ask whether thermodynamics limits the accuracy with which we can measure time.

This question has been the topic of several recent works [11, 18–20]. These works find that there exists a fundamental connection between the accuracy of ticking clocks and their irreversible entropy production or energy dissipation. In particular, they find that a larger accuracy requires a larger entropy production and energy dissipation. This is in agreement with a large class of inequalities known as thermodynamic uncertainty relations (TURs) in non-equilibrium and stochastic thermodynamics [21, 22]. These TURs state that the accuracy (the ratio of mean to variance) with which currents can be measured is bounded from above by quantities that serve as a measure of thermodynamic cost, such as the entropy production. Examples of such currents are the electric current flowing through a resistor or the stream of particles flowing through a molecular motor. Recently, significant effort has been made to formulate TURs for general open quantum systems and go beyond the framework of thermodynamics [23, 24]. Ultimately, such relations aim to quantify the notion that the generation of a highly accurate signal requires a large amount of resources, in particular, highly irreversible dynamics.

In this work, we try to explore the relation between the accuracy and entropy production per tick of ticking clocks. In contrast to previous works, we go beyond the thermodynamic setting and instead adopt an information-theoretic perspective: a ticking clock is a quantum system that emits temporal information to its outside [14]. We thus raise the question of whether the theory of quantum information imposes any constraints on the relation between the entropy production per tick of a ticking clock and its accuracy. Here, the entropy production per tick is not thermodynamic in nature. Instead, it is an information-theoretic quantity that measures the exchange of information of the clock with its environment during each tick. Because this information transfer can be pinpointed as the fundamental origin of irreversibility of the clock’s dynamics, the entropy production per tick of a clock also serves as a measure for its irreversibility.

We rely on a ticking clock model which has been proposed recently and can be derived from a set of axiomatic principles. This model will be introduced in Chapter I. Having established a fundamental framework, we face the task of defining an appropriate measure for the entropy production per tick of a ticking clock in Chapter II. To this end, we first review previous notions of entropy production in thermodynamic ticking clocks and in general open quantum systems. Eventually, we motivate an expression for the entropy production per tick of a ticking clock from first principles. In Chapter III, we finally investigate the relationship between the accuracy and our measure for the entropy production per tick of a ticking clock.

# Chapter I

## Ticking clock model

When investigating the task of timekeeping using ticking clocks theoretically and from an information-theoretic perspective, it is crucial to devise an appropriate model that captures the key characteristics of such devices. In this work, we rely on the ticking clock model introduced in Ref. [16] motivated by axiomatic principles. This model both generalizes and refines previous ticking clock models [12, 14]. In this chapter, we will introduce this ticking clock model following Ref. [16].

First, we remind the reader of the difference between ticking clocks and other timekeeping devices, such as stopwatches. A timekeeping device designed to measure the elapsed time between events is considered a stopwatch. In particular, such a device will require an external start and stop signal and thus relies on an observer who actively retrieves the temporal information the device provides, e.g., by performing a measurement. In contrast, we think of a ticking clock as a timekeeping device that outputs information about time in the form of individual events, referred to as ticks, that occur at approximately regular intervals. The clock outputs this information in an autonomous fashion which does not require any external signal. Consider, for example, a typical wall clock. The internal mechanism of a wall clock is designed to output ticks independent of the presence or absence of an external observer. Moreover, the information is provided in a passive and continuous fashion, either visually through its clock face or via its ticking sound. Importantly, the process of information retrieval, i.e., observing whether a tick occurred or not, does not disturb the dynamics of the clock. Note that such fundamental differences between these two types of devices should be reflected in their mathematical description. As such, our ticking clock model is to be distinguished from a stopwatch model.

Here, we model a clock to be composed of two distinct parts: a clockwork ( $C$ ) and a register ( $R$ ). The clockwork is referred to as the part of the clock that provides its timing – the internal

parts of a clock which trigger a tick through their dynamics. The information transfer between the clockwork and the observer is mediated by the register. The register's state provides the observer with information about the ticks of the clock and undergoes changes based on the clockwork's state. Meaning, the coupling of the clockwork to the register results in a change in the state of the register at each tick. In fact, it is the change in the state of the register which constitutes a tick. Importantly, the state of the register can be continuously measured by an observer without affecting the dynamics of the clockwork and thus its ticks. Taking a wall clock as an example of a typical ticking clock, we can identify its oscillator as the clockwork and the clock face as the register, see Fig. I.1.

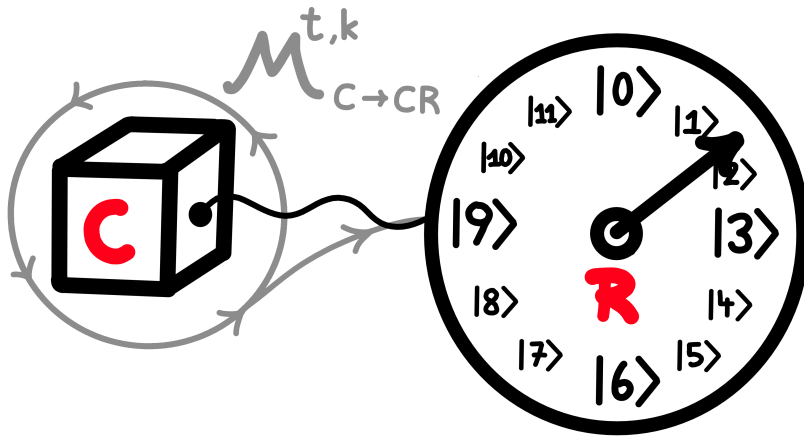


Figure I.1: Illustration of a wall clock in the view of our ticking clock model. The wall clock consists of an oscillator that takes on the role of a clockwork (C) and a clock face that serves as a register (R). The clock provides the observer information about time in the form of a continuous stream of “tick” and “no-tick” events, where no-tick events correspond to the silence in between the ticks [14]. The clockwork provides the timing for the clock’s ticks which are themselves recorded in the register. These dynamics can be described by a set of quantum channels ( $\mathcal{M}_{C \rightarrow CR}^{t,k}$ ) $_{t \geq 0, k \in (0, N_T)}$  which map an initial state of the clockwork that is paired with a fixed state  $|k\rangle_R$  of the register to a state of the clockwork and register a time interval  $t$  later (here  $N_T = 11$ ).

The clock is modeled by a quantum system living in a bipartite Hilbert space  $\mathcal{H}_C \otimes \mathcal{H}_R$ , where  $d = \dim(\mathcal{H}_C)$  and  $N_T + 1 = \dim(\mathcal{H}_R)$  denote the dimensions of the clockwork and register Hilbert spaces, respectively. We choose the  $N_T + 1$  orthonormal states in  $\mathcal{H}_R$  denoted by  $\{|0\rangle_R, |1\rangle_R, \dots, |N_T\rangle_R\}$  to represent no tick, 1 tick, ..., and  $N_T$  ticks, respectively. Thus, these register states convey the information about time provided by the clock. The register is considered to be “classical”, such that at every stage of the dynamics of the clock no coherences establish in the chosen basis. This is motivated by the fact that the temporal information

emitted by a clock is typically classical. The classicality of the register then guarantees that only classical information can be obtained by measuring it. Moreover, this property allows for the register to be continuously measured in the chosen basis without disturbing the clockwork dynamics, because there exist no coherences which could be destroyed by a measurement to begin with. Additionally, we consider two distinct types of registers: periodic registers and cut-off registers. The state of a cut-off register will keep advancing as more ticks are observed until it reaches the state  $|N_T\rangle_R$ , that is, until  $N_T$  ticks are observed. After that point, the clockwork dynamics become decoupled from the register in the sense that no further change in the register can be inflicted, i.e., the register remains in the state  $|N_T\rangle_R$ . For a periodic register, having reached the state  $|N_T\rangle_R$  the next tick will trigger the register to change back to the state  $|0\rangle_R$ . This is akin to the clock face of a typical wall clock repeating itself every 12 or 24 hours. As such, by looking at the state of the register one can only determine the number of ticks of the clock up to multiples of its period ( $|n\rangle_R = |n \text{ mod. } (N_T + 1)\rangle_R \forall n \in \mathbb{Z}$ ). Nevertheless, an observer can still keep track of the ticks in real-time and thereby circumvent this issue.

The clock – comprised of clockwork and register – is a (generally) open quantum system. As such, changes in its state are most generally described by completely-positive trace-preserving (CPTP) maps [25, 26]. In particular, these CPTP maps governing the evolution of the clock form a family parametrized by the coordinate time  $t \in \mathbb{R}_{\geq 0}$ :

$$\mathcal{M}_{\text{CR} \rightarrow \text{CR}}^t(\cdot) : \rho_{\text{CR}}^0 \rightarrow \rho_{\text{CR}}(t), \quad (\text{I.1})$$

where we introduce the short-hand notation

$$\mathcal{M}_{\text{C} \rightarrow \text{CR}}^{t,k}(\cdot) = \mathcal{M}_{\text{CR} \rightarrow \text{CR}}^t((\cdot) \otimes |k\rangle\langle k|_R) : \rho_{\text{C}}^0 \rightarrow \rho_{\text{CR}}(t), \quad (\text{I.2})$$

with  $k = 0, 1, \dots, N_T$ . Here,  $\rho_{\text{C}}$ ,  $\rho_{\text{R}}$ , and  $\rho_{\text{CR}}$  denote arbitrary states of the clockwork, register, and the clock (both clockwork and register), respectively. The ticking clock channel in Eq. (I.1) specifies the evolution from an initial state of the clock, here w.l.o.g. at coordinate time  $t = 0$ , to the state of the clock at coordinate time  $t$ . The coordinate time  $t$  serves as an (unknown) bookkeeping parameter that increases as time passes. For these maps to govern the evolution of a ticking clock, we will require them to satisfy a set of properties. In the following, we will state the conditions we impose on the dynamical maps  $(\mathcal{M}_{\text{CR} \rightarrow \text{CR}}^t)_{t \geq 0}$  as axioms. To start, we restrict ourselves to the particular case of ticking clocks with periodic registers.

**Axiom 1** (Uniform continuity condition).

$$\mathcal{M}_{\text{CR} \rightarrow \text{CR}}^0 = \mathcal{I}_{\text{CR}}, \quad (\text{I.3})$$

$$\lim_{t \rightarrow 0^+} \|\mathcal{M}_{\text{CR} \rightarrow \text{CR}}^t - \mathcal{I}_{\text{CR}}\| = 0. \quad (\text{I.4})$$

Axiom 1 ensures that the clock undergoes no evolution if no time passes and that any change occurring in the clockwork and register happens at a finite speed.

**Axiom 2** (Self-timing condition).

$$\mathcal{M}_{\text{CR} \rightarrow \text{CR}}^{t_1+t_2} = \mathcal{M}_{\text{CR} \rightarrow \text{CR}}^{t_1+t_2} = \mathcal{M}_{\text{CR} \rightarrow \text{CR}}^{t_2} \circ \mathcal{M}_{\text{CR} \rightarrow \text{CR}}^{t_1} \quad \forall t_1, t_2 \geq 0, \quad (\text{I.5})$$

where  $\circ$  denotes the composition of quantum channels.

Axiom 2 ensures that the ticking clock channel is Markovian. Equation (I.5) is also known as the semigroup property or divisibility condition. It ensures that the clockwork is self-timing, meaning that no other external system can act as a source of timing. In particular, if Axiom 2 was not satisfied then the ticking clock channel to be applied in each instance would depend on the particular value of the coordinate time itself. This would, in turn, require an additional system that serves as a reference for time.

**Axiom 3** (Leading order condition). *Given a register starting in the state  $|k\rangle\langle k|_{\text{R}}$ , denote the probability that the  $l$ th tick has already occurred at coordinate time  $t$  but not the  $(l+1)$ th tick as*

$$p_l^{(k)}(t) = \text{tr} \left[ \mathcal{M}_{\text{C} \rightarrow \text{CR}}^{t,k} (\rho_{\text{C}}) |l\rangle\langle l|_{\text{R}} \right]. \quad (\text{I.6})$$

Then

$$\lim_{t \rightarrow 0^+} \frac{\sum_{l=0, l \notin \{k, f(k)\}}^{N_{\text{T}}} p_l^{(k)}(t)}{p_{f(k)}^{(k)}(t)} = 0 \quad \forall \rho_{\text{C}}, \quad (\text{I.7})$$

where  $f(k) = (k+1) \bmod. (N_{\text{T}} + 1)$ .

Axiom 3 ensures that the clock cannot skip a tick. That is, if the clock ticked  $k$  times at some coordinate time  $t$  and the  $(k+1)$ th tick occurs at a later coordinate time  $t' > t$ , then in the time interval between the two ticks the probability of observing the  $(k+2)$ th tick or later ticks vanishes.

**Axiom 4** (Time invariance symmetry condition).

$$\text{tr}_{\text{R}} \left[ \mathcal{M}_{\text{C} \rightarrow \text{CR}}^{t,k} (\rho_{\text{C}}) |k+l\rangle\langle k+l|_{\text{R}} \right] \quad (\text{I.8})$$

is independent of  $k$   $\forall t$ , where  $l \in \mathbb{Z}$  such that  $k+l = 0, 1, \dots, N_{\text{T}}$ .

Axiom 4 ensures that the clockwork dynamics are invariant under translation of the input and output register states by the same amount. In particular, such a property is reasonable to expect from an ordinary ticking clock: the probability that a ticking clock ticked after evolving

for a time  $t$  should not depend on the particular state its register was initialized in.

As stated previously, Axioms 1–4 represent the necessary conditions that a clock with a periodic register should fulfill. The reason for stating these axioms for ticking clocks with a periodic register is due to the presence of periodic boundary conditions which makes it easier to state the necessary conditions. One could, however, also think of formulating analogous conditions for ticking clocks with a cut-off register. Instead, we consider the following axiom which states the necessary conditions for a clock with a cut-off register based on Axioms 1–4 in a compact form.

**Axiom 5** (Cut-off register condition). *For every ticking clock channel with a cut-off register  $\mathcal{M}_{\text{CR} \rightarrow \text{CR}}^t$  there exists a ticking clock channel with a periodic register  $\bar{\mathcal{M}}_{\text{CR} \rightarrow \text{CR}}^t$  which satisfies Axioms 1–4 such that in the limit  $t \rightarrow 0^+$ :*

$$\mathcal{M}_{\text{C} \rightarrow \text{CR}}^{t,k}(\rho_C) = \bar{\mathcal{M}}_{\text{C} \rightarrow \text{CR}}^{t,k}(\rho_C) + o(t), \quad (\text{I.9})$$

for all  $k = 0, 1, \dots, N_T - 1$ , and

$$\text{tr}_C \left[ \mathcal{M}_{\text{C} \rightarrow \text{CR}}^{t,N_T}(\rho_C) \right] = |N_T\rangle\langle N_T|_R + o(t) \quad \forall \rho_C, \quad (\text{I.10})$$

where  $o(\cdot)$  denotes little-o notation.

Axiom 5 captures the fact that ticking clocks with a cut-off register evolve similarly to ticking clocks with a periodic register. The crucial difference is that when the last state of the register  $|N_T\rangle_R$  is reached, no further change within the register can take place in case of a cut-off register, i.e., these clocks stop ticking.

Having stated all five axioms governing the dynamics of ticking clocks, it is worth pointing out that one could also consider other ticking clock models with altered versions of the present axioms. For example, one may consider a ticking clock model which allows for ticking clocks that do not fulfill the time variance symmetry condition stated in Axiom 4. That being said, we believe that the present choice of axioms constitutes a reasonable set of properties that characterize “accurate” ticking clocks.

**Definition 1** (Ticking clock). *A ticking clock is a pair  $(\rho_{\text{CR}}^0, (\mathcal{M}_{\text{CR} \rightarrow \text{CR}}^t)_{t \geq 0})$ , where  $\rho_{\text{CR}}^0$  is the state of the clockwork and register at coordinate time  $t = 0$  and the ticking clock channels  $\mathcal{M}_{\text{CR} \rightarrow \text{CR}}^t$  governing their dynamics satisfy Axioms 1–4 in case of a periodic register and Axioms 2 and 5 in case of a cut-off register.*

For ticking clocks with a cut-off register no further change in the register can happen once it reached its last state  $|N_T\rangle_R$ , i.e., the clock stops ticking. Therefore, two ticking clocks with

a cut-off register which only differ in the dynamics of their clockwork after that point exhibit identical ticking statistics and can thus, for all practical means, be considered identical. This is captured by the following definition.

**Definition 2** (Clockwork equivalence). *Two ticking clocks with a cut-off register are said to be clockwork equivalent if their underlying ticking clock channels with a periodic register  $\bar{\mathcal{M}}_{\text{CR} \rightarrow \text{CR}}^t$  are identical but the state of their clockwork when the input register state is  $|N_T\rangle_R$ , given by*

$$\text{tr}_R [\mathcal{M}_{\text{C} \rightarrow \text{CR}}^{t;N_T} (\rho_C)], \quad (\text{I.11})$$

*differ for some  $t \geq 0$  and choices of  $\rho_C$ .*

Now that we have established the notion of a ticking clock we can revisit the requirement of a classical register. The condition that no coherences should develop with respect to the chosen basis of the register  $\{|0\rangle_R, |1\rangle_R, \dots, |N_T\rangle_R\}$  requires the dynamics of the clock to be of the following form:

$$\mathcal{M}_{\text{C} \rightarrow \text{CR}}^{t,k} (\rho_C^0) = \sum_{n=0}^{N_T} \tilde{\rho}_C^{(n;k)}(t) \otimes |n\rangle\langle n|_R, \quad (\text{I.12})$$

for all  $k = 0, 1, \dots, N_T$ ,  $t \geq 0$ , and initial clockwork states  $\rho_C^0$ , where  $\tilde{\rho}_C^{(n;k)}(t)$  denote arbitrary subnormalized states of the clockwork. In the following, subnormalized quantum states will generally be denoted by  $\tilde{\rho}$ . This is equivalent to the requirement that  $\mathcal{M}_{\text{C} \rightarrow \text{CR}}^t (\rho_C^0)$  must be block-diagonal in the chosen basis of the register  $\{|0\rangle_R, |1\rangle_R, \dots, |N_T\rangle_R\}$  for all  $t \geq 0$ . Clearly, with dynamics of the form Eq. (I.12) any measurement of the state of the register in the basis  $\{|0\rangle_R, |1\rangle_R, \dots, |N_T\rangle_R\}$  will leave the state of the clock invariant. Thus, Eq. (I.12) properly captures the requirement that the register of a clock should be able to be continuously monitored without affecting its dynamics.

**Definition 3** (Classical register). *A ticking clock has a classical register if its ticking clock channels  $\mathcal{M}_{\text{C} \rightarrow \text{CR}}^{t,k}$  are of the form stated in Eq. (I.12) for all  $k = 0, 1, \dots, N_T$  and  $t \geq 0$ .*

As we will see later in this work, it will be useful to distinguish between “classical” and “quantum” ticking clocks. We define a classical ticking clock as follows.

**Definition 4** (Classical ticking clock). *A ticking clock is considered classical if there exists a preferred orthonormal basis  $\{|i\rangle_C\}_{i=0}^{d-1}$  of  $\mathcal{H}_C$  for which the clockwork remains incoherent during its dynamics:*

$$\text{tr}_R [\mathcal{M}_{\text{CR} \rightarrow \text{CR}}^t (\rho_{\text{CR}}^0)] = \sum_i p_i(t) |i\rangle\langle i|_C, \quad \forall t \geq 0. \quad (\text{I.13})$$

On the contrary, a quantum ticking clock will be any ticking clock that is not classical. Intuitively, a classical ticking clock can arise from a general quantum ticking clock if its

internal state decoheres quickly with respect to the time scale on which the ticks are generated.

The definition of a ticking clock and the conditions its dynamics need to fulfill allow us to give an intuitive representation for the allowed ticking clock channels  $\mathcal{M}_{\text{CR} \rightarrow \text{CR}}^t$ .

**Proposition 1** (Ticking clock representation). *The pair  $(\rho_{\text{C}}^0, (\mathcal{M}_{\text{CR} \rightarrow \text{CR}}^t)_{t \geq 0})$  forms a ticking clock (Def. 1) with a classical register (Def. 3) up to clockwork equivalence (Def. 2) if and only if there exists a Hermitian operator  $H$  and two finite sequences of operators  $\{L_j\}_{j=1}^{N_{\text{L}}}$ , and  $\{J_j\}_{j=1}^{N_{\text{L}}}$ , which are all independent of  $t$ , such that for all  $t \geq 0$  and  $N_{\text{T}} \in \mathbb{N}_{>0}$ ,*

$$\mathcal{M}_{\text{CR} \rightarrow \text{CR}}^t(\cdot) = e^{\mathcal{L}_{\text{CR}} t}(\cdot), \quad (\text{I.14})$$

$$\mathcal{L}_{\text{CR}}(\cdot) = -i[\bar{H}, (\cdot)] + \sum_{j=1}^{N_{\text{L}}} \bar{L}_j(\cdot) \bar{L}_j^\dagger - \frac{1}{2} \{ \bar{L}_j^\dagger \bar{L}_j, (\cdot) \} + \sum_{j=1}^{N_{\text{L}}} \bar{J}_j^{(l)}(\cdot) \bar{J}_j^{(l)\dagger} - \frac{1}{2} \{ \bar{J}_j^{(l)\dagger} \bar{J}_j^{(l)}, (\cdot) \}, \quad (\text{I.15})$$

where  $\bar{H} = H \otimes \mathbb{1}_{\text{R}}$ ,  $\bar{L}_j = L_j \otimes \mathbb{1}_{\text{R}}$ ,  $\bar{J}_j^{(l)} = J_j^{(l)} \otimes O_{\text{R}}^{(l)}$ , with

$$O_{\text{R}}^{(l)} = |1\rangle\langle 0|_{\text{R}} + |2\rangle\langle 1|_{\text{R}} + \cdots + |N_{\text{T}}\rangle\langle N_{\text{T}} - 1|_{\text{R}} + l|0\rangle\langle N_{\text{T}}|_{\text{R}}. \quad (\text{I.16})$$

Here,  $l = 0$  in the case of a cut-off register and  $l = 1$  for a periodic register. The register is initialized in the state  $|0\rangle\langle 0|_{\text{R}}$  such that  $\rho_{\text{CR}}^0 = \rho_{\text{C}}^0 \otimes |0\rangle\langle 0|_{\text{R}}$ .

In Proposition 1 we do not place any restrictions on  $N_{\text{L}} \in \mathbb{N}_{>0}$ . Using Choi's theorem [27], one can show that w.l.o.g.  $N_{\text{L}} = d^2 - 1$  [16]. Meaning, for any choice of  $\{L_j\}_{j=1}^{N_{\text{L}}}$  and  $\{J_j\}_{j=1}^{N_{\text{L}}}$  with  $N_{\text{L}} \in \mathbb{N}_{>0}$  one can find a new set of operators  $\{L'_j\}_{j=1}^{d^2-1}$  and  $\{J'_j\}_{j=1}^{d^2-1}$  which result in the same dynamics. In the following, we will refer to the set of operators  $\{L_j\}$  and  $\{J_j\}$  as no-tick and tick operators, respectively. This nomenclature is motivated by the fact that the tick operators are associated with the operator  $O_{\text{R}}^{(l)}$  which advances the register state, i.e., causes ticks to be generated. On the contrary, the no-tick operators appear paired with the identity operator  $\mathbb{1}_{\text{R}}$  and thus do not cause any change in the register.

Note that the coupling of the clockwork to the register is such that the clock cannot tick “backward” and no ticks can be skipped. This is intuitive if one associates the register with an observer that keeps track of the ticks of the clock by counting recurring “tick” events. This observer simply chooses not to associate backward ticks with any particular events, such as the reverse processes of the tick events. To illustrate this, consider a typical pendulum clock as an example. The observer has the freedom to associate any particular event with a tick: one observer may identify a single swing of the pendulum from left to right as a tick and not count swings from right to left as backward ticks, whereas another may identify swings of the pendulum from left to right as forward ticks and swings from right to left as backward ticks.

Both observers rely on the same clockwork but use different counting strategies to obtain information about time in the form of ticks from the occurrence of certain events associated with the clockwork. Importantly, by adopting the perspective of the former observer we do not disregard the existence of the reverse process of the tick event – the swing from right to left – but simply choose not to associate a backward tick with it. Similarly, the observer we consider does not skip or miss any tick events, but continuously monitors the clockwork. Here, w.l.o.g. we associate with any valid clockwork an observer with the above-described counting scheme, i.e., a corresponding register.

To gain a better understanding of the dynamics of a ticking clock, it is particularly useful to look at the form of the ticking clock channel  $\mathcal{M}_{\text{C} \rightarrow \text{CR}}^{\delta t, k}(\cdot)$  for a small time step  $\delta t$  from which the dynamics for arbitrary coordinate times follows.

**Lemma 1** (Implicit ticking clock representation). *The pair  $(\rho_{\text{C}}^0, (\mathcal{M}_{\text{CR} \rightarrow \text{CR}}^t)_{t \geq 0})$  forms a ticking clock (Def. 1) with a classical register (Def. 3) up to clockwork equivalence (Def. 2) if and only if there exists a Hermitian operator  $H$  and two finite sequences of operators  $\{L_j\}_{j=1}^{N_L}$ , and  $\{J_j\}_{j=1}^{N_L}$ , which are all independent of  $t, k$  such that for all  $t \geq 0$  and  $k = 0, 1, \dots, N_{\text{T}}$ ,*

$$\mathcal{M}_{\text{C} \rightarrow \text{CR}}^{t, k}(\rho_{\text{C}}^0) = \lim_{N \rightarrow \infty, N \in \mathbb{N}} (\mathcal{M}_{\text{CR} \rightarrow \text{CR}}^{t/N, k})^{\circ(N-1)} \circ \mathcal{M}_{\text{C} \rightarrow \text{CR}}^{t/N, k}(\rho_{\text{C}}^0), \quad (\text{I.17})$$

where

$$\mathcal{M}_{\text{C} \rightarrow \text{CR}}^{\delta t, k}(\cdot) = (\cdot) \otimes |k\rangle\langle k|_{\text{R}} + \delta t \mathcal{C}_{(1, k)}(\cdot) \otimes |k\rangle\langle k|_{\text{R}} + \delta t \mathcal{C}_{(2, k)}(\cdot) \otimes |k+1\rangle\langle k+1|_{\text{R}} + F_{\text{C} \rightarrow \text{CR}}^{\delta t, k}(\cdot), \quad (\text{I.18})$$

with

$$\mathcal{C}_{(1, k)}(\cdot) = -i[H, (\cdot)] - \sum_{i=1}^{N_L} \frac{1}{2} \{L_i^\dagger L_i + \theta(k) J_i^\dagger J_i, (\cdot)\} + L_i(\cdot) L_i^\dagger, \quad (\text{I.19})$$

$$\mathcal{C}_{(2, k)}(\cdot) = \theta(k) \sum_{i=1}^{N_L} J_i(\cdot) J_i^\dagger, \quad (\text{I.20})$$

and  $F_{\text{C} \rightarrow \text{CR}}^{\delta t, k}(\rho_{\text{C}}) = o(\delta t)$  entry-wise. For ticking clocks with a periodic register  $\theta(k) = 1$  for all  $k$ , whereas  $\theta(k) = 1 - \delta_{k, N_{\text{T}}}$  in the cut-off register case, where  $\delta_{\cdot, \cdot}$  denotes the Kronecker delta. The register is initialized in the state  $|0\rangle\langle 0|_{\text{R}}$  such that  $\rho_{\text{CR}}^0 = \rho_{\text{C}}^0 \otimes |0\rangle\langle 0|_{\text{R}}$ .

Similar to Proposition 1, we can find a representation for the dynamics of the clockwork itself.

**Proposition 2** (Clockwork representation). *Given a ticking clock (Def. 1) with a classical periodic register (Def. 3) which is written in the representation of Proposition 1, its clockwork channel defined as*

$$\mathcal{M}_{\text{C} \rightarrow \text{C}}^t(\cdot) = \text{tr}_{\text{R}} [\mathcal{M}_{\text{CR} \rightarrow \text{CR}}^t((\cdot) \otimes |k\rangle\langle k|_{\text{R}})] \quad (\text{I.21})$$

is independent of  $k$  for all  $t \geq 0$  and can be written as

$$\mathcal{M}_{C \rightarrow C}^t(\cdot) = e^{\mathcal{L}_C t}(\cdot), \quad (\text{I.22})$$

where  $\mathcal{L}_C$  is of the form given in Eq. (I.15) with  $\bar{H} \rightarrow H$ ,  $\bar{L}_j \rightarrow L_j$  and  $\bar{J}_j^{(l)} \rightarrow J_j$ . For a ticking clock with a classical cut-off register written in the representation of Proposition 1, there exists a clock that is clockwork equivalent (Def. 2), such that its clockwork admits the representation stated above.

While the detailed proofs of Proposition 1 and 2, as well as Lemma 1 can be found in Ref. [16], we will review the underlying principles in the following. Any one-parameter family of CPTP maps  $(\mathcal{M}^t)_{t \geq 0}$  which is uniformly continuous (Axiom 1) and satisfies the semigroup property (Axiom 2) form a so-called (quantum) dynamical semigroup [28]. Based on these properties, it is clear that the description of the evolution in terms of the entire family of dynamical maps is highly redundant. They allow us to write

$$\mathcal{M}^t = \lim_{N \rightarrow \infty, N \in \mathbb{N}} (\mathcal{M}^{t/N})^{\circ N} \quad \forall t \geq 0. \quad (\text{I.23})$$

Thus, it suffices to specify the dynamical map for an arbitrarily small time step. One can prove that the maps of a dynamical semigroup can be written as [29]

$$\mathcal{M}^t = e^{\mathcal{L}t} = \sum_{n=0}^{\infty} t^n \frac{\mathcal{L}^{\circ n}}{n!}, \quad (\text{I.24})$$

where  $\mathcal{L}$  is the generator of the dynamical semigroup. As such, the evolution is described by a first-order differential equation

$$\frac{d}{dt} \rho(t) = \mathcal{L} \rho(t) \longleftrightarrow \rho(t) = e^{\mathcal{L}t} \rho(0), \quad (\text{I.25})$$

which is called the quantum Markovian master equation [30, 31].

One can show that any generator  $\mathcal{L}$  of a quantum dynamical semigroup admits the form [30, 31]:

$$\mathcal{L}(\cdot) = -i[H, (\cdot)] + \sum_{i=1}^{d^2-1} A_i(\cdot) A_i^\dagger - \frac{1}{2} \{A_i^\dagger A_i, (\cdot)\}, \quad (\text{I.26})$$

where  $H$  is a Hermitian operator and  $\{A_i\}_{i=1}^{d^2-1}$  are a set of arbitrary operators with  $d = \dim(\mathcal{H})$  being the dimension of the relevant Hilbert space  $\mathcal{H}$ . When written in the form given in Equation (I.26), the so-called Lindblad form, the generator  $\mathcal{L}$  is typically referred to as a Lindbladian, where the operators  $\{A_i\}$  are called Lindblad or jump operators [26]. Moreover, the quantum Markovian master equation is then referred to as a Lindblad master equation. Looking

back at the representations of the ticking clock and clockwork given in Proposition 1 and 2, respectively, we observe that in both cases the dynamics are governed by a Lindblad master equation. In particular, any Lindblad master equation can serve as a valid description of the dynamics of the clockwork itself. As such, *a priori* any general open quantum system whose dynamics are described by a Lindblad master equation can serve as a clockwork. Note that the Markovianity of its evolution is what justifies the identification of the clockwork as the single source of timing for the clock. Moreover, the fact that the dynamics generated by a Lindblad master equation are generally non-unitary and thus irreversible makes it clear that the clockwork emits temporal information in the form of ticks in an irreversible fashion. We see, on the other hand, that the clock itself consisting of clockwork and register only admits a description in terms of a special class of Lindblad master equations (see Proposition 1). Because Axioms 1 and 2 alone allow us to describe the evolution of the clock by a general Lindblad master equation, we can see this as a consequence of the conditions imposed in Axioms 3,4, and 5, as well as Def. 3. These restrict the interaction between clockwork and register, as well as the form of the register itself. Therefore, these are precisely the aspects of a ticking clock that distinguish it from any ordinary open quantum system.

A Lindblad master equation represents the most general type of Markovian and time-homogeneous master equation describing the evolution of open quantum systems [26]. It turns out that the Lindblad master equation allows for an accurate description of many physical processes which justifies the assumption of Markovianity beyond the simplicity of the resulting dynamical equations [26, 30]. In fact, one can derive the Lindblad master equation from an underlying unitary Hamiltonian evolution a total system comprised of system and environment, where the environment simply constitutes those parts of the total system which we decide not to model explicitly. More precisely, there are two known types of limits – the weak and singular coupling limits – under which a Lindblad master equation can be derived from the interaction of the system with an infinite dimensional environment via a time-independent Hamiltonian, i.e., under which the assumption of Markovianity is met [26, 32]. In the weak-coupling limit, one assumes that the interaction between the system and the environment is small. This results in the degrees of freedom of the environment changing fast with respect to the system [31]. Conversely, in the singular coupling limit, one assumes that the system couples strongly to its environment resulting in fast system variables. In the context of our ticking clock model, this guarantees that any ticking clock can be realized via the inclusion of a large, macroscopic environment such that the total system evolves according to a time-independent Hamiltonian. This is crucial, as it shows that there exists a physical realization of any ticking clock that is autonomous. An autonomous clock contains all necessary resources for it to run and there is no external system that provides timing [12, 18]. Note that this environment must, however, not necessarily be thermal. In fact, the question of what minimal resources are required to

run a given ticking clock in an autonomous fashion is still open [16, 18].

## I.1 Examples of ticking clocks

To gain a better intuition on the inner workings of a ticking clock and for later reference, we discuss two examples explicitly in this section: the so-called ladder clock and the quasi-ideal clock.

### I.1.1 Ladder ticking clock

The “ladder ticking clock” is a classical ticking clock that has been proven to be the most accurate classical ticking clock in Ref. [14] and was first considered in Ref. [13]. Choosing some orthonormal basis  $\{|j\rangle\}_{j=1}^d$  for the Hilbert space of the clockwork  $\mathcal{H}_C$ , the clock can be represented as stated in Proposition 1 with the following choice of no-tick and tick operators:

$$L_j = |j+1\rangle\langle j|, \quad J_j = 0, \quad (\text{I.27})$$

$$L_d = 0, \quad J_d = |1\rangle\langle d|, \quad (\text{I.28})$$

with  $N_L = d$  and  $H = 0$ . The clock is initialized in the state  $\rho_{CR}^0 = |1\rangle\langle 1|_C \otimes |0\rangle\langle 0|_R$ . Note that the clockwork is initialized in a pure state and that the clock is a so-called reset clock.

**Definition 5** (Reset ticking clock). *A ticking clock (Def. 1) which admits a representation given by Proposition 1 is considered a reset clock if*

$$\sum_{j=1}^{N_L} J_j \rho_C J_j^\dagger \propto \rho_C^0 \quad \forall \rho_C, \quad (\text{I.29})$$

where  $\rho_C^0$  is the initial state of the clockwork.

Looking back at the implicit ticking clock representation given in Lemma 1, we have  $\mathcal{C}_{(2,k)}(\cdot) = \theta(k) \sum_{j=1}^{N_L} J_j(\cdot) J_j^\dagger$  as the dynamical map associated with the generation of a tick in each infinitesimal time step. Thus, a reset clock corresponds to a ticking clock which maps the clockwork back to its initial state in each tick. As we will see, this makes the dynamics and tick statistics of such clocks particularly simple.

The working principle of the ladder ticking clock is illustrated in Fig. I.2. The evolution of the clockwork is given by a (classical) stochastic biased random walk up a  $d$ -dimensional ladder associated with the orthonormal basis  $\{|i\rangle\}_{i=1}^d$ . Given that the clock is classical, the clockwork  $\rho_C(t)$  remains diagonal in the basis  $\{|i\rangle\}_{i=1}^d$  at all times and can thus be represented state vector  $\vec{v}_C(t)$  that contains its diagonal elements. In this notation, using the representation

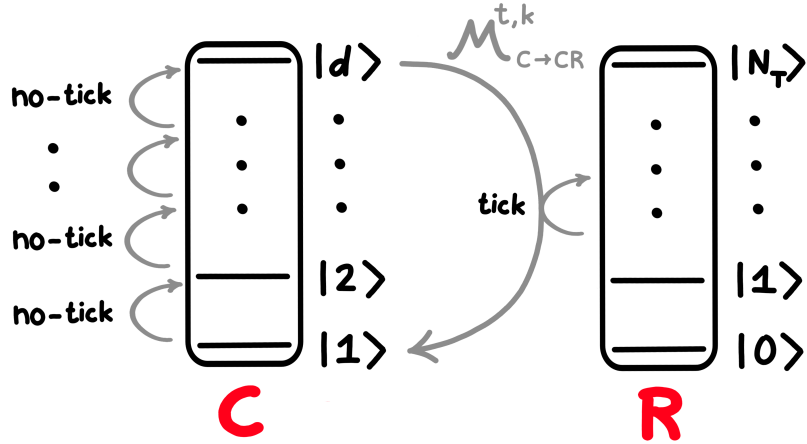


Figure I.2: Illustration of the working principle of the ladder ticking clock composed of a clockwork (C) made of a  $d$ -dimensional ladder and a register (R) depicted as a  $(N_T + 1)$ -dimensional ladder. Transitions from the top of the ladder to its ground state trigger a tick event which results in the advancement of the register's state, whereas transitions within the ladder constitute no-tick events. These dynamics are governed by a particular set of quantum channels  $(\mathcal{M}_{C \rightarrow CR}^{t,k})_{t \geq 0, k \in (0, N_T)}$ .

given by Proposition 2 the Lindblad master equation governing the evolution of the clockwork of the ladder clock can be rewritten as

$$\frac{d}{dt}\vec{v}_C(t) = \mathcal{P}\vec{v}_C(t), \quad \mathcal{P} = \begin{pmatrix} -1 & 0 & 0 & \cdots & 1 \\ 1 & -1 & 0 & \cdots & 0 \\ 0 & 1 & -1 & \cdots & 0 \\ \vdots & \vdots & \vdots & \ddots & \vdots \\ 0 & 0 & 0 & \cdots & -1 \end{pmatrix}, \quad (\text{I.30})$$

where  $\vec{v}_C(0) = \vec{v}_C^0 = (1, 0, \dots, 0)^T$  and  $\mathcal{P}$  is a transition rate matrix [33].

The dynamics specified in Eq. (I.30) can be interpreted as follows. At  $t = 0$  the clockwork starts in the ground state of the ladder  $|1\rangle_C$ . In each time step the population can move up the ladder, where only adjacent states of the ladder are coupled (with periodic boundary conditions) and the rate at which population moves from state  $|k\rangle_C \rightarrow |(k + 1) \bmod. d\rangle_C$  is given by the population of the state  $|k\rangle_C$ . The coupling of the clockwork to the register is such that only the transitions from the most-upper state of the ladder to its ground state  $|d\rangle_C \rightarrow |1\rangle_C$  are coupled to an advancement of the register, i.e., the generation of a tick. This can be seen from the fact that this transition is mediated by the tick operator, whereas all other transitions within the clockwork are governed by the no-tick operators, see Eq. (I.27)

and (I.28).

### I.1.2 Quasi-ideal ticking clock

The “quasi-ideal ticking clock” [14, 15] is a highly-accurate quantum ticking clock. The clock can be represented as stated in Proposition 1 with the following choice of tick and no-tick operators

$$L_j = 0, \quad J_j = \sqrt{2V_j}|\Psi\rangle\langle\theta_j|, \quad (\text{I.31})$$

with  $N_L = d$  and an initial state  $\rho_{\text{CR}}^0 = |\Psi\rangle\langle\Psi|_C \otimes |0\rangle\langle 0|_R$ . The coefficient  $\{V_j\}_{j=0}^{d-1}$  follow a distribution peaked near  $j = d - 1$ . Note that this clock is also a reset clock with a pure initial state of its clockwork. The Hamiltonian is given by a truncated harmonic oscillator with level spacing  $w$ :

$$H = \sum_{n=0}^{d-1} nw|E_n\rangle\langle E_n|. \quad (\text{I.32})$$

We denote the complementary basis to  $\{|E_j\rangle\}_{j=0}^{d-1}$  obtained by taking the discrete Fourier transform as  $\{|\theta_j\rangle\}_{j=0}^{d-1}$ , where

$$|\theta_j\rangle = \frac{1}{\sqrt{d}} \sum_{n=0}^{d-1} e^{-2\pi i n j / d} |E_n\rangle. \quad (\text{I.33})$$

The initial state of the quasi-ideal clock is then given as a coherent complex Gaussian superposition of Fourier basis states

$$|\Psi\rangle = \sum_{k \in \mathcal{S}_d(k_0)} A e^{\frac{\pi^2}{\sigma_0^2}(k-k_0)^2} e^{2\pi i n_0(k-k_0)/d} |\theta_k\rangle, \quad (\text{I.34})$$

with  $\mathcal{S}_d(k_0)$  denoting a set of  $d$  consecutive integers all centered around  $k_0 \in \mathbb{R}$ , where  $k_0$  determines the mean position of the Gaussian and  $\sigma_0$  denotes its width. Choosing  $\sigma_0 \approx d$  then yields an initial state which is well approximated by an energy eigenstate. Moreover,  $wn_0$  is the mean energy of the initial state with  $n_0 \in (0, d - 1)$ . The dynamics of the quasi-ideal clock (with appropriate choices of its remaining parameters) are such that the complex Gaussian starts off highly peaked around the state  $|\theta_0\rangle$  at  $t = 0$ . Over time it shifts to a distribution that is highly concentrated around the state  $|\theta_{d-1}\rangle$  which leads to a tick generation with high probability, thereby resetting the clock.

## I.2 Accuracy of ticking clocks

A crucial characteristic of any ticking clock is its accuracy. *A priori* one can consider many different measures for the accuracy of a ticking clock [12–14]. However, all measures have in

common that they are solely a function of measurement results obtained from the register. As such, these measures are independent of the particular dynamics of the clockwork which generated the corresponding ticks. A good way to assess the accuracy of a ticking clock is to look at its so-called tick delay functions  $\{\tau^{(k)}(t)\}_{k=1}^{N_T}$ . Here,  $\tau^{(k)}(t)$  denotes the delay function of the  $k$ th tick: the probability that  $(k-1)$  ticks occurred during the time interval  $[0, t)$  and the  $k$ th tick occurs in the infinitesimal time interval  $[t, t+\delta t]$  is then given by  $\tau^{(k)}(t)\delta t$ ,  $\delta t > 0$ .

The delay function of the  $k$ th tick can be computed as

$$\tau^{(k)}(t) = \lim_{\delta t \rightarrow 0^+} \frac{\text{tr} \left[ \mathbb{1}_C \otimes |k\rangle\langle k|_R \left( \mathcal{M}_{C \rightarrow CR}^{\delta t, k-1} \left( \tilde{\rho}_C^{(k-1)}(t) \right) - \tilde{\rho}_C^{(k-1)}(t) \otimes |k-1\rangle\langle k-1|_R \right) \right]}{\delta t}, \quad (\text{I.35})$$

where

$$\tilde{\rho}_C^{(k)}(t) = \text{tr}_R \left[ \mathbb{1}_C \otimes |k\rangle\langle k|_R \mathcal{M}_{C \rightarrow CR}^{t, 0} \left( \rho_C^0 \right) \right]. \quad (\text{I.36})$$

Intuitively, an accurate clock will have tick delay functions with a small width. That is, the delay functions of an ideal clock which we would describe as being infinitely accurate will be given by Dirac delta distributions  $\tau^{(k)}(t) = \delta(t - \mu_k)$ , where  $\mu_k$  denotes the expected time at which the  $k$ th tick occurs. In general, we compute the expected time  $\mu_k$  and the variance  $\sigma_k^2$  of the  $k$ th tick as

$$\mu_k = \int_0^\infty \tau^{(k)}(t) t dt, \quad (\text{I.37})$$

$$\sigma_k^2 = \int_0^\infty \tau^{(k)}(t) (t - \mu_k)^2 dt. \quad (\text{I.38})$$

Note that the tick delay functions are normalized probability densities

$$\int_0^\infty \tau^{(k)}(t) dt = 1, \quad (\text{I.39})$$

for all  $k = 1, \dots, N_T$ .

For the rest of this work, we will be concerned with the limit  $N_T \rightarrow \infty$  where the distinction between cut-off registers and periodic registers becomes irrelevant. For brevity, we will refer to these clocks as ticking clocks throughout this work if not stated otherwise. Note that at finite memory, the accuracy of a ticking clock is generally dependent on whether the clock has a periodic register or a cut-off register. The crucial property of clocks with periodic registers is that the dynamics of the clockwork at times after the first tick has occurred are still relevant for the first tick's statistics, i.e., its accuracy but also other quantities such as its entropy (as we will see later). This is because for a ticking clock with a periodic register, the first tick statistics encompasses all ticks, labeled by  $k$ , for which  $1 = k \bmod. N_T$ . Note that the class

of ticking clocks with a cut-off register encompasses the class of ticking clocks with a periodic register given that the observer keeps track of the ticks in real-time and is thus not affected by the periodic nature of the register. In particular, by restricting ourselves to this particular class of registers the delay functions obtained for clocks in the ticking clock model presented here are identical in how they are related to the dynamics of the clockwork as in previous works, such as Refs. [14, 18]. Thus, we can make use of previous results on the accuracy of ticking clocks, in particular Ref. [14]. Using the representation given in Lemma 1, the expression for the tick delay function given in Eq. (I.35) then reduces to

$$\tau^{(k)}(t) = \text{tr} \left[ \sum_j J_j \tilde{\rho}_C^{(k-1)}(t) J_j^\dagger \right]. \quad (\text{I.40})$$

As a measure of accuracy of the  $k$ th tick, we consider the quantity  $R_k = \mu_k^2 / \sigma_k^2$  [14]. We use this measure to compare the accuracy of different clocks:

- ticking clock A has the same accuracy as ticking clock B if and only if  $R_k^A = R_k^B \forall k \in \mathbb{N}_{>0}$ ,
- ticking clock A is strictly more accurate than ticking clock B if and only if  $R_k^A > R_k^B \forall k \in \mathbb{N}_{>0}$ ,
- ticking clock A is more accurate than ticking clock B if and only if  $R_k^A \geq R_k^B \forall k \in \mathbb{N}_{>0}$  but the two clocks do not have the same accuracy.

Note that this measure is invariant under rescaling of coordinate time  $t \rightarrow t/a$ ,  $a > 0$ . This captures the fact that the accuracy of a clock should be the same, irrespective of whether the expected time at which the ticks occur is small or large. Moreover, the accuracy takes on a simple form for reset clocks. Because reset clocks reset their clockwork to its initial state after every tick, each tick event is independently and identically distributed. Thus, the delay function of the  $k$ th tick is given by a convolution of  $k$  delay functions of the first tick

$$\tau^{(k)}(t) = \underbrace{(\tau^{(1)} * \tau^{(1)} * \dots * \tau^{(1)})(t)}_{k \text{ times}} \quad (\text{I.41})$$

This yields

$$R_k = kR_1 \forall k \in \mathbb{N}_{>0}, \quad (\text{I.42})$$

meaning that the accuracy of its later ticks can solely be expressed in terms of the accuracy of the first tick. The proof for Eq. (I.41) and (I.42) can be found in Appendix B.1. This has the intuitive interpretation that for reset clocks  $R_1$  corresponds to the number of ticks that the clock generates on average before the next tick has a standard deviation  $\sigma_1$  equal to the mean time between ticks  $\mu_1$ . Also note that in this case,  $1/R_1$  corresponds to the Allan

variance, an accuracy measure frequently used for clocks [34], with an observation period of  $\mu_1$ .

In Ref. [14] it has been shown that the maximal achievable accuracy for a classical ticking clock with a  $d$ -dimensional clockwork is given by  $R_k = kd$  and can be achieved by the ladder ticking clock (see Section I.1.1). Moreover, it was shown that there exists a quantum ticking clock which achieves  $R_k = kR_1$  with  $R_1 \geq d^{2-\epsilon} + o(d^{2-\epsilon})$  for any arbitrary  $\epsilon > 0$  in the large  $d$  limit. This demonstrates a quantum-over-classical advantage in the task of timekeeping. The quantum ticking clocks that achieve such accuracy are quasi-ideal ticking clocks (see Section I.1.2) with carefully tuned parameters. In Ref. [17] it has been shown that this quantum bound is essentially tight when considering ticking clocks that only tick once. Note that both the ladder ticking clocks and quasi-ideal ticking clocks are reset clocks with an initial clockwork state that is pure. It is intuitive that reset clocks are the optimal clocks in terms of accuracy because they generate a sequence of independent and identically distributed tick events. The accuracy of later ticks is then solely determined by the accuracy of the first tick  $R_1$ .

### I.3 Classical ticking clocks

It turns out to be useful to adopt an alternative notation for describing classical ticking clocks (Def. 4) which we hinted at in our discussion of the ladder ticking clock (see Section I.1.1). For a classical ticking clock, the density operator of the clockwork is guaranteed to remain incoherent throughout its dynamics. Thus, it suffices to describe the clockwork by a state vector  $\vec{v}_C \in \mathbb{R}^d$  whose entries correspond to the diagonal entries of its density matrix in the preferred basis

$$\rho_C = \sum_{i=0}^{d-1} v_{C,i} |i\rangle\langle i|_C \longleftrightarrow \vec{v}_C = \sum_{i=0}^{d-1} v_{C,i} \vec{e}_i, \quad (\text{I.43})$$

with  $\sum_i v_{C,i} = 1$ ,  $v_{C,i} \geq 0 \forall i$ , and  $\{\vec{e}_i\}$  some orthonormal basis of  $\mathbb{R}^d$ . In the case of a classical register (Def. 3), the joint state of clockwork and register is also diagonal when choosing the basis of the register as  $\{|0\rangle_R, |1\rangle_R, \dots, |N_T\rangle_R\}$ . Thus, we can similarly represent the state  $\rho_{CR}$  by a set of subnormalized state vectors  $\{\tilde{v}_C^{(k)}\}_{k=0}^{N_T}$ , where  $\tilde{v}_C^{(k)} \in \mathbb{R}^d$  represents the state of the clockwork within the subspace associated with the state  $|k\rangle_R$  of the register

$$\hat{\rho}_C^{(k)} = \text{tr}_R [\rho_{CR} |k\rangle\langle k|_R] \longleftrightarrow \tilde{v}_C^{(k)}. \quad (\text{I.44})$$

The state of the clockwork can be retrieved as

$$\vec{v}_C = \sum_{k=0}^{N_T} \tilde{v}_C^{(k)}. \quad (\text{I.45})$$

This allows us to simplify the representations given in Proposition 1 and Lemma 1 following Ref. [14].

**Corollary 1** (Classical ticking clock representation). *The dynamics of a classical ticking clock (Def. 4) with a classical (periodic or cut-off) register (Def. 3) in the limit  $N_T \rightarrow \infty$  are governed by a set of coupled first-order differential equations*

$$\frac{d}{dt} \vec{v}_C^{(k)}(t) = \begin{cases} \mathcal{N} \vec{v}_C^{(0)}(t), & \text{for } k = 0 \\ \mathcal{N} \vec{v}_C^{(k)}(t) + \mathcal{T} \vec{v}_C^{(k-1)}(t), & \text{for } k \neq 0 \end{cases}, \quad (\text{I.46})$$

where  $\mathcal{N}$  and  $\mathcal{T}$  are two real  $d \times d$ -matrices satisfying

$$\mathcal{N}_{ij} = \begin{cases} \leq 0, & \text{for } i = j \\ \geq 0, & \text{for } i \neq j \end{cases}, \quad \mathcal{T}_{ij} \geq 0 \quad \forall i, j, \quad (\text{I.47})$$

and

$$\sum_{i=0}^{d-1} \mathcal{N}_{ij} + \mathcal{T}_{ij} = 0 \quad \forall j. \quad (\text{I.48})$$

The initial conditions to Eq. (I.46) are given by

$$\vec{v}_C^{(k)}(0) = \begin{cases} \vec{v}_C^0, & \text{for } k = 0 \\ 0, & \text{for } k \neq 0 \end{cases}, \quad (\text{I.49})$$

which corresponds to the choice of  $|0\rangle_R$  as the initial register state at  $t = 0$ .

We will prove Corollary 1 in the following. Consider the representation of the ticking clock channel for an infinitesimal time step  $\mathcal{M}_{C \rightarrow CR}^{\delta t, k}$  given in Lemma 1. Because we consider the limit  $N_T \rightarrow \infty$ , we are not concerned with the cases where the memory runs full, i.e., where the state  $|N_T\rangle_R$  is reached. Thus, the distinction between cut-off and periodic registers becomes irrelevant. In order for the dynamics to generate an incoherent clockwork state, we require the clockwork state obtained by application of the channels  $\mathcal{C}_{(1,k)}$  and  $\mathcal{C}_{(2,k)}$  with a diagonal input state to be themselves diagonal. This yields the following dynamics for the diagonal entries of the clockwork, or equivalently the corresponding state vector,

$$\mathcal{C}_{(1,k)}(\rho_C) \leftrightarrow \mathcal{N} \vec{v}_C, \quad \mathcal{C}_{(2,k)}(\rho_C) \leftrightarrow \mathcal{T} \vec{v}_C, \quad (\text{I.50})$$

where

$$\mathcal{N}_{nm} = -\delta_{n,m} \langle n | \sum_j (L_j^\dagger L_j + J_j^\dagger J_j) | n \rangle + \sum_j |\langle n | L_j | m \rangle|^2, \quad (\text{I.51})$$

$$\mathcal{T}_{nm} = \sum_j |\langle n | J_j | m \rangle|^2, \quad (\text{I.52})$$

with  $\{|i\rangle\}_{i=0}^{d-1}$  the preferred basis of the clockwork in which it remains incoherent. Given the freedom in the choice of no-tick and tick operators specified in Lemma 1, one can check that Eq. (I.33) and (I.34) allow for all possible no-tick and tick generators,  $\mathcal{N}$  and  $\mathcal{T}$ , as specified in Eq. (I.47) and (I.48). Having obtained an expression for the ticking clock channel for an infinitesimal time step  $\mathcal{M}_{\text{C} \rightarrow \text{CR}}^{\delta t, k}(\cdot)$  in vector notation, the dynamics of the clockwork can straightforwardly be written as a set of coupled first-order differential equations (Eq. (I.46)).

Equation (I.46) corresponds to a stochastic Markovian sequence of events [14] which arises from the general dynamics of a ticking clock governed by a quantum Markovian master equation when restricting the dynamics and the initial state to remain diagonal in some preferred basis. We refer to the matrices  $\mathcal{N}$  and  $\mathcal{T}$  as no-tick and tick generator, respectively. The dynamics given by Eq. (I.46) can be explained as follows: in each infinitesimal time step there are two contributions to the state  $\vec{v}_\text{C}^{(k)}$   $k > 0$ , being from the no-tick event governed by the no-tick generator  $\mathcal{N}$  and the tick event governed by the tick generator  $\mathcal{T}$ . The tick events are associated with a transition between different tick subspaces, whereas transitions within a tick subspace correspond to no-tick events. Note that if we are not interested in tracking the evolution of the clockwork with respect to the individual tick subspaces, we have

$$\frac{d}{dt}\vec{v}_\text{C}(t) = (\mathcal{N} + \mathcal{T})\vec{v}_\text{C}(t) = \mathcal{P}\vec{v}_\text{C}(t), \quad (\text{I.53})$$

with  $\vec{v}_\text{C}(0) = \vec{v}_\text{C}^0$ . Equation (I.53) corresponds to a forward equation describing a continuous-time Markov chain with a transition rate matrix  $\mathcal{P} = \mathcal{N} + \mathcal{T}$  [33]. This represents the classical analogous of the clockwork representation given in Proposition 2.

Not only does this ‘‘classical’’ notation allow for a simplified picture of the dynamics of a classical ticking clock, it also removes any redundancy in the description of classical ticking clocks. The dynamics of a quantum ticking clock can be specified by choosing a Hermitian operator  $H$ , as well as two sets of tick and no-tick operators,  $\{J_j\}_{j=1}^{d^2-1}$  and  $\{L_j\}_{j=1}^{d^2-1}$ , see Proposition 1. On the contrary, for classical ticking clocks, it suffices to specify two real  $d \times d$ -matrices satisfying additional constraints. Thus, when analyzing and optimizing the entropy production of classical ticking clocks we will make use of this reduction in the degrees of freedom by adopting the classical notation.

Revisiting the ladder ticking clock discussed in Section I.1.1, it can be stated in the representation given in Corollary 1 by choosing

$$\mathcal{N} = \begin{pmatrix} -1 & 0 & 0 & \cdots & 0 \\ 1 & -1 & 0 & \cdots & 0 \\ 0 & 1 & -1 & \cdots & 0 \\ \vdots & \vdots & \vdots & \ddots & \vdots \\ 0 & 0 & 0 & \cdots & -1 \end{pmatrix}, \quad \mathcal{T}_{ij} = \begin{cases} 1, & \text{if } i = 0, j = d-1 \\ 0, & \text{otherwise} \end{cases}, \quad (\text{I.54})$$

and  $\vec{v}_C^0 = \vec{e}_0 = (1, 0, \dots, 0)^T$  which represents the ground state of the ladder. The matrix  $\mathcal{N}$  governs the transitions within the ladder which are not connected to the generation of any ticks, whereas  $\mathcal{T}$  governs the transitions from the top of the ladder to its ground state and the generation of ticks.

In analogy to Eq. (I.38) the delay function of the  $k$ th tick can then be computed as

$$\tau^{(k)}(t) = \|\mathcal{T}\vec{v}_C^{(k-1)}(t)\|, \quad (\text{I.55})$$

where  $\|\vec{v}\| = \sum_i v_i$  and the tick generator  $\mathcal{T}$  takes the role of the channel  $\mathcal{C}_{(2,k)}$  (see Eq. (I.50)). The condition for a classical ticking clock to be a reset clock (Def. 5) can be stated as

$$\mathcal{T}\vec{v}_C \propto \vec{v}_C^0 \quad \forall \vec{v}_C. \quad (\text{I.56})$$

This can be achieved by choosing  $\mathcal{T}$  to be a rank-1 matrix, where each column is proportional to  $\vec{v}_C^0$ . Importantly, for classical ticking clocks, one can show that reset clocks which start with an initially pure clockwork are the most accurate classical ticking clocks.

**Theorem 1** (Reset ticking clocks are most accurate). *For every classical ticking clock (Def. 4) written in the representation of Corollary 1 with accuracies  $\{R_k\}_{k \in \mathbb{N}_{>0}}$ , there exists a classical ticking clock with accuracies  $\{R'_k\}_{k \in \mathbb{N}_{>0}}$  such that  $R'_k \geq R_k \forall k \in \mathbb{N}_{>0}$ . This ticking clock is a reset clock (Def. 5) with a clockwork of the same dimension that is initialized in a pure state. In particular, it can be constructed from the original clock by*

- initializing the clockwork in a well-chosen canonical state:  $\vec{v}_C^0 = \vec{e}_i$  for some  $i \in (0, d-1)$ ,
- setting all but one of the rows of the tick generator  $\mathcal{T}$  to zero, and shifting the single non-zero row to the location of the chosen initial canonical state, such that  $\mathcal{T}\vec{v}_C \propto \vec{v}_C^0 \forall \vec{v}_C$ .

The proof of this theorem can be found in Ref. [14]. While we expect a similar theorem to hold in the case of general quantum ticking clocks, it has not yet been proven. In the following, we will outline the intuition on why reset clocks should be optimal in terms of their accuracy:

For reset clocks, one can optimize the dynamics to result in the highest accuracy of the first tick for the given initial clockwork state and simply reset to the initial state after each tick. The only possible way such a scheme would not be optimal is if one could tune the mean time of the later ticks to adjust for any time gained or lost due to previous ticks occurring too early or too late. Indeed, there exist physical systems with events that exhibit such a property, e.g., based on electron transport [35] or photon emission [36]. It remains to be seen whether quantum clocks with such tick events can yield higher accuracies than reset clocks. Intuitively, determining whether previous ticks happened too early or too late itself requires an accurate timekeeping device that needs to be incorporated into the clockwork. As such, one expects the increased accuracy of such ticking clocks to come at the cost of a clockwork with increased dimension.

## Chapter II

# Entropy production per tick of a ticking clock

A closed quantum system undergoes unitary Hamiltonian evolution governed by Schrödinger’s equation [25, 26, 37]. Under such dynamics, both the von Neumann entropy and energy of the system are conserved (see Appendix A for a brief review of the properties of the von Neumann entropy). Furthermore, because the evolution is unitary it is completely reversible, i.e., time-reversal symmetric. This reflects the fact that the system does not interchange any information or energy with another system. In contrast, the dynamics of an open quantum system cannot, in general, be described by a unitary time evolution. Thus, both the von Neumann entropy and energy of the open quantum system can undergo change. This can be attributed to the fact that the (open) system is now coupled to another quantum system – its environment. Any open quantum system is inevitably part of a larger closed system undergoing unitary Hamiltonian evolution, which may be the entire universe as a whole. As a consequence, to guarantee the conservation of energy and von Neumann entropy of this larger closed system, any change in von Neumann entropy or energy of the open quantum system must be compensated by a corresponding change in the remaining degrees of freedom [38, 39].

Because the von Neumann entropy of a quantum system can be interpreted as its information content [40, 41], this establishes a global conservation law for information in quantum theory [42]. Compare this to the second law of thermodynamics which states that the “thermodynamic” entropy of an isolated system can never decrease: Clausius theorem states that the change in the system entropy  $\Delta S_S$  (thermodynamic notion of entropy) when exchanging an amount of heat  $Q$  with a thermal reservoir (where a positive heat corresponds to heat flow from system to reservoir) at temperature  $T$  is bounded by  $\Delta S_S \geq -\beta Q$ . Here,  $\beta = 1/k_B T$  and  $k_B$  denotes the Boltzmann constant. Equality is achieved if and only if the heat exchange is done reversibly, whereas any irreversible process necessarily leads to  $\Delta S_S > -\beta Q$ . Thus,

the irreversible entropy production  $\Sigma$  in classical thermodynamics is identified as

$$\Sigma = \Delta S_S + \beta Q \geq 0. \quad (\text{II.1})$$

Evidently, the von Neumann entropy of the overall closed system is not a suitable candidate for the microscopic analogous of thermodynamic entropy because it is conserved under the unitary dynamics governing the evolution of the total system. This fact can be regarded as the main difficulty in formulating an analogous law to the second law of thermodynamics in non-thermodynamic, possibly microscopic, and quantum-mechanical settings [39, 43, 44]. Such a law should quantify the irreversibility of the underlying dynamics and thus fundamentally relies on identifying an analogous quantity to the entropy production  $\Sigma$  in classical thermodynamics. Importantly, it may depend on the particular physical system under consideration and the dynamical laws governing its evolution. As such, a unifying theory of (irreversible) entropy production that applies for all kinds of processes, both classical and quantum in nature, has not yet been established [45].

A ticking clock corresponds to a quantum system that is generally open and undergoes non-unitary evolution (see Chapter I). In fact, one can regard the openness of a ticking clock as a direct consequence of its purpose – measuring time. This necessitates the presence of irreversible dynamics which break time-reversal symmetry and allow the ticking clock to single out a direction of time [18]. As such, any ticking clock will generally be coupled to its environment and participate in an exchange of information. In a thermodynamic setting, it is the thermodynamic entropy that must inevitably increase over the course of a tick and which quantifies the irreversibility of the clock, as we will find shortly in Section II.1. Clearly, the identification of this quantity as the relevant measure for the irreversibility of a ticking clock relies on the applicability of the second law of thermodynamics. In particular, there have been several works discussing the entropy production of ticking clocks recently [11, 18–20]. However, these investigations have been restricted to certain classes of ticking clocks in a thermodynamic setting. Furthermore, the expressions for the entropy per tick of ticking clocks put forward in these works were based on the particular physical realization of the ticking clocks. The clocks studied in Refs. [11, 18, 19], for example, are all driven by heat exchange with thermal reservoirs. In such a setup, measures for the entropy production per tick related to the heat exchange per tick emerge naturally.

For a general ticking clock described by our ticking clock model in Chapter I, these conditions may not be met. In particular, for a given ticking clock there may be various physical realizations that do not rely on thermal baths. Thus, while the ticking clocks in Refs. [11, 18, 19] can be described using our ticking clock model, the analysis of their entropy produc-

tion was not carried out in this general framework. In this chapter, we address the task of devising an appropriate measure for the entropy production per tick of a ticking clock in the context of the axiomatic framework introduced in Chapter I. This measure should apply for any ticking clock as given by Proposition 1, where we restrict ourselves to cut-off registers, or equivalently, periodic registers in the limit  $N_T \rightarrow \infty$ . The measure should therefore be applicable independent of the specific physical realization of the ticking clock. In particular, our notion of the entropy production per tick of a ticking clock should not be restricted to a thermodynamic setting, i.e., a situation where the environment is given by thermal reservoirs. Nevertheless, we can draw inspiration from this special case. Thus, we start with a review of previous results regarding the entropy production per tick of ticking clocks and its connection to accuracy in a thermodynamic setting.

## II.1 Entropy production of thermodynamic ticking clocks

In Ref. [18], the relation between the accuracy and entropy production per tick of a ticking clock whose clockwork is driven by the heat flow between two thermal reservoirs is studied. It is based on the smallest quantum heat engine introduced in Ref. [46] and we will refer to it as the “thermodynamic ticking clock” in the following. The thermal environment of the clock allows for its entropy production to be analyzed by means of thermodynamic concepts.

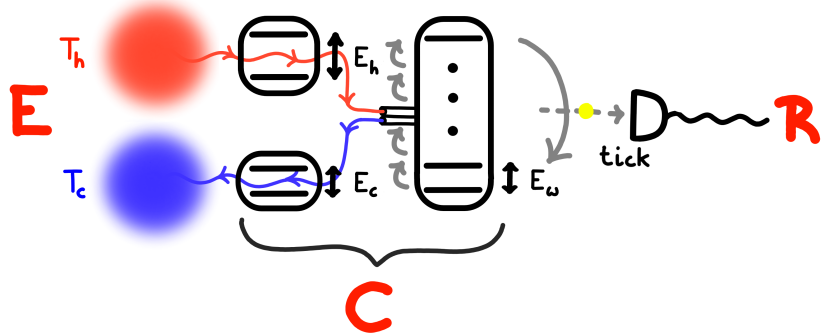


Figure II.1: Illustration of the working principle of the thermodynamic ticking clock. The clockwork (C) is composed of two qubits each coupled to a separate heat bath, as well as a  $d$ -dimensional ladder. The clockwork is powered by the heat flow between the two heat baths which constitute the environment (E) of the clockwork. A tick in the register (R) is triggered by the detection of a photon that is spontaneously emitted from the top of the ladder.

Figure II.1 illustrates the working principle of the thermodynamic ticking clock. Its clockwork consists of two qubits, each coupled to a separate thermal reservoir. One qubit, labeled  $h$ , is connected to a hot bath at temperature  $T_h$  and has an energy gap  $E_h$ . The other qubit,

labeled  $c$ , is connected to a cold bath at temperature  $T_c$  and has an energy gap  $E_c < E_h$ . Initially, each of the two qubits is in equilibrium with its bath and thus given by a thermal state at the corresponding bath temperature. Both baths are modeled as idealized, infinitely large heat reservoirs. The two qubits make up a heat engine that is coupled to a third subsystem of the clockwork with  $d$  equally-spaced energy levels, where the level spacing is  $E_w = E_h - E_c$ . In the following, this system will be referred to as the  $d$ -dimensional ladder to which we associate the orthonormal basis  $\{|i\rangle_w\}_{i=0}^{d-1}$ . Ultimately, the heat flow induced by the temperature difference  $T_h - T_c$  between the two thermal reservoirs powers the heat engine comprised of the two qubits. Through the coupling between the heat engine and the ladder, the heat flow then delivers energy to cause a drift of population up the ladder. The top level of the ladder  $|d-1\rangle_w$  is assumed to be out of equilibrium with respect to the photon field of the environment at temperature  $T_c$ . Thus, there may be spontaneous emission of a photon with energy  $E_\gamma = (d-1)E_w$  which results in the ladder decaying to its ground state  $|0\rangle_w$ . The probability of the reverse process, i.e., photon absorption from the ground state of the ladder, is negligible given that the temperature of the environment is small compared to the energy of the photon  $E_\gamma \ll k_B T_c$ . The photon is then detected via an ideal photon detector. This detection event constitutes a tick of the clock and is coupled to an advancement of the register. Once the ladder returns to its ground state after the clock ticks, the process repeats itself. In particular, one assumes that the entire clockwork is reset to its initial state with vanishing correlations between all subsystems of the clockwork and thermalized qubits

$$\rho_C^0 = \frac{e^{-\beta_h E_h \sigma_h^\dagger \sigma_h}}{Z_h} \otimes \frac{e^{-\beta_c E_c \sigma_c^\dagger \sigma_c}}{Z_c} \otimes |0\rangle\langle 0|_w, \quad (\text{II.2})$$

where  $Z_{h,c}$  are the partition function necessary for proper normalization of the hot and cold qubit states,  $\sigma_{h,c} = |0\rangle\langle 1|_{h,c} + |1\rangle\langle 0|_{h,c}$ , and  $\beta_{h,c} = 1/k_B T_{h,c}$ . That is, one treats the ticking clock as an approximate reset clock. In the weak-coupling limit, the two engine qubits are only weakly perturbed by their coupling to the ladder and this assumption is valid. This clock can be represented using Proposition 1 by choosing [16]

$$L_1 = \sqrt{\gamma_h} \sigma_h, \quad L_2 = \sqrt{\gamma_h e^{-\beta_h E_h}} \sigma_h^\dagger, \quad (\text{II.3})$$

$$L_3 = \sqrt{\gamma_c} \sigma_c, \quad L_4 = \sqrt{\gamma_c e^{-\beta_c E_c}} \sigma_c^\dagger, \quad (\text{II.4})$$

$$J_1 = \sqrt{\Gamma_{\text{em}}} |0\rangle\langle d-1|_w, \quad J_2 = J_3 = J_4 = 0, \quad (\text{II.5})$$

where  $N_L = 4$ ,  $\gamma_{h,c}$  are the dissipative rates of the qubits, and  $\Gamma_{\text{em}}$  is the spontaneous emission rate. The total Hamiltonian  $H = H_0 + H_{\text{int}}$  is comprised of a free Hamiltonian  $H_0$  and an

interaction Hamiltonian  $H_{\text{int}}$  which are given by

$$H_0 = \sum_{j \in \{h,c\}} E_j |0\rangle\langle 0|_j + \sum_{n=0}^{d-1} n E_w |n\rangle\langle n|_w, \quad (\text{II.6})$$

and

$$H_{\text{int}} = g \sum_{n=0}^{d-1} (|0\rangle_h |1\rangle_c |k+1\rangle_w \langle 0|_c \langle 1|_h \langle k|_w + \text{h.c.}), \quad (\text{II.7})$$

respectively. Here,  $g$  is the interaction strength with  $g \ll E_c, E_h, E_w$  in the weak-coupling limit.

Because the environment is comprised of two thermal reservoirs and the clock approximately resets after each tick, the ticking clock can be seen as a thermodynamic machine that operates in a cyclic fashion, where each cycle is terminated by a tick and all cycles are approximately identical. The entropy production of the  $k$ th tick of the ticking clock  $\Sigma_k$  can thus be assessed by a thermodynamic analysis of a single operation cycle of the machine, that is  $\Sigma_k \approx \Sigma_1 \forall k \in \mathbb{N}_{>0}$ . In each cycle of this thermal machine, a photon with energy

$$E_\gamma = (d-1)E_w = (d-1)E_h - (d-1)E_c \quad (\text{II.8})$$

is emitted, where an amount of heat  $Q_h = (d-1)E_h$  is supplied to the machine by the hot bath and an amount of heat  $Q_c = (d-1)E_c$  is dissipated into the cold bath. The heat  $Q_c$  can be identified as the minimum energy expenditure per tick of the clock, because a large part of the photon energy  $E_\gamma$  can be recycled, e.g., by dumping it back into the hot bath. It is precisely this heat dissipation in each tick of the clock with which one associates an entropy production.

In particular, in each cycle the thermodynamic entropy of the hot bath decreases by  $\Delta S_h = -\beta_h Q_h$  while the thermodynamic entropy of the cold bath increases by  $\Delta S_c = \beta_c Q_c$  as a result of the heat flow from the hot bath to the cold bath. Thus, the change in thermodynamic entropy of the total system comprised of the clockwork and thermal baths is

$$\Sigma_1^{\text{th}} = \Delta S_h + \Delta S_c = \beta_c Q_c - \beta_h Q_h = (\beta_c - \beta_h)Q_c - \beta_h E_\gamma \geq 0, \quad (\text{II.9})$$

which can be identified as the entropy production per tick of this ticking clock [18]. Assuming that the full amount of energy  $E_\gamma$  is dumped back into the hot reservoir, the entropy production per tick is instead by

$$\Sigma_1^{\text{th}'} = (\beta_c - \beta_h)Q_c \propto Q_c. \quad (\text{II.10})$$

Based on Eq. (II.9) and (II.10), we see that the heat dissipated per tick  $Q_c$  is closely related

to entropy production per tick. In particular, it shows that a large amount of dissipated heat  $Q_c$  results in a large entropy production. Such an analysis is valid if the assumption that the clock resets to its initial state after each tick hold.

Note that there will inevitably be additional energy costs in operating such a thermodynamic clock which are not assessed here. For example, the preparation (and the inevitable reset) of the initial state of the register represents an additional contribution to the entropy production and energy dissipation. This can be seen as a consequence of Landauer's erasure principle [38, 47]. Landauer's erasure principle states that a reduction of entropy in the degrees of freedom that encode information must be compensated by a corresponding increase in entropy of the remaining degrees of freedom. Furthermore, any measurement process, here given by the photon detection, comes at its own thermodynamic cost [48]. Additionally, one may associate an entropy production with the irreversibility of spontaneous photon emission. Perfect irreversibility corresponds to a vanishing rate of photon absorption  $\Gamma_{\text{abs}} \rightarrow 0$ . The rates of spontaneous photon emission and absorption satisfy a detailed balanced condition  $\Gamma_{\text{em}}/\Gamma_{\text{abs}} = e^{\beta_c E_\gamma}$ . Assuming a finite energy spacing of the ladder  $E_w$  (where  $E_\gamma = (d-1)E_w$ ) the limit  $\Gamma_{\text{em}}/\Gamma_{\text{abs}} \rightarrow \infty$  can then be achieved by requiring a vanishing background temperature  $T_c \rightarrow 0$ . The entropy production associated with the photon emission and absorption events can then be expressed as  $\ln(\Gamma_{\text{em}}/\Gamma_{\text{abs}}) = \beta_c E_\gamma = \beta_c(Q_h - Q_c)$  and thus needs to diverge for perfect irreversibility. This additional diverging contribution to the entropy production is not taken into account for the entropy production per tick  $\Sigma_1^{\text{th}}$  ( $\Sigma_1^{\text{th}'}$ ) of the thermodynamic ticking clock. In the present case, one analyses a particular source of entropy production of the clock and energy cost – the dissipated heat – which is associated with the dynamics of the clockwork. Given that there are other sources of entropy production and energy cost, the presented quantities should be understood as lower bounds.

Investigating different types of such thermodynamic clocks numerically, one finds a fundamental trade-off between the accuracy  $R_1$  of the ticking clock ( $R_k \approx kR_1$ ) and the dissipated heat  $Q_c$  per tick, or equivalently, the entropy production per tick  $\Sigma_1^{\text{th}}$  (Eq. (II.9)). This trade-off is depicted in Fig. II.2. A clock that achieves a particular accuracy must produce a minimal amount of entropy per tick  $\Sigma_{1,\min}^{\text{th}}$ . This minimal amount seems to increase with increasing accuracy of the clock. In that sense, the entropy production per tick acts as a resource for measuring time.

In the weak-coupling limit, where the interaction between the ladder and the engine qubits is weak and the coherence of the ladder is negligible, the dynamics of the ladder can be approximated well by a (classical) biased random walk. We make the simplifying assumption that the clock ticks immediately once the population reaches the top of the ladder and that  $d$  is

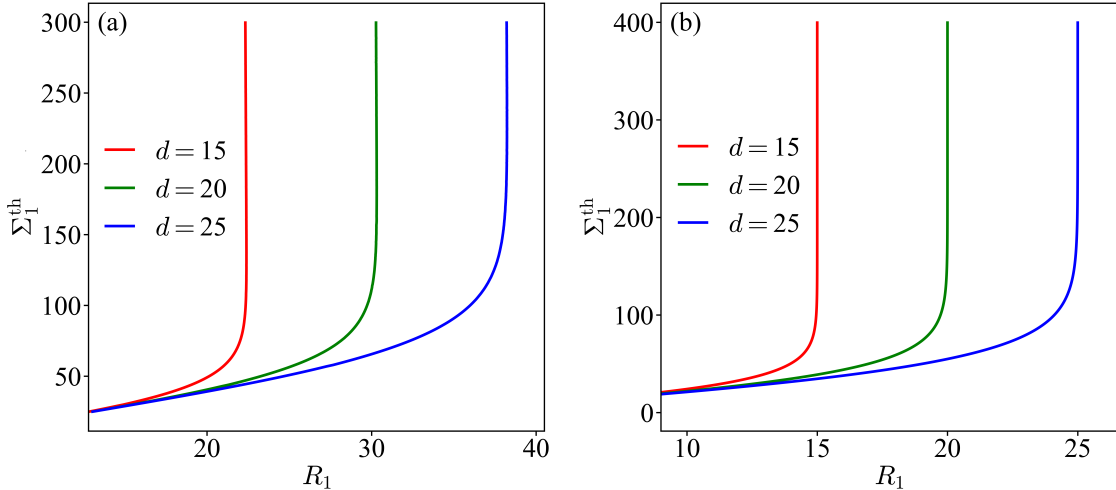


Figure II.2: Illustration of the trade-off between the entropy production per tick  $\Sigma_k^{\text{th}}$  ( $\Sigma_k^{\text{th}} \approx \Sigma_1^{\text{th}} \forall k \in \mathbb{N}_{>0}$ ), see Eq. (II.9), and accuracy  $R_1$  of thermodynamic ticking clocks ( $R_k \approx kR_1 \forall k \in \mathbb{N}_{>0}$ ). For a fixed dimension  $d$  of the clockwork's ladder, the entropy production increases with increasing accuracy and diverges as a limiting accuracy is approached. While a higher-dimensional ladder allows for the same accuracy to be achieved at a lower entropy production, there seems to exist a minimal entropy production per tick  $\Sigma_{1,\min}^{\text{th}}$  at a given accuracy irrespective of the ladder dimension  $d$ . The results in panel (a) are obtained by numerical simulations of various thermodynamic ticking clocks, where the parameters are chosen in accordance with Ref. [18]. That is, at a fixed dimension of the ladder  $d$  we vary the energy spacing of the cold qubit  $E_c$ . The other parameters are held fixed and are given by  $k_B T_c = E_w$ ,  $k_B T_h = 1000E_w$  and  $g = \hbar\gamma = \hbar\Gamma_{\text{em}} = 0.05E_w$ , with  $E_w = \hbar w$  and  $w = 1/0.05$  rad/s. Note that this choice ensures  $k_B T_c = E_w < E_\gamma = (d-1)E_w$ , such that the re-absorption of a photon occurs at a vanishing probability. The results in panel (b) are obtained using the approximation given in Eq. (II.13) which holds in the weak-coupling limit. The remaining parameters are chosen as for panel (a). Compared to the “quantum” ticking clocks depicted in panel (a), the ticking clocks governed by classical dynamics in panel (b) achieve a lower maximal accuracy with the same ladder dimension (and comparable entropy production).

large, such that the dynamics of the ladder can be well described without taking into account its behavior at the ladder boundaries. The rates at which the population of the ladder moves up  $p_{\uparrow}$  or down  $p_{\downarrow}$  then satisfy a detailed balance condition [18]

$$p_{\uparrow}/p_{\downarrow} = e^{-\beta_v E_w}, \quad (\text{II.11})$$

where

$$\beta_v = \frac{\beta_h E_h - \beta_c E_c}{E_h - E_c} = \frac{-\Sigma_1^{\text{th}}}{Q_h - Q_c}. \quad (\text{II.12})$$

In this case, the accuracy of the thermodynamic clock is given by

$$R_1(d) = dtanh\left(\frac{\Sigma_1^{\text{th}}}{2d}\right) \quad (\text{II.13})$$

In the limit of a large ladder dimension  $d$  the accuracy is directly proportional to the entropy production per tick

$$\lim_{d \rightarrow \infty} R_1(d) = \frac{\Sigma_1^{\text{th}}}{2}. \quad (\text{II.14})$$

Equations (II.13) and (II.14) establish a direct relationship between the accuracy of ticking clocks and its entropy production. Once more, one finds a minimal amount of irreversible entropy per tick which is necessary to achieve a particular accuracy (see Fig. II.2(b)). This minimal amount increases with increasing accuracy of the clock and can be achieved in the limit  $d \rightarrow \infty$ . Thus, it is given by  $\Sigma_{1,\min}^{\text{th}}(R_1) = 2R_1$ , see Eq. (II.14). Note that the exact same relations (Eq. (II.13) and (II.14)) have been found previously for other ticking clock models based on classical biased random walks in which the transition rates are governed by a detailed balance condition (Eq. (II.11)) using TURs [10].

These results show that the entropy production per tick (or equivalently the dissipated heat per tick) of thermodynamic ticking clocks serves as a fundamental resource for measuring time. To achieve a certain accuracy, these clocks necessarily need to produce a minimal amount of entropy production per tick (see Fig. II.2). Given that the accuracy serves as a measure of the strength of the arrow of time provided by the ticking clock, this establishes a connection between the arrow of time and the irreversibility of a ticking clock – the latter being quantified by the irreversible entropy production per tick. In the same turn, these results link the second law of thermodynamics and the arrow of time. Similarly, there seems to be a minimal energy cost (in the form of dissipated heat) which increases with increasing accuracy of such clocks. There remains the question of whether this connection between the accuracy of a clock and its entropy production is specific to the particular class of ticking clocks under consideration or a general property of ticking clocks – and thus a fundamental aspect of measuring time.

To this end, one can think of splitting the inner workings of a ticking clock into two fundamental processes: [11]

- a process that pushes the clockwork (or a subsystem thereof) out of equilibrium,
- a stochastic, effectively irreversible process given by an out-of-equilibrium system evolving towards equilibrium that results in a tick.

In the case of the thermodynamic ticking clocks, the ladder is pushed out-of-equilibrium with respect to the background photon field through its interaction with the engine qubits. Even-

ually, this results in the effectively irreversible emission of a photon and the registration of a tick. If the probability of photon emission is temporally concentrated, this constitutes a highly accurate clock. Here, the tick-generating process is effectively irreversible which avoids the clock from ticking backward and singles out a particular direction of time. In fact, for any ticking clock described by the ticking clock model in Chapter I this irreversible aspect is inherently built into the coupling of its clockwork and register because the model does not describe clocks that can tick backward. Note that other works consider ticking clocks that are allowed to tick backwards [10], but nevertheless come to similar conclusions on the relationship between their accuracy and entropy production.

From a thermodynamic point of view, biasing a process in favor of its time reverse requires the free energy of the system to decrease during the process [11, 18]. This fundamentally connects clocks to the second law of thermodynamics and irreversible entropy production. In the case of thermodynamic ticking clocks, the necessary driving force is provided by the heat flow between two thermal heat baths of different temperatures. In this case, the efficiency for converting heat to work is ultimately limited by the Carnot efficiency [46]  $\eta_C = 1 - T_c/T_h$  achieved by a heat engine operating reversibly, and therefore infinitely slow. Even in the limit  $T_c/T_h \rightarrow 0$  such that  $\eta_C \rightarrow 1$ , this would result in a clock that ticks infinitely slow. Hence, every thermodynamic ticking clock that ticks in a finite amount of time inevitably requires a minimal amount of heat  $Q_c = (1 - \eta_C)Q_h$  to be dissipated and a minimal amount of irreversible entropy to be produced as a consequence [18]. Note that this type of argument applies to any clock driven by idealized thermal baths. In general, however, a ticking clock may be driven by non-equilibrium resources. An autonomous ticking clock operating at a finite speed that does not produce any entropy per tick would constitute an autonomous machine that operates at a finite speed with unit efficiency. Under the assumption that no quantum machines can operate at a finite speed and achieve unit efficiency, one expects that any autonomous ticking clock must inevitably produce some amount of entropy per tick and dissipate some amount of energy. We will re-examine this assumption later in this work.

This conjecture is supported by several recent works [11, 19, 20] which study various types of ticking clocks and all find a fundamental connection between the accuracy of these clocks and their irreversible entropy production or energy dissipation. While the precise relationship between the accuracy and these quantities varies, all works find that a larger accuracy necessitates a larger entropy production and energy dissipation. In particular, in Ref. [19] this relation is confirmed when investigating a nano-electromechanical clock both experimentally and theoretically. In Ref. [20], the relationship is confirmed for escapement pendulum clocks, quartz oscillator clocks, clocks based on lasers, nano-mechanical clocks driven by an electron tunneling current, radiocarbon ( $C^{14}$ ) clocks, and various thermal clocks in a theoretical study.

And Ref. [11] finds similar results for a general class of clocks driven by heat engines which extend the thermodynamic ticking clock model of Ref. [18]. These results further enforce the idea that entropy production and energy dissipation constitute necessary resources for the process of timekeeping. The key challenge which remains is thus to investigate the precise connection between accuracy and entropy production per tick for arbitrary ticking clocks within the general framework provided in Chapter I.

## II.2 Entropy production in open quantum systems

As pointed out earlier, there does not currently exist a unifying theory of entropy production that is valid for general quantum (and classical) processes [39, 43, 45]. The most central property of any measure for entropy production common to all approaches is that it should characterize and quantify the degree of irreversibility of processes. There have been various different approaches to devising such a quantity in the context of stochastic thermodynamics, open quantum systems, or quantum information theory. In this section we briefly review the progress in the field, focusing on results from open quantum systems and quantum information theory. A more extensive review can be found in Ref. [45]. Crucially, the absence of a unified framework underlying the concept of entropy production requires us to propose a measure of the entropy production per tick of a ticking clock from first principles. Nevertheless, existing approaches to identify sources of entropy production can serve as a motivation for our measure of the entropy production per tick of ticking clocks.

### II.2.1 Entropy production as correlation between system and environment

We start by analyzing a situation in which a quantum system S interacts with its environment E via a global unitary  $U$ . We assume that the system and environment are initially uncorrelated  $\rho_{SE} = \rho_S \otimes \rho_E$  with arbitrary reduced states of system and environment  $\rho_S$  and  $\rho_E$ , respectively. The joint state of system and environment after the interaction is given by

$$\rho'_{SE} = U\rho_S \otimes \rho_E U^\dagger. \quad (\text{II.15})$$

The reduced states of system and environment after the interaction can be obtained via a partial trace as  $\rho'_S = \text{tr}_E [\rho'_{SE}]$  and  $\rho'_E = \text{tr}_S [\rho'_{SE}]$ , respectively. In particular, such a setup has been considered in Refs. [39, 47]. We can evaluate the von Neumann entropy of the initial and final states as

$$S(\rho_{SE}) = S(\rho_S) + S(\rho_E), \quad (\text{II.16})$$

$$S(\rho'_{SE}) = S(\rho'_S) + S(\rho'_E) - I(\rho'_{SE}), \quad (\text{II.17})$$

where  $I$  denotes the quantum mutual information (see Appendix A for more details on the quantum mutual information). In the following, we will simply refer to the von Neumann entropy as entropy if not stated otherwise. Noting that the entropy is conserved under unitary evolution

$$S(\rho_{\text{SE}}) = S(\rho'_{\text{SE}}), \quad (\text{II.18})$$

we have

$$S(\rho'_S) - S(\rho_S) + S(\rho'_E) - S(\rho_E) = I(\rho'_{\text{SE}}) \geq 0 \quad (\text{II.19})$$

$$\Delta S_S + \Delta S_E = I(\rho'_{\text{SE}}) \geq 0, \quad (\text{II.20})$$

where  $\Delta S_S = S(\rho'_S) - S(\rho_S)$  and  $\Delta S_E = S(\rho'_E) - S(\rho_E)$  denote the change in entropy of the system and environment, respectively. Equality is achieved if and only if the final state is a product state with  $\rho'_{\text{SE}} = \rho'_S \otimes \rho'_E$ , because

$$S(\rho'_{\text{SE}}) = S(\rho'_S) + S(\rho'_E) \quad (\text{II.21})$$

if and only if  $\rho'_{\text{SE}}$  is a product state.

If we consider a unitary of the form  $U = U_S \otimes U_E$ , we have

$$\rho'_{\text{SE}} = U_S \rho_S U_S^\dagger \otimes U_E \rho_E U_E^\dagger = \rho'_S \otimes \rho'_E. \quad (\text{II.22})$$

Thus, a system S which undergoes a unitary (and thereby reversible) evolution on its own and does not interact with the environment E cannot establish any correlations with the latter. Moreover, intuitively the amount of correlation (or equivalently the strength of the entanglement) that build up between system and environment is indicative of the strength of their interaction. As pointed out previously, it is precisely the interaction with an environment present in an open quantum system that makes its dynamics generally irreversible. While the joint evolution of system and environment is unitary, and thereby reversible, the irreversibility of the system's evolution governed by the CPTP map  $\mathcal{E}$  as  $\rho'_S = \mathcal{E}(\rho_S) = \text{tr}_E[\rho'_{\text{SE}}]$  can be seen as a consequence of tracing over the degrees of freedom of the environment. In particular, tracing over, i.e., discarding the environment, embodies the assumption that after the interaction one no longer has access to its degrees of freedom. Therefore, irreversibility emerges as a consequence of discarding any information about E from the perspective of the system S in the form of correlations. This is illustrated in Fig. II.3.

In fact, this aspect can be viewed as a general ansatz for identifying the origins of irreversibility in system-environment interactions, and thus for devising a measure for the irreversible entropy production. Here, Eq. (II.20) can be seen as a manifestation of the second

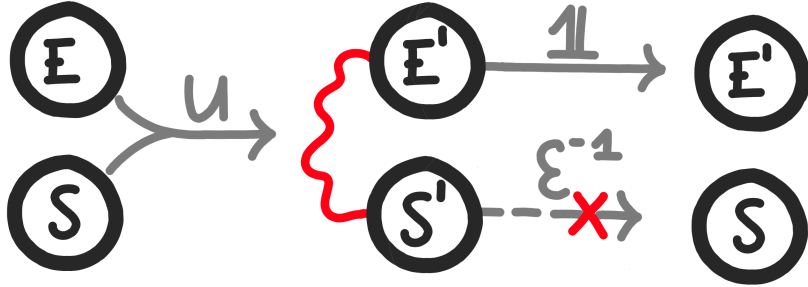


Figure II.3: Illustration of the setup in which the correlations between system and environment can be pinpointed as the origin for irreversible entropy production: a system ( $S$ ) and environment ( $E$ ) which are initially uncorrelated undergo a joint evolution governed by the unitary  $U$ . The resulting states of the system and environment,  $S'$  and  $E'$ , respectively, will become entangled (and thus correlated) through their interaction (red connection). In general, one cannot completely restore the initial state  $S$  of the system (and its potential correlations with other systems) via the application of a quantum channel  $\mathcal{E}^{-1}$  on the system alone. That is, one cannot revert the evolution of the system alone without accessing the state of the environment due to the built-up correlations. The dynamics can, in general, (only) be reversed completely by application of the inverse unitary  $U^{-1}$  to the joint state of system  $S'$  and environment  $E'$ .

law of thermodynamics in the present setting with  $\Sigma = I(\rho'_{SE})$  taking the role of an irreversible entropy production. Starting with full knowledge of all degrees of freedom involved, irreversibility emerges when we deem certain information irretrievable or inaccessible. Equivalently, we can view this as a transition from an observer who has complete knowledge of all involved systems as permitted by quantum theory to an observer who only has complete knowledge of the system but not of its environment.

The assumption of an observer who has only limited knowledge about the state of the system and environment in the form of a small set of well-defined macroscopic properties is central to thermodynamics [49–52]. In particular, the first law itself is a reflection of this, as it states that in a thermodynamic process not all forms of energy changes are equal. It makes a distinction between work as the type of energy that is “useful” in an operational sense, and heat, which is any form of energy change that is not work – and thus not useful [53–55]. This distinction arises from the fact that the observer core to thermodynamics only has limited knowledge, and thus control, of the microscopic degrees of freedom underlying energy in the form of heat. This is in contrast to the macroscopic degrees of freedom underlying energy in the form of work. Moreover, it is standard in thermodynamics to assume that the correlations between system and environment vanish initially [47], which reflects the fact that the observer does not have knowledge or control over them. In fact, by leveraging the (classical or quantum)

correlations between system and environment the laws of thermodynamics can be violated, for example in the form of heat flowing spontaneously from a cold to a hot bath [45, 50, 53, 56, 57]. Thus, by transitioning to the viewpoint of a more oblivious observer we move closer to the framework of thermodynamics in which the concept of irreversibility emerges as the second law. Note, however, that the procedure outlined above is not restricted to a situation where the environment is made of ideal thermal reservoirs. In the context of information theory, the correlations quantified by the quantum mutual information  $I(\rho'_{SE})$  can be interpreted as the shared information between system and environment, or equivalently, the information about the system which leaks to the environment as a consequence of their interaction (and vice-versa) [25, 40]. Therefore, this procedure also establishes a direct link between irreversibility, as measured by the irreversible entropy production, and the information which is exchanged between system and environment in the process.

Let us assume that the environment is initially in a thermal state  $\rho_E = e^{-\beta H} / \text{tr}[e^{-\beta H}]$ , where  $H$  is the corresponding Hamiltonian and  $\beta = 1/k_B T$  the inverse temperature. Then, one can show that

$$\Delta S_S + \beta (\text{tr}[H\rho'_E] - \text{tr}[H\rho_E]) = I(\rho'_{SE}) + S(\rho'_E \| \rho_E) \geq 0, \quad (\text{II.23})$$

where one can identify the change in energy of the reservoir as the amount of exchanged heat  $Q_E = (\text{tr}[H\rho'_E] - \text{tr}[H\rho_E])$  during the process. Here,  $S(\rho \| \sigma)$  denotes the quantum relative entropy (see Appendix A for further details on the quantum relative entropy). Then

$$\Delta S_S + \beta Q_E = I(\rho'_{SE}) + S(\rho'_E \| \rho_E) \geq 0, \quad (\text{II.24})$$

or equivalently

$$\beta Q_E = I(\rho'_{SE}) + S(\rho'_E \| \rho_E) - \Delta S_S \geq -\Delta S_S. \quad (\text{II.25})$$

The corresponding proof can be found in Appendix B.2. Consequently, one can identify the following expression for the entropy production  $\Sigma$  in such a scenario

$$\Sigma = I(\rho'_{SE}) + S(\rho'_E \| \rho_E) = \Delta S_S + \beta Q_E \geq 0. \quad (\text{II.26})$$

Here,  $I(\rho'_{SE})$  quantifies the shared information (in the form of correlations) between system S and environment E which is discarded when losing access to the environment, whereas  $S(\rho'_E \| \rho_E)$  quantifies how far the environment E evolved from its initial state. While the first contribution to the entropy production is bounded as [58]

$$I(\rho'_{SE}) \leq 2\min\{S(\rho'_S), S(\rho'_E)\}, \quad (\text{II.27})$$

the second term given by the quantum relative entropy is unbounded.

If the initial state of the environment is instead given by multiple uncorrelated thermal baths  $\rho_E = \rho_{E_1} \otimes \rho_{E_2} \otimes \rho_{E_3} \otimes \dots$  at different temperatures  $T_i$ , the expression for the entropy production in Eq. (II.26) can be rewritten as [39, 45]

$$\Sigma = \Delta S_S + \sum_i \beta_i Q_{E_i}, \quad (\text{II.28})$$

where the sum runs over all thermal baths  $\{E_i\}$ . In that case, the second term attributed to the change in entropy of the thermal reservoirs  $\sum_i \beta_i Q_{E_i}$  is also partially based on the contributions of intra-environmental correlations which build up between the different thermal reservoirs as a consequence of their common interaction with the system [45]. Equation (II.20) defines a purely information-theoretic quantity that makes no reference to thermodynamic concepts, such as work or heat. Nevertheless, in a thermodynamic setting, it gives rise to Eq. (II.26) which embodies the fact that one has no access to the state of the reservoir and only possesses knowledge of the energy that has flown into it as heat. Moreover, the standard form of the second law of thermodynamics emerges naturally, see Eq. (II.28).

Consider the special case where the unitary map has a global fixed point  $\rho_S^*$  satisfying

$$U(\rho_S^* \otimes \rho_E) U^\dagger = \rho_S^* \otimes \rho_E. \quad (\text{II.29})$$

Then, Eq. (II.26) can be rewritten as (see Appendix B.2 for a proof)

$$\Sigma = S(\rho_S \| \rho_S^*) - S(\rho'_S \| \rho_S^*). \quad (\text{II.30})$$

Equation (II.30) has been proposed as a measure for the entropy production of quantum systems undergoing evolution according to a quantum Markovian master equation [26, 59]. Note that in this special case the entropy production can be expressed solely based on the properties of the system alone, irrespective of its environment. Importantly, this measure is applicable when dealing with a large class of problems involving so-called thermal operations [60–62]. These are operations involving a thermal environment for which the map describing the joint unitary evolution between the system and environment has a thermal state of the system as a global fixed point.

The expression for the entropy production in Eq. (II.26) differs from Eq. (II.20) by the addition of the term  $S(\rho'_E \| \rho_E) \geq 0$ . Thus, Eq. (II.20) represents a lower bound to the measure of entropy production given in Eq. (II.26). The additional contribution  $S(\rho'_E \| \rho_E)$  is motivated by the fact that it allows for the identification of heat flow when considering thermal environments.

Different expressions for  $\Sigma$  may be applicable depending on the assumptions one makes about the aspects of the system-environment dynamics that become inaccessible or irretrievable. For example, the expression in Eq. (II.20) corresponds to the assumption that one loses complete access to the correlations between system and environment, whereas Eq. (II.26) embodies the assumption that one additionally loses the ability to perform operations on the environment itself. Consequently, even in the case of a thermal environment Eq. (II.20) has been considered as the relevant expression for the entropy production in some works [53]. This can be justified as follows: consider the case of an environment which is initially prepared in a thermal state and a joint unitary of the form  $U_{SE} = \mathbb{1}_S \otimes U_E$ . Then,  $\rho'_E = U_E \rho_E U_E^\dagger$  and  $\rho'_S = \rho_S$ . Even though the state of the system remains unchanged, and thus  $S(\rho'_S) - S(\rho_S) = 0$ , according to Eq. (II.26) there is, in general, a non-zero amount of heat  $Q_E = \text{tr} [H (\rho'_E - \rho_E)]$  dissipated. This results in an entropy production of  $\Sigma = \beta Q_E$  associated with this process. Meaning, this definition assigns to heat increases of the internal energy of the environment which – depending on the observer – cannot be considered to be irreversibly lost, but instead can be recovered.

Alternative, one can identify the relevant expression for the heat in this context as the difference in entropy of the environment  $\beta Q = S(\rho'_E) - S(\rho_E)$ . This is in the spirit of heat being a flow of energy between environment and system, in some way different from work. Where work is the flow of energy that is still accessible and could therefore be re-extracted. In the context of entropy production, this re-definition of heat corresponds to dropping the second contribution given by the quantum relative entropy in Eq. (II.26) or equivalently adopting the expression in Eq. (II.20). Finally, note that one may attempt a comparison of the relative importance of the two terms in Eq. (II.26) to justify this choice [39, 45, 53]. In the thermodynamic limit where a thermal reservoir is assumed to remain at equilibrium  $\rho'_E = \rho_E$ , the contribution  $S(\rho'_E \parallel \rho_E)$  vanishes and the two definitions of heat coincide [39, 45, 53, 63, 64]. This captures the fact that an ideal thermal reservoir only exchanges entropy with the system but does not irreversibly produce it. While it was often assumed that the second contribution given by the quantum relative entropy is also negligible for reasonably large thermal reservoirs [39, 45, 53], a recent study [63] shows that this is not always the case.

To conclude, we may directly apply this approach to the thermodynamic ticking clock discussed in Section II.1 under the assumption that there exists a joint unitary evolution of clockwork and the environment composed of the two thermal baths  $E_h$  and  $E_c$ . The initial joint state of clockwork and environment is given by

$$\rho_{\text{tot}} = \rho_C^0 \otimes \rho_{E_h} \otimes \rho_{E_c}, \quad (\text{II.31})$$

where  $\rho_{E_h, c}$  is the thermal state of the hot and cold thermal bath, respectively. An instance

after each tick, the joint state of the clock and environment is given as

$$\rho'_{\text{tot}} = \rho_C^0 \otimes \rho'_{E_h E_c}, \quad (\text{II.32})$$

where we used the fact that the thermodynamic ticking clock is – to a good approximation – a reset clock. We connect the two state  $\rho_{\text{tot}}$  and  $\rho'_{\text{tot}}$  via a joint unitary evolution. This allows us to apply Eq. (II.28) with  $\Delta S_S = 0$ . Adopting the appropriate sign convention for the exchanged heat of the two reservoirs, we obtain

$$\Sigma = \beta_c Q_c - \beta_h Q_h. \quad (\text{II.33})$$

Because we assume idealized thermal baths in the thermodynamic limit, the two notions of heat discussed above coincide and we recover the original expression for the entropy production per tick of the thermodynamic ticking clock.

### II.2.1.a Connection to Landauer's erasure principle

In 1867 James Clerk Maxwell proposed a thought experiment that suggested a potential violation of the second law of thermodynamics: the lowering of the entropy of a gas of particles without exerting any work on it. This violation was thought to be accomplished by Maxwell's demon – an entity that has knowledge of all the position and momenta of the gas particles [65]. The paradox was later resolved by the findings of Rolf Landauer who suggested that the erasure of information (which is necessarily logically irreversible) from any information-bearing degrees of freedom must necessarily be accompanied by an increase in entropy in the non-information-bearing degrees of freedom [38, 66, 67]. This establishes a deep connection between information theory and thermodynamics. For a thermal environment at temperature  $T$  this is equivalent to the statement that an amount

$$\beta Q_E \geq -\Delta S_S \quad (\text{II.34})$$

of heat needs to be dissipated given a decrease in entropy of the system by  $\Delta S_S$ . This is known as Landauer's principle and the inequality in Eq. (II.34) is typically referred to as the Landauer bound. Applied to Maxwell's demon, Eq. (II.34) implies that the heat dissipated during the inevitable reset of the demon's memory restores the second law of thermodynamics.

For a long time, there has been no rigorous treatment of Landauer's principle and assessment of the assumptions under which the principle is valid. This has been achieved in recent works [39, 47]. In fact, the minimal setting in which Landauer's bound holds coincides with the setting considered in this section: a quantum system  $S$  which interacts with an environment  $E$  via a global unitary  $U$ , where the system and environment are initially uncorrelated

$\rho_{SE} = \rho_S \otimes \rho_E$ . If one wants to formulate Landauer’s principle in terms of heat exchange, rather than entropy exchange, one needs the additional assumption of an environment that is initially in a thermal state. This setting is minimal in the sense that, if one drops any of these assumptions the Landauer bound can be violated [47]. Recalling the results from the previous section, we found

$$\Delta S_E = I(\rho'_{SE}) - \Delta S_S \geq -\Delta S_S, \quad (\text{II.35})$$

and

$$\beta Q_E = I(\rho'_{SE}) + S(\rho'_E \| \rho_E) - \Delta S_S \geq -\Delta S_S, \quad (\text{II.36})$$

where for Eq. (II.36) we additionally assume that the environment is initialized in a thermal state. In fact, Eq. (II.35) and (II.36) correspond to improved Landauer bounds (see Eq. (II.34)) given that they are formulated as equality constraints.

### II.3 Observer-dependent clockwork states

The notion of entropy, whether information-theoretic or thermodynamically, is relative to an observer’s knowledge [49–52, 68]. Unlike many other physical quantities, such as the energy of a system, it is crucially dependent on the choice of observer [51]. This “anthropomorphic” nature of entropy in contrast to the “physical” nature of quantities like energy has been well understood for decades [51]. Clearly, an observer which has complete knowledge of the position and velocity of each particle in a gas, such as Maxwell’s demon [65–67] after performing a measurement on every gas particle, would ascribe the gas zero entropy [52]. For the macroscopic observer who does not possess any such microscopic knowledge about the gas, the entropy of the gas is the entropy of a thermal state (which may be arbitrarily large). This is, however, no contradiction, because both observers would agree on each other’s assessment of the entropy when being conditioned on each other’s knowledge [52].

The reason that entropy appears to be a property of the system alone in standard thermodynamics arises from the fact, that one is concerned with a common, implicit observer which has access to a small set of well-defined macroscopic properties of the system, but whose uncertainty about the state of the system is otherwise maximal [49–52]. In particular, if one does not condition the state of the system (and thereby its entropy) on the observer’s knowledge, apparent violations of the laws of thermodynamics can be observed. Different observers may, for example, disagree on the amount of extractable work of a thermodynamic system – and thus on its entropy – given that they have different levels of “subjective” knowledge of the underlying microstates. This is intuitive, as the amount of extractable work of a thermodynamic system indeed varies depending on the observer’s level of knowledge about the system. In fact, if the entropy of a macrostate did not depend on the observer’s knowledge of the under-

lying microstates, the quantity would fail at its core thermodynamic function of quantifying the amount of extractable work [51]. Thus, to identify the appropriate notion of the entropy produced per tick of a ticking clock we need to decide on an appropriate observer relative to which this entropy is assessed. Importantly, one needs to decide what level of knowledge this observer possesses about the state of the clock itself.

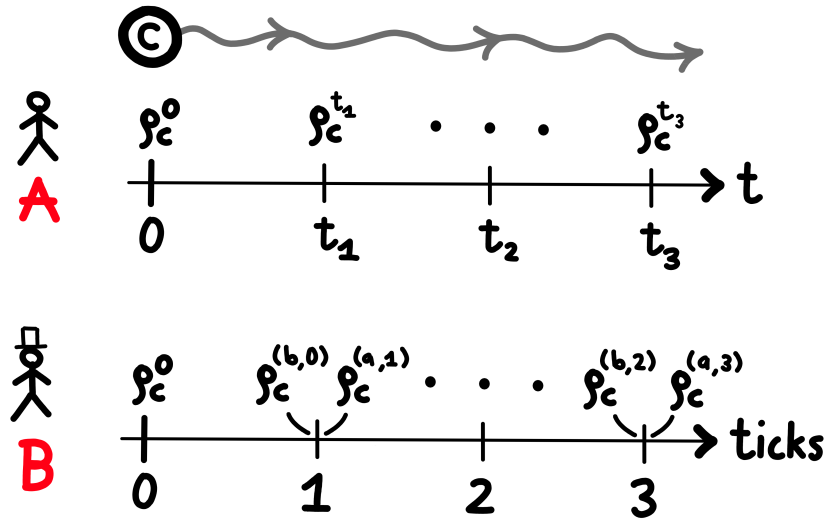


Figure II.4: Illustration of the different descriptions of a ticking clock based on two observers with different levels of knowledge. Observer A has knowledge of the coordinate time  $t$  and can thus ascribe the clockwork (C) of a ticking clock a state  $\rho_C^t$  at any point in time. In this work, we instead adopt the viewpoint of observer B which does not have any knowledge of the coordinate time but only has access to the register (R) of the ticking clock. That is, observer B only gains information about time in the form of the ticks of the ticking clock. While observer B cannot ascribe the clockwork a state at each point in time, his level of knowledge allows him to distinguish between the states of the clockwork before (b) and after (a) each tick event. Given the ticking clock just ticked for the  $k$ th time, observer B denotes the state of the clockwork an instance before and after the tick as  $\rho_C^{(b,k-1)}$  and  $\rho_C^{(a,k)}$ , respectively.

Ticking clocks are devices designed to measure time and provide temporal information to the observer in the form of ticks. Thus, the observer relative to which the entropy production per tick is assessed should only possess as much information about time as the ticking clock itself provides. Hence, we here consider an observer that has no knowledge of the background coordinate time  $t > 0$ , but has access to the state of the register of the clock, i.e., its ticks. Figure II.4 illustrate the states of the clockwork which an observer that only has access to the state of the register can effectively distinguish, in contrast to an observer that has complete knowledge of coordinate time. Crucially, the quantum state assigned to the clock should be conditioned on the observer's knowledge [49, 50]. This conditioning is performed by integrat-

ing out coordinate time, which renders the states of the clock relative to the observer time independent [49]. Based on these observer-dependent quantum states assigned to the clock, an appropriate measure for the entropy production per tick can then be derived. Note that any observer-dependent state of the clock will be of the form  $\rho_{\text{CR}} = \rho_{\text{C}}^{(k)} \otimes |k\rangle\langle k|_{\text{R}}$   $k \in \mathbb{N}$ , that is a product state of the clockwork and a fixed state of the register. This is because at any point in time the observer measures the register to be in a fixed state. In fact, the measurement of the register is what allows the observer to gain information about time and construct its observer-dependent states of the clock. Thus, the expression for the entropy production of the  $k$ th tick will, in general, be a function of the relevant observer-dependent clockwork states of the  $k$ th tick. Looking at Fig. II.4, for the  $k$ th tick we identify these states to be  $\rho_{\text{C}}^{(\text{a},k-1)}$ ,  $\rho_{\text{C}}^{(\text{b},k-1)}$ , and  $\rho_{\text{C}}^{(\text{a},k)}$ , because the clockwork (from an observers point of view) undergoes the following transition after the  $(k-1)$ th tick:

$$\rho_{\text{C}}^{(\text{a},k-1)} \rightarrow \rho_{\text{C}}^{(\text{b},k-1)} \rightarrow \rho_{\text{C}}^{(\text{a},k)}. \quad (\text{II.37})$$

It is precisely with this transition between different states of the clockwork – and the resulting tick in the register – that we associate an entropy production. In this section, we are concerned with finding an appropriate expression for these observer-dependent clockwork states.

For a ticking clock specified by  $(\rho_{\text{C}}^0 \otimes |0\rangle\langle 0|_{\text{R}}, (\mathcal{M}_{\text{CR} \rightarrow \text{CR}}^t)_{t \geq 0})$ , the unnormalized state of the clockwork at coordinate time  $t$  given that the register is still observed to be in state  $|0\rangle_{\text{R}}$  is

$$\tilde{\rho}_{\text{C}}^{(0)}(t) = \text{tr}_{\text{R}} \left[ \mathbb{1}_{\text{C}} \otimes |0\rangle\langle 0|_{\text{R}} \mathcal{M}_{\text{C} \rightarrow \text{CR}}^{t,0} (\rho_{\text{C}}^0) \right]. \quad (\text{II.38})$$

Given the probability density

$$P^{(0 \rightarrow 1)}(t) = \lim_{\delta t \rightarrow 0^+} \frac{\text{tr} \left( \mathbb{1}_{\text{C}} \otimes |1\rangle\langle 1|_{\text{R}} \left( \mathcal{M}_{\text{C} \rightarrow \text{CR}}^{\delta t,0} \left( \tilde{\rho}_{\text{C}}^{(0)}(t) \right) - \tilde{\rho}_{\text{C}}^{(0)}(t) \otimes |0\rangle\langle 0|_{\text{R}} \right) \right)}{\delta t}, \quad (\text{II.39})$$

the probability to observe the register in state  $|1\rangle_{\text{R}}$  at time  $t \geq 0$  (i.e., the probability that the clock has *not* yet ticked from  $|0\rangle_{\text{R}} \rightarrow |1\rangle_{\text{R}}$  in the interval  $[0, t)$ ) and observe a tick from  $|0\rangle_{\text{R}}$  to  $|1\rangle_{\text{R}}$  in the infinitesimal time interval  $[t, t + \delta t]$  is  $\delta t \cdot P^{(0 \rightarrow 1)}(t)$ , where  $\delta t > 0$ . Note that  $P^{(0 \rightarrow 1)}(t)$  corresponds to the delay function of the first tick of the clock  $\tau^{(1)}(t)$  (see Eq. (I.35)).

For an observer that does not have access to coordinate time  $t > 0$ , the state of the clockwork an instance before the first tick is then appropriately described as

$$\rho_{\text{C}}^{(\text{b},0)} = \int_0^\infty P^{(0 \rightarrow 1)}(t) \rho_{\text{C}}^{(0)}(t) dt. \quad (\text{II.40})$$

This state of the clockwork is time-independent and arises from a weighting of the state  $\rho_C^{(0)}(t)$  for all coordinate times  $t \in [0, \infty)$  by its probability of ticking in the next infinitesimal time step given by  $P^{(0 \rightarrow 1)}(t) dt$ . Similarly, the relevant state of the clockwork an instance after the first tick is observed can be calculated as

$$\rho_C^{(a,1)} = \int_0^\infty P^{(0 \rightarrow 1)}(t) \lim_{\delta t \rightarrow 0^+} \frac{\text{tr}_R \left[ \mathbb{1}_C \otimes |1\rangle\langle 1|_R \mathcal{M}_{C \rightarrow CR}^{\delta t,0} \left( \rho_C^{(0)}(t) \right) \right]}{\text{tr} \left[ \mathbb{1}_C \otimes |1\rangle\langle 1|_R \mathcal{M}_{C \rightarrow CR}^{\delta t,0} \left( \rho_C^{(0)}(t) \right) \right]} dt, \quad (\text{II.41})$$

where

$$\lim_{\delta t \rightarrow 0^+} \frac{\text{tr}_R \left[ \mathbb{1}_C \otimes |1\rangle\langle 1|_R \mathcal{M}_{C \rightarrow CR}^{\delta t,0} \left( \rho_C^{(0)}(t) \right) \right]}{\text{tr} \left[ \mathbb{1}_C \otimes |1\rangle\langle 1|_R \mathcal{M}_{C \rightarrow CR}^{\delta t,0} \left( \rho_C^{(0)}(t) \right) \right]} \quad (\text{II.42})$$

corresponds to the state of the clockwork an instance after the tick from  $|0\rangle_R$  to  $|1\rangle_R$  has been observed in the interval  $[t, t + \delta t]$ . Using the expression for  $\mathcal{M}_{C \rightarrow CR}^{\delta t,0}$  provided in Lemma 1, Eq. (II.42) can be written as

$$\frac{\sum_j J_j \rho_C^{(0)}(t) J_j^\dagger}{\text{tr} \left[ \sum_j J_j \rho_C^{(0)}(t) J_j^\dagger \right]} = \frac{1}{P^{(0 \rightarrow 1)}(t)} \sum_j J_j \tilde{\rho}_C^{(0)}(t) J_j^\dagger. \quad (\text{II.43})$$

And the state of the clockwork just after the first tick (Eq. (II.41)) can then be rewritten as

$$\rho_C^{(a,1)} = \int_0^\infty \sum_j J_j \tilde{\rho}_C^{(0)}(t) J_j^\dagger dt. \quad (\text{II.44})$$

The initial clockwork state at  $t = 0$  given by  $\rho_C^0$ , as well as  $\rho_C^{(b,0)}$  (Eq. (II.40)), and  $\rho_C^{(a,1)}$  (Eq. (II.41)) constitute the three relevant observer-dependent clockwork states for assessing the entropy production of the first tick of a ticking clock. Note that if the ticking clock is a reset clock (Def. 5), we have

$$\rho_C^{(a,1)} = \rho_C^0 \int_0^\infty P^{(0 \rightarrow 1)}(t) dt = \rho_C^0. \quad (\text{II.45})$$

Thus, we obtain the intuitive result that the observer-dependent clockwork state after the first tick of a reset clock corresponds to the initial state of the clockwork – its reset state.

For the subsequent ticks, there may *a priori* be different approaches to define the relevant observer-dependent clockwork states. Here, we discuss three different approaches explicitly. We show how to rule out two approaches by requiring the resulting observer-dependent clockwork states, and thus the measure for the entropy production per tick derived from these states, to possess certain desired properties.

**Approach 1:** In a first approach, the observer-dependent states of the clockwork are defined as follows. We calculate the unnormalized state of the clockwork given that the observer measures the register still to be in state  $|k-1\rangle_R$  a time interval  $t$  after the  $(k-1)$ th tick occurred as

$$\tilde{\rho}_C^{(k-1)}(t) = \text{tr}_R \left[ \mathbb{1}_C \otimes |k-1\rangle\langle k-1|_R \mathcal{M}_{C \rightarrow CR}^{t,k-1} \left( \rho_C^{(a,k-1)} \right) \right]. \quad (\text{II.46})$$

The state of the clockwork an instance before the  $k$ th tick occurs is then defined as

$$\rho_C^{(b,k-1)} = \int_0^\infty P^{(k-1 \rightarrow k)}(t) \rho_C^{(k-1)}(t) dt. \quad (\text{II.47})$$

Here,

$$P^{(k-1 \rightarrow k)}(t) = \lim_{\delta t \rightarrow 0^+} \frac{\text{tr} \left[ \mathbb{1}_C \otimes |k\rangle\langle k|_R \left( \mathcal{M}_{C \rightarrow CR}^{\delta t,k-1} \left( \tilde{\rho}_C^{(k-1)}(t) \right) - \tilde{\rho}_C^{(k-1)}(t) \otimes |k-1\rangle\langle k-1|_R \right) \right]}{\delta t}, \quad (\text{II.48})$$

which can be rewritten as

$$P^{(k-1 \rightarrow k)}(t) = \text{tr} \left[ \sum_j J_j \tilde{\rho}_C^{(k-1)}(t) J_j^\dagger \right]. \quad (\text{II.49})$$

Equation (II.49) corresponds to the probability density characterizing the  $k$ th ticking event. The probability of observing the register in state  $|k-1\rangle_R$  a time interval  $t$  after the  $(k-1)$ th tick (i.e., the probability that the clock has *not* yet ticked from  $|k-1\rangle_R \rightarrow |k\rangle_R$  in the interval  $t$ ) and observing a tick from  $|k-1\rangle_R$  to  $|k\rangle_R$  in the infinitesimal time interval  $[t, t + \delta t]$  is  $\delta t \cdot P^{(k-1 \rightarrow k)}(t)$ , where  $\delta t > 0$ . Similarly, the state of the clockwork an instance after the  $k$ th tick is

$$\rho_C^{(a,k)} = \int_0^\infty P^{(k-1 \rightarrow k)}(t) \frac{\sum_j J_j \tilde{\rho}_C^{(k-1)}(t) J_j^\dagger}{\text{tr} \left[ \sum_j J_j \tilde{\rho}_C^{(k-1)}(t) J_j^\dagger \right]} dt, \quad (\text{II.50})$$

or equivalently

$$\rho_C^{(a,k)} = \int_0^\infty \sum_j J_j \tilde{\rho}_C^{(k-1)}(t) J_j^\dagger dt. \quad (\text{II.51})$$

This first approach is based on taking  $\rho_C^{(a,k-1)}$  as a starting state of the clockwork to assess the relevant clockwork states of the  $k$ th tick. In particular, given that the clock is a reset clock we have seen that  $\rho_C^{(a,1)} = \rho_C^0$  (see Eq. (II.45)). Thus, by treating a reset clock using approach 1 we have

$$\rho_C^{(a,k)} = \rho_C^0, \quad \rho_C^{(b,k)} = \rho_C^{(b,0)} \quad \forall k \in \mathbb{N}, \quad (\text{II.52})$$

where  $\rho_C^{(a,0)} = \rho_C^0$  by definition. Recall that the entropy production of the  $k$ th tick will be a function of the three clockwork states  $\rho_C^{(a,k-1)}, \rho_C^{(b,k-1)}$ , and  $\rho_C^{(a,k)}$ . For a reset clock, the three clockwork states of the  $k$ th tick are identical to the states of the first tick. Thus, for reset clocks, the entropy production per tick will be independent of the particular tick under consideration. This is a desirable property because the ticking events of a reset clock are independent and identically distributed. Similar to the thermodynamic ticking clock discussed in Section II.1, one can think of reset clocks undergoing a cyclic process where the clockwork ends up in the initial state after the completion of each tick. As such, we ascribe this ticking process a particular entropy production per tick that is identical for all ticks.

**Approach 2:** In a second approach, one takes

$$\tilde{\rho}_C^{(k-1)}(t) = \text{tr}_R \left[ \mathbb{1}_C \otimes |k-1\rangle\langle k-1|_R \mathcal{M}_{C \rightarrow CR}^{t,0} (\rho_C^0) \right] \quad (\text{II.53})$$

as the state of the clockwork at coordinate time  $t$  (as measured from the initialization of the clock at  $t = 0$ ) before the  $k$ th tick occurred. Following similar steps as in the first approach, the observer-dependent clockwork states are then calculated as

$$\rho_C^{(b,k-1)} = \int_0^\infty P^{(k-1 \rightarrow k)}(t) \tilde{\rho}_C^{(k-1)}(t) dt, \quad (\text{II.54})$$

and

$$\rho_C^{(a,k)} = \int_0^\infty \sum_j J_j \tilde{\rho}_C^{(k-1)}(t) J_j^\dagger dt, \quad (\text{II.55})$$

where

$$P^{(k-1 \rightarrow k)}(t) = \lim_{\delta t \rightarrow 0^+} \frac{\text{tr} \left[ \mathbb{1}_C \otimes |k\rangle\langle k|_R \left( \mathcal{M}_{C \rightarrow CR}^{\delta t, k-1} \left( \tilde{\rho}_C^{(k-1)}(t) \right) - \tilde{\rho}_C^{(k-1)}(t) \otimes |k-1\rangle\langle k-1|_R \right) \right]}{\delta t}. \quad (\text{II.56})$$

One can show that this second approach yields the same expression for  $\rho_C^{(a,k)}$  as approach 1, whereas they generally differ in their expression for  $\rho_C^{(b,k-1)}$ . The key difference to approach 1 is, that in approach 2 we take the initial clockwork state  $\rho_C^0$  as a starting state for every tick, as opposed to the state just after the previous tick.

Earlier, we have motivated an important property of the entropy production per tick of a ticking clock: it should be independent of the tick under consideration when considering reset clocks. We can check whether the observer-dependent clockwork states calculated using approach 2 allow for an expression that satisfies this property. Similar to the first approach, we have  $\rho_C^{(a,k)} = \rho_C^0$  for a reset clock. However, in this second approach  $\rho_C^{(b,k-1)}$  (Eq. (II.54)) is, in general, still dependent on  $k$ . This can be seen from the fact that  $P^{(k-1 \rightarrow k)}(t)$  corresponds

the delay function corresponding to the  $k$ th tick  $\tau^{(k)}(t)$ . As such, it is typically dependent on  $k$  even for reset clocks. In Fig. B.1 in Appendix B.3, we confirm numerically that  $\rho_C^{(b,k-1)}$  is still dependent on  $k$  even in case of reset clocks by considering the ladder clock as an example of a reset clock. Thus, in contrast to the first approach this second, alternative approach would not yield an expression for the entropy per tick which is independent of the tick under consideration when considering reset clocks. Consequently, approach 1 is preferred over approach 2.

**Approach 3:** In a third approach we define

$$\tilde{\rho}_C^{(1)}(t, t') = \text{tr}_R \left[ \mathbb{1}_C \otimes |1\rangle\langle 1|_R \mathcal{M}_{C \rightarrow CR}^{t', 1} \left( \frac{\sum_j J_j \rho_C^{(0)}(t) J_j^\dagger}{\text{tr} \left[ \sum_j J_j \rho_C^{(0)}(t) J_j^\dagger \right]} \right) \right], \quad (\text{II.57})$$

where

$$\tilde{\rho}_C^{(0)}(t) = \text{tr}_R \left[ \mathbb{1}_C \otimes |0\rangle\langle 0|_R \mathcal{M}_{C \rightarrow CR}^{t, 0} (\rho_C^0) \right]. \quad (\text{II.58})$$

Equation (II.57) corresponds to the unnormalized state of the clock at coordinate time  $t + t'$  (as measured from the initialization of the clock at  $t = 0$ ) given that the register is observed to be in the state  $|1\rangle_R$  and a tick from  $|0\rangle_R \rightarrow |1\rangle_R$  was observed at coordinate time  $t$ . Because the observer does not have any knowledge of  $t$  or  $t'$ , the state of the clock right before the second tick is

$$\rho_C^{(b,1)} = \int_0^\infty \int_0^\infty P^{(0 \rightarrow 1)}(t) P^{(1 \rightarrow 2)}(t, t') \rho_C^{(1)}(t, t') dt dt', \quad (\text{II.59})$$

with

$$P^{(1 \rightarrow 2)}(t, t') = \lim_{\delta t \rightarrow 0^+} \frac{\text{tr} \left[ \mathbb{1}_C \otimes |2\rangle\langle 2|_R \left( \mathcal{M}_{C \rightarrow CR}^{\delta t, 1} \left( \tilde{\rho}_C^{(1)}(t, t') \right) - \tilde{\rho}_C^{(1)}(t, t') \otimes |1\rangle\langle 1|_R \right) \right]}{\delta t}. \quad (\text{II.60})$$

Similarly, the state of the clock right after the second tick is

$$\rho_{CR}^{(a,2)} = \int_0^\infty \int_0^\infty P^{(0 \rightarrow 1)}(t) P^{(1 \rightarrow 2)}(t, t') \frac{\sum_j J_j \rho_C^{(1)}(t, t') J_j^\dagger}{\text{tr} \left[ \sum_j J_j \rho_C^{(1)}(t, t') J_j^\dagger \right]} dt dt'. \quad (\text{II.61})$$

Following this approach, the state of the clock an instance before and after the  $k$ th tick is then

$$\begin{aligned} \rho_C^{(b,k-1)} = & \int_0^\infty \int_0^\infty \dots \int_0^\infty P^{(0 \rightarrow 1)}(t) P^{(1 \rightarrow 2)}(t, t') \dots P^{(k-1 \rightarrow k)}(t, t', \dots, t^{(k-1)}) \\ & \rho_C^{(k-1)}(t, t', \dots, t^{(k-1)}) dt dt' \dots dt^{(k-1)}, \end{aligned} \quad (\text{II.62})$$

and

$$\rho_C^{(a,k)} = \int_0^\infty \int_0^\infty \dots \int_0^\infty P^{(0 \rightarrow 1)}(t) P^{(1 \rightarrow 2)}(t, t') \dots P^{(k-1 \rightarrow k)}(t, t', \dots, t^{(k-1)}) \frac{\sum_j J_j \rho_C^{(k-1)}(t, t', \dots, t^{(k-1)}) J_j^\dagger}{\text{tr} \left[ \sum_j J_j \rho_C^{(k-1)}(t, t', \dots, t^{(k-1)}) J_j^\dagger \right]} dt dt' \dots dt^{(k-1)} \quad (\text{II.63})$$

respectively. For reset clocks, we have  $\sum_j J_j \rho_C^{(k-1)}(t, t', \dots, t^{(k-1)}) J_j^\dagger \propto \rho_C^0$  and thus  $\rho_C^{(a,k)} = \rho_C^0 \forall k \in \mathbb{N}$ , as well as  $\rho_C^{(b,k)} = \rho_{CR}^{(b,0)} \forall k \in \mathbb{N}$ . We see that this approach does yield observer-dependent clockwork states that are independent of the tick under consideration for reset clocks. One can show that this approach yields the same expression for  $\rho_C^{(a,k)}$  as approach 1, whereas it differs in its expression for  $\rho_C^{(b,k-1)}$  (see Appendix B.3 for a proof). The crucial differences between approaches 1 and 3 will be explored in the following.

Approach 3 can be motivated as follows: consider an observer which has witnessed the clock tick  $(k - 1)$  times already. However, he is unaware of the specific coordinate times  $\mathcal{S}_t = \{t, t + t', t + t' + t'', \dots\}$  at which these ticks happened. Thus, he considers each possible set  $\mathcal{S}_t$  of coordinate times at which these ticks may have occurred and calculates the corresponding state of the clock before and after the  $k$ th tick accordingly (see Eq.(II.62) and (II.63)). Integrating over all possible coordinate times for each tick, each state is weighted by the probability of the first tick occurring in the infinitesimal time interval  $[t, t + \delta t]$ , the second tick occurring in the infinitesimal time interval  $[t + t', t + t' + \delta t]$ , and so on. Clearly, because the expression of  $P^{(k-1 \rightarrow k)}$  involves a sequence of states of the clockwork corresponding to a specific sequence of coordinate times  $\mathcal{S}_t = \{t, t + t', t + t' + t'', \dots\}$ , it is dependent on the time interval between all previous ticks  $P^{(k-1 \rightarrow k)}(t, t', \dots, t^{k-1})$ .

In contrast, approach 1 can be motivated as follows: after each tick, we invoke the fact that the observer has no knowledge of the precise coordinate time at which the tick occurred. Thus, the appropriate state of the clock after the  $(k - 1)$ th tick for such an observer is given by  $\rho_C^{(a,k-1)}$  (Eq. (II.51)). Any subsequent assessment of the clock dynamics will then proceed from this state onwards. Clearly, in this approach, we invoke the observer's oblivion of the exact time at which each tick happened earlier in the calculation compared to approach 3. This renders the resulting expressions in approach 1 independent of the time interval between previous ticks. We can therefore think of approach 1 as follows: it treats subsequent ticks as independent, in the sense that it incorporates the action of previous ticks only in an average fashion while ignoring correlations between the ticking times (see Appendix B.3 for a detailed comparison of approach 1 and 3). Note that this puts the analysis of all ticks on an equal footing. The precise tick under consideration merely determines the initial state of

the clockwork and register which is considered for the analysis, that is the observer-dependent state of the clockwork just after the previous tick. Axiom 4 of our ticking clock model guarantees that the analysis of the entropy production per tick of the  $k$ th tick ( $k > 1$ ) of a clock then simply reduces to an analysis of the first tick ( $k = 1$ ) for a different initial clockwork state, namely the observer-dependent clockwork state after the  $(k - 1)$ th tick given by  $\rho_C^{(a,k-1)}$ .

To illustrate this, imagine the observer is handed a clock just after its  $(k - 1)$ th tick and wants to assess the entropy production of the next tick of the clock. The observer is, however, not aware of the fact that this clock ticked  $(k - 1)$  times beforehand already. One obtains an ensemble description of this situation, for example, by analyzing the clock many times with varying coordinate times  $S_t$  at which the first  $(k - 1)$  ticks occur. This ensemble description is appropriately reflected by ascribing the clockwork the initial state  $\rho_C^{(a,k-1)}$ . Thus, this is identical to a situation where the observer analyses the first tick of a clock with the same clockwork dynamics  $(\mathcal{M}_{\text{CR} \rightarrow \text{CR}}^t)_{t \geq 0}$  but initialized in the state  $\rho_C^{(a,k-1)}$ , as opposed to  $\rho_C^0$ . This situation is depicted in Fig. II.5.

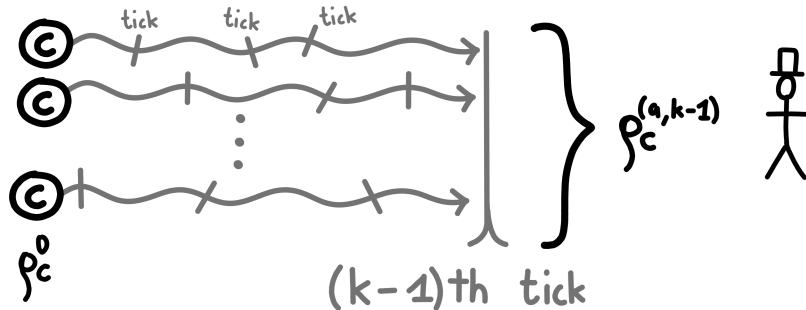


Figure II.5: Illustration of an observer which is handed a ticking clock after its  $(k - 1)$ th tick. The observer-dependent clockwork state  $\rho_C^{(a,k-1)}$  takes into account all possible times at which the previous ticks could have occurred.

If we agree that an observer who is oblivious of the previous ticks of a clock can still assess the entropy production per tick faithfully, we must agree that approach 1 is appropriate for constructing the observer-dependent clockwork states. Or in other words, by adopting approach 1 we decide to construct a measure for the entropy production per tick which differs for the various ticks only in the initial state of the clockwork. The entropy produced in the  $k$ th tick of a clock is equivalent to the entropy produced in the first tick of the clock when initialized in another clockwork state, being  $\rho_C^{(a,k-1)}$ . Because we believe that this is a reasonable property for a measure of the entropy production per tick of a ticking clock, we prefer approach 1 over approach 3 to calculate the observer-dependent clockwork states.

To conclude, we have motivated our choice for the relevant observer-dependent clockwork states by requiring that a reasonable measure of the entropy production per tick of a ticking clock satisfies the following properties:

- the entropy production per tick of a reset clock should be independent of the particular tick under consideration,
- the entropy production of the  $k$ th tick of a ticking clock  $(\rho_C^0, (\mathcal{M}_{\text{CR} \rightarrow \text{CR}}^t)_{t \geq 0})$  is identical to the entropy production of the first tick of a clock with the same clock dynamics  $(\mathcal{M}_{\text{CR} \rightarrow \text{CR}}^t)_{t \geq 0}$  but which is initialized in the state  $\rho_C^{(a,k-1)}$ .

Based on the observer-dependent clockwork states calculated using approach 1 we can now propose a measure for the entropy per tick.

## II.4 Modelling a ticking clock's environment

For ticking clocks in a thermodynamic setting, there has been significant evidence of a fundamental relation between their accuracy and the entropy production per tick which arises due to heat dissipation (see Section II.1). More generally, the irreversibility of the dynamics of an open quantum system, such as a ticking clock, can ultimately be attributed to the interaction with its environment (see Section II.2.1). In particular, if there is no interaction between system and environment, the dynamics of the system itself can still be well described by reversible unitary dynamics. Hence, to devise a measure for the entropy production per tick for a ticking clock  $(\rho_C^0, (\mathcal{M}_{\text{CR} \rightarrow \text{CR}}^t)_{t \geq 0})$ , we first need an appropriate notion of its environment.

Here, we adopt the perspective of an observer who does not have explicit knowledge of the environment generating the underlying dynamics of the clock. This is because, given a particular ticking clock specified by  $(\rho_C^0, (\mathcal{M}_{\text{CR} \rightarrow \text{CR}}^t)_{t \geq 0})$ , there may be several different environments that all yield the appropriate clock dynamics. In particular, we do not want to limit our measure of entropy production to thermal environments. Instead, because we want to define a property based on the dynamics of the clock alone, we assign all these clocks an equal entropy production per tick. In the following, we discuss two different approaches to modeling the environment associated with a ticking clock. These are based on common tools from quantum information theory used to construct quantum channels and quantum states via dilation of the system to a larger Hilbert space, i.e., to a system that encompasses both the ticking clock as well as its environment. Thus, we “go to the church of the larger Hilbert space” to model the environment of a ticking clock [69, 70]. This is illustrated in Fig. II.6. Ultimately, our measure for the entropy production per tick will be based on an environment modeled by such an approach.

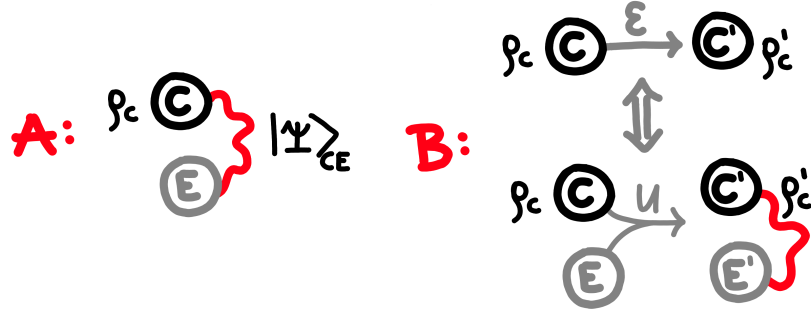


Figure II.6: Illustration of the two procedures for modeling the environment (E) of the clockwork (C) of a ticking clock: the dilation of (A) clockwork states, or (B) ticking channels. (A) Given a mixed state of the clockwork  $\rho_C$ , its purifying system constitutes the environment. By construction, the joint state of the clockwork and its environment is then pure  $|\Psi\rangle_{CE}$ . (B) Given that the clockwork undergoes an evolution according to a quantum channel  $\mathcal{E}$ , the ancillary system which allows for this evolution to be expressed as joint unitary dynamics (with a unitary operator  $U$ ) constitutes the environment. In both approaches (A and B), the clockwork and its environment will generally be entangled (red connection). These correlations can be identified as the key source of entropy production (see Section II.2.1).

### II.4.1 Dilation of quantum states

One way to define an environment only from the state of the clockwork is via purification [25, 69, 70]. That is, given a state of the clockwork  $\rho_C$  the joint state of clockwork and environment is defined as any pure state  $\rho_{CE} = |\Psi\rangle\langle\Psi|_{CE}$ , such that

$$\rho_C = \text{tr}_E [|\Psi\rangle\langle\Psi|_{CE}], \quad \rho_E = \text{tr}_C [|\Psi\rangle\langle\Psi|_{CE}]. \quad (\text{II.64})$$

Here, the environment E corresponds to the purifying system of the clockwork C. A purification represents the most general procedure for modeling a minimal environment from an information-theoretic perspective, such that the joint system of clock and environment can be considered closed, i.e., be described by a pure state (see Fig. II.6). In that sense, the environment encompasses all degrees of freedom other than the system itself.

Any bipartite pure state can be written in the following form using Schmidt decomposition [25, 69, 70]

$$|\Psi\rangle_{CE} = \sum_{i=1}^{d_{\min}} \sqrt{\lambda_i} |\xi_i\rangle_C \otimes |\eta_i\rangle_E, \quad (\text{II.65})$$

where  $\{|\xi_i\rangle\}_C$  and  $\{|\eta_i\rangle\}_E$  are two orthonormal bases of the Hilbert spaces  $\mathcal{H}_C$  and  $\mathcal{H}_{EC}$  of the subsystem C and E, respectively. These two Hilbert spaces are of dimensions  $d_C = \dim(\mathcal{H}_C)$  and  $d_E = \dim(\mathcal{H}_E)$ . Here,  $d_{\min} = \min(d_C, d_E)$  with  $\sum_{i=1}^{d_{\min}} \lambda_i = 1$ ,  $\lambda_i \geq 0 \forall i$ . The Schmidt

coefficients  $\{\lambda_i\}_{i=1}^{d_{\min}}$  are the eigenvalues of the reduced states of the two subsystems C and E

$$\rho_C = \text{tr}_E [|\Psi\rangle\langle\Psi|_{CE}] = \sum_{i=1}^{d_{\min}} \lambda_i |\xi_i\rangle\langle\xi_i|_C, \quad (\text{II.66})$$

$$\rho_E = \text{tr}_C [|\Psi\rangle\langle\Psi|_{CE}] = \sum_{i=1}^{d_{\min}} \lambda_i |\eta_i\rangle\langle\eta_i|_E. \quad (\text{II.67})$$

The two reduced states  $\rho_E$  and  $\rho_C$  have the same eigenvalues and are therefore characterized by the same von Neumann entropy  $S(\rho_E) = S(\rho_C)$ .

For any particular state of the clockwork  $\rho_C$  there will be multiple possible choices of purifying systems, i.e., choices of environments E. Consider, for example, the state  $\rho_{CEE'} = |\Psi\rangle\langle\Psi|_{CE} \otimes |\phi\rangle\langle\phi|_{E'}$  with the purifying system now being labeled by EE' with

$$\rho_C = \text{tr}_{EE'} [|\Psi\rangle\langle\Psi|_{CE} \otimes |\phi\rangle\langle\phi|_{E'}]. \quad (\text{II.68})$$

But any environment to the clockwork C in state  $\rho_C$  will have an entropy equal to the system's entropy  $S(\rho_C)$  as shown above via Schmidt decomposition. Furthermore, the correlations between the clockwork and any potential environment will be given by

$$I(|\Psi\rangle\langle\Psi|_{CE}) = S(\rho_C) + S(\rho_E) - S(|\Psi\rangle\langle\Psi|_{CE}) = 2S(\rho_C) \propto S(\rho_C), \quad (\text{II.69})$$

with  $S(|\Psi\rangle\langle\Psi|_{CE}) = 0$ . That is, for any choice of purifying system E the correlations between system S and E will be given by  $2S(\rho_C)$ .

To conclude, we find that the environments of the clockwork constructed via purification all have equal entropy and exhibit equal correlations with the clockwork because these are properties of the clockwork itself. Given that these are the precise quantities of interest when devising a measure of irreversibility (see Sections II.1 and II.2), all such environments are equivalent when assessing the entropy production per tick of a ticking clock. In other words, all choices of purifying systems reduce to the same expression for the entropy production per tick and are thus implicitly accounted for.

## II.4.2 Dilation of quantum channels

Stinespring's representation theorem [69, 70] states that any quantum channel  $\mathcal{E}$ , i.e., CPTP map, between density matrices can be represented (dilated) by a joint unitary evolution on a

larger dimensional Hilbert space which includes the environment E as an additional system:

$$\rho'_C = \mathcal{E}(\rho_C) = \text{tr}_E \left[ U \rho_C \otimes |0\rangle\langle 0|_E U^\dagger \right]. \quad (\text{II.70})$$

This represents a general procedure for modeling an environment given a non-unitary evolution of an open quantum system (see Fig. II.6). Here, the environment corresponds to the additional quantum system on which the joint evolution can be represented by a unitary evolution. Importantly, the fact that the joint evolution is unitary guarantees that no other system takes part in the dynamics, and all resources are included in this description.

Given that the joint evolution is unitary

$$\rho'_{CE} = U \rho_C \otimes |0\rangle\langle 0|_E U^\dagger, \quad (\text{II.71})$$

we have

$$S(\rho'_{CE}) = S(\rho_{CE}), \quad (\text{II.72})$$

where

$$S(\rho_{CE}) = S(\rho_C \otimes |0\rangle\langle 0|_E) = S(\rho_C), \quad (\text{II.73})$$

$$S(\rho'_{CE}) = S(\rho'_C) + S(\rho'_E) - I(\rho'_{CE}). \quad (\text{II.74})$$

Thus, the change in entropy of the environment can be expressed as

$$\Delta S_E = S(\rho'_E) - S(\rho_E) = S(\rho_C) - S(\rho'_C) + I(\rho'_{CE}) = I(\rho'_{CE}) - \Delta S_C \geq 0, \quad (\text{II.75})$$

$$\Delta S_E \geq -\Delta S_C, \quad (\text{II.76})$$

where  $\Delta S_C = S(\rho'_C) - S(\rho_C)$  is the corresponding change in system entropy. The correlations between system and environment are given as

$$I(\rho'_{CE}) = \Delta S_C + \Delta S_E = \Delta S_C + S(\rho'_E) \geq 0. \quad (\text{II.77})$$

Let us purify the initial clockwork state  $\rho_C$  as  $|\Psi\rangle\langle\Psi|_{CP}$  with a purifying system P and extend the quantum channel  $\mathcal{E}$  to act trivially on the purifying system

$$\mathcal{E} \longrightarrow \mathcal{E}'_{CE} = \mathcal{E}_C \otimes \mathcal{I}_P. \quad (\text{II.78})$$

Note that  $\mathcal{E}'$  is guaranteed to be a valid CPTP map due to the complete positivity of the channel  $\mathcal{E}$ . By the Stinespring representation theorem, we have

$$\rho'_{CP} = \mathcal{E}'(|\Psi\rangle\langle\Psi|_{CP}) = \text{tr}_E \left[ U_{CE} \otimes \mathbb{1}_P |\Psi\rangle\langle\Psi|_{CP} \otimes |0\rangle\langle 0|_E U_{CE}^\dagger \otimes \mathbb{1}_P \right], \quad (\text{II.79})$$

where

$$\rho'_C = \text{tr}_P [\rho'_{CP}] = \mathcal{E}(\rho_C) = \text{tr}_E [U_{CE}\rho_C \otimes |0\rangle\langle 0|_E U_{CE}^\dagger], \quad (\text{II.80})$$

and

$$\rho'_P = \text{tr}_C [\rho'_{CP}] = \mathcal{I}(\rho_P) = \rho_P. \quad (\text{II.81})$$

Note that the joint state of CPE after application of the unitary  $U_{CE} \otimes \mathbb{1}_P$  in Eq. (II.79) is also pure, because a unitary evolution conserves purity. Replacing C by CP in Eq. (II.75) and (II.77) and noting that  $S(|\Psi\rangle\langle\Psi|_{CP}) = 0 = S(|\Psi\rangle\langle\Psi|'_{CPE})$  we have

$$\Delta S_E = S(\rho'_{CP}) \geq 0, \quad (\text{II.82})$$

and

$$I_{CP:E}(\rho'_{CPE}) = 2S(\rho'_{CP}) \propto S(\rho'_{CP}) \geq 0. \quad (\text{II.83})$$

Therefore, we see that by purifying the initial state of the clockwork and tracking the evolution of the resulting pure state, we can directly assess the change in entropy of the environment  $\Delta S_E$  (Eq. (II.75)) arising when considering the quantum channel  $\mathcal{E}$  without any explicit reference to the environment itself. That is, all environments and unitary operators that result in the state  $\rho'_{CP}$  of the system CP after a joint evolution will yield the same entropy production per tick if the latter is given by the change in entropy of the environment, or equivalently, the built-up correlations between the system CP and its environment E (see Eq. (II.83)). As such, these are *intrinsic* properties of the clockwork and its dynamics irrespective of the particular environment which is used in its realization [49]. Note that if the initial state of the clockwork is already pure  $\rho_C = |\Psi\rangle\langle\Psi|_C$ , then  $S(\rho'_{CP}) = S(\rho'_C)$ . In this special case, the relevant quantity  $S(\rho'_{CP})$  corresponds to the change in entropy of the clockwork itself during the process. In general, using the triangle inequality (see Appendix A) we have

$$S(\rho'_{CP}) \geq |S(\rho'_C) - S(\rho_C)|. \quad (\text{II.84})$$

One may think that the restriction to pure initial states of the environment E in the above analysis is unphysical. Firstly, note that while the actual environment responsible for generating the dynamics may be impure, we find quantities intrinsic to the clockwork and its dynamics by substituting this environment with an alternative environment that is initially in a pure state and gives rise to the same dynamics. As such, it is this pure environment that is most useful for gauging the properties of the clock irrespective of its physical implementation. Consider, for example, the case where the evolution of the system governed by the quantum channel  $\mathcal{E}$  can be expressed as

$$\rho'_C = \mathcal{E}(\rho_C) = \text{tr}_E [U\rho_C \otimes \rho_E U^\dagger]. \quad (\text{II.85})$$

That is, a situation where the clockwork undergoes a joint unitary evolution with a generally mixed state of the environment  $\rho_E$ . Then, we have

$$\Delta S_E = S(\rho'_E) - S(\rho_E) \leq S(\rho'_E), \quad (\text{II.86})$$

and

$$I(\rho'_{CE}) = \Delta S_C + \Delta S_E \leq \Delta S_C + S(\rho'_E), \quad (\text{II.87})$$

where equality hold if and only if  $\rho_E$  is a pure state. Let us purify the initial state of the environment  $\rho_E$  as  $|\Psi\rangle\langle\Psi|_{EE'}$  with a purifying system labeled  $E'$ . Equation (II.85) can then be rewritten as

$$\rho'_C = \mathcal{E}(\rho_C) = \text{tr}_{EE'} \left[ U_{CE} \otimes \mathbb{1}_{E'} \rho_C \otimes |\Psi\rangle\langle\Psi|_{EE'} U_{CE}^\dagger \otimes \mathbb{1}_{E'} \right]. \quad (\text{II.88})$$

We have

$$\Delta S_{EE'} = S(\rho'_{EE'}) - S(\rho_{EE'}) = S(\rho'_{EE'}), \quad (\text{II.89})$$

and

$$I_{C:EE'}(\rho'_{CEE'}) = \Delta S_C + \Delta S_{EE'} = \Delta S_C + S(\rho'_{EE'}). \quad (\text{II.90})$$

Here, Eq. (II.89) and (II.90) upper bound the expressions in Eq. (II.86) and (II.87), respectively. Meaning, the change in entropy of the environment and the built-up correlations between the clockwork and environment given a joint unitary evolution with an initially mixed state of the environment is upper bounded by the expressions obtained using Stinespring dilation, where the initial state of the environment is pure. Moreover, in the case where the evolution can be written in the form of Eq. (II.85) one can always construct a joint unitary evolution with a pure initial state of the environment obtained via purification (see Eq. (II.88)). Here, if we purify the initial clockwork state  $\rho_C$  as  $|\Psi\rangle\langle\Psi|_{CP}$  and extend the corresponding quantum channel, we have

$$S(\rho'_{CP}) = S(\rho'_{EE'}). \quad (\text{II.91})$$

Thus, using the triangle inequality (see Appendix A) we obtain

$$S(\rho'_{CP}) \geq |S(\rho'_E) - S(\rho_E)|. \quad (\text{II.92})$$

So the quantity  $S(\rho'_{CP})$  constitutes an upper bound to the absolute change in entropy of any environment  $E$  which may start in a generally mixed state and be sufficient to describe the dynamics of the clockwork through joint unitary evolution.

From a point of view of the clockwork itself, one cannot distinguish between these two situations. This becomes clear when picturing two physical scenarios: one in which the envi-

ronment is identified as the subsystems labeled  $EE'$  which starts in a pure state initially and shows trivial dynamics on subsystem  $E'$  itself. In the other scenario, the environment is only identified as the subsystem  $E$ , which is (generally) in a mixed state initially. Because both environments generate the same dynamics on the clockwork, there is no way judging from the evolution of the clockwork alone whether one is currently witnessing the first or second situation. The choice of which subsystems should constitute the environment then lies in the hands of an observer who has, at least partial, knowledge of the environment. Note that we set out to define an expression for the entropy production per tick of a ticking clock irrespective of the environment which realizes the clock. Thus, such a disagreement on the identification of subsystems as the relevant environment emerges naturally. In this work, we adopt a viewpoint of an observer that has no knowledge of the environment at all, i.e., only has access to the clock itself and its dynamics. When modeling the environment by means of Stinespring dilation of the corresponding quantum channel with a pure initial state of the environment, we account for both these scenarios implicitly. By doing so, we upper-bound the change in the entropy of the environment and the built-up correlations, and thus the entropy production per tick which will be derived from these quantities.

#### II.4.2.a Information leakage of noisy quantum channel

Note that  $S(\rho'_{\text{CP}})$  is a known quantity called ‘‘entropy exchange’’ [25, 71–74] (or sometimes entropy production [75]) when analyzing the transmission through noisy quantum channels using concepts from quantum information theory. Here, the noisy quantum channel is given by the CPTP map  $\mathcal{E}$ . It is called ‘‘noisy’’ because, in general, the evolution of the system is not unitary and as such, the system is not isolated from its environment. As we have seen above, the quantity  $S(\rho'_{\text{CP}})$  is generally not equal to the change in the entropy of the clockwork  $C$  itself or the physical environment which realizes the dynamics via a joint unitary evolution. Instead, it quantifies the information exchanged between the clockwork and the ‘‘rest of the universe’’ during its generally non-unitary evolution. In particular, one can show that it gains operational meaning in quantum cryptographic protocols: the entropy exchange then upper-bounds the amount of information that an eavesdropper can potentially acquire when the noisy quantum channel is used for communication between two parties [71]. Here, the environment of the system includes the measurement apparatus of the eavesdropper which disturbs the system and acts as a source of noise for the quantum channel. Moreover, consider the entanglement fidelity  $F_e$  given as

$$F_e = \text{tr} [\rho'_{\text{CP}} |\Psi\rangle\langle\Psi|_{\text{CP}}]. \quad (\text{II.93})$$

Equation (II.93) quantifies how well the initial entangled state  $|\Psi\rangle_{\text{CP}}$  is preserved under the evolution by the quantum channel  $\tilde{\mathcal{E}}_{\text{CP}} = \mathcal{E}_C \otimes \mathcal{I}_P$ . Importantly, the entanglement fidelity does

not only measure how well the state of the clockwork C is preserved under the evolution but also how well the coherences with its purifying system P are conserved. As such, it is a strong measure of the amount of disturbance that the state of the clockwork experiences during its evolution. One can show that the entanglement fidelity, similar to the entropy exchange, is also an intrinsic quantity depending only on the state of the clockwork C and on its dynamics [71]. A connection between  $F_e$  and  $S(\rho'_{CP})$  is given by the quantum Fano inequality

$$S(\rho'_{CP}) \leq S_{\text{bin}}(F_e) + (1 - F_e) \ln(d^2 - 1), \quad (\text{II.94})$$

where  $S_{\text{bin}}(p) = -p \ln(p) - (1 - p) \ln(1 - p)$  is the binary Shannon entropy and  $d$  is the dimension of the clockwork Hilbert space. This inequality connects the disturbance experienced by the clockwork, as quantified by  $F_e$ , to the information which “leaks” into the environment, as quantified by  $S(\rho'_{CP})$ . Looking at Eq. (II.94), if the entropy exchange is large, the entanglement fidelity must necessarily be small. That is, the system is disturbed strongly. This enforces the notion that in quantum information theory, noise (or disturbance) is caused by an information exchange with the environment of the system.

## II.5 Measures of entropy production per tick of a ticking clock

In this section, we construct appropriate measures for the (irreversible) entropy production per tick of a ticking clock based on the relevant observer-dependent states of the clockwork motivated in Section II.3 and the corresponding environment which we construct using the methods discussed in Section II.4. Ultimately, these measures are motivated by the findings in Section II.1 regarding the entropy production per tick of thermodynamic ticking clocks, as well as recent advances regarding entropy production in open quantum systems reviewed in Section II.2.

### II.5.1 Based on dilation of clockwork states

In a first approach to define a measure for the entropy production per tick, we assess the environment of the ticking clock by purifying the relevant observer-dependent clockwork states before and after each tick, see Section II.4.1. As motivated previously, the entropy production of the  $k$ th tick will generally depend on the following clockwork states:  $\rho_C^{(a,k-1)}$ ,  $\rho_C^{(b,k-1)}$ , and  $\rho_C^{(a,k)}$ . The entropy of the environment of the clockwork at these instances is given by  $S(\rho_C^{(a,k-1)})$ ,  $S(\rho_C^{(b,k-1)})$ , and  $S(\rho_C^{(a,k)})$ , respectively. This also corresponds, up to a constant factor of 2, to the correlations between clockwork and environment, as measured by the quantum mutual information (see Eq. (II.69)). Eventually, we will be interested in assessing the change in entropy of the environment or the change in the correlations between system and

environment during the ticking process. Naively, one can identify

$$\Sigma_k^{(A)} = S(\rho_C^{(a,k)}) - S(\rho_C^{(a,k-1)}) \quad (\text{II.95})$$

and

$$\Sigma_k^{(B)} = S(\rho_C^{(b,k-1)}) - S(\rho_C^{(a,k-1)}) \quad (\text{II.96})$$

as two potential quantities measuring this change. While  $\Sigma_k^{(A)}$  (Eq. (II.95)) measures these changes by assessing the environment of the clockwork in the instances just after the  $(k-1)$ th and  $k$ th tick,  $\Sigma_k^{(B)}$  (Eq. (II.96)) evaluates the environment of the clockwork in the instances just after and before the  $(k-1)$ th and  $k$ th tick, respectively. Note that these two quantities are not guaranteed to be non-negative. Consider, for example, the case where the clockwork is initialized in a maximally mixed state  $\rho_C^0 = \frac{1}{d}\mathbb{1}$  but which resets to a pure state of the clockwork after its first tick. Then,  $\Sigma_1^{(A)} = S(\frac{1}{d}\mathbb{1}) = \ln(d)$  and  $\Sigma_1^{(B)} \leq 0$  in general, where equality can only be achieved if  $\rho_C^{(b,0)} = \frac{1}{d}\mathbb{1}$ .

A crucial property of any measure for the entropy production per tick of a ticking clock  $\Sigma_k$  is that it should be invariant under purification of the clockwork state  $\rho_C^{(a,k-1)}$ . Thus, we modify the two measures as follows:

$$\Sigma_k^{(A)} = S(\rho_{CP}^{(a,k)}) - S(|\Psi\rangle\langle\Psi|_{CP}^{(a,k-1)}) = S(\rho_{CP}^{(a,k)}) \geq 0, \quad (\text{II.97})$$

$$\Sigma_k^{(B)} = S(\rho_{CP}^{(b,k-1)}) - S(|\Psi\rangle\langle\Psi|_{CP}^{(a,k-1)}) = S(\rho_{CP}^{(b,k-1)}) \geq 0, \quad (\text{II.98})$$

where

$$\rho_{CP}^{(b,k-1)} = \int_0^\infty P^{(k-1 \rightarrow k)}(t) \rho_{CP}^{(k-1)}(t) dt, \quad (\text{II.99})$$

$$\rho_{CP}^{(a,k)} = \int_0^\infty P^{(k-1 \rightarrow k)}(t) \frac{\sum_j \tilde{J}_j \rho_{CP}^{(k-1)}(t) \tilde{J}_j^\dagger}{\text{tr} \left[ \sum_i \tilde{J}_i \rho_{CP}^{(k-1)}(t) \tilde{J}_i^\dagger \right]} dt = \int_0^\infty \sum_j \tilde{J}_j \tilde{\rho}_{CP}^{(k-1)}(t) \tilde{J}_j^\dagger dt, \quad (\text{II.100})$$

with

$$\tilde{\rho}_{CP}^{(k-1)}(t) = \text{tr}_R \left[ \mathbb{1}_{CP} \otimes |k-1\rangle\langle k-1|_R \tilde{\mathcal{M}}_{CP \rightarrow CPR}^{t,k-1} \left( |\Psi\rangle\langle\Psi|_{CP}^{(a,k-1)} \right) \right]. \quad (\text{II.101})$$

Here,  $|\Psi\rangle\langle\Psi|_{CP}^{(a,k-1)}$  corresponds to the purification of the clockwork state  $\rho_C^{(a,k-1)}$  with purifying system  $P$

$$\text{tr}_P \left[ |\Psi\rangle\langle\Psi|_{CP}^{(a,k-1)} \right] = \rho_C^{(a,k-1)}. \quad (\text{II.102})$$

The new ticking clock channels  $(\tilde{\mathcal{M}}_{CPR \rightarrow CPR}^t)_{t \geq 0}$  can be obtained from the original channels  $(\mathcal{M}_{CR \rightarrow CR}^t)_{t > 0}$  via

$$\tilde{\mathcal{M}}_{CPR \rightarrow CPR}^t = \mathcal{M}_{CR \rightarrow CR}^t \otimes \mathcal{I}_P \quad \forall t \geq 0. \quad (\text{II.103})$$

Equivalently,

$$\tilde{\mathcal{M}}_{\text{CP} \rightarrow \text{CPR}}^{t,k} = \mathcal{M}_{\text{C} \rightarrow \text{CR}}^{t,k} \otimes \mathcal{I}_P \quad \forall t \geq 0, k \in \mathbb{N}. \quad (\text{II.104})$$

The corresponding representation given in Proposition 1 can be obtained by the following substitutions

$$L_{j,C} \longrightarrow \tilde{L}_{j,\text{CP}} = L_{j,C} \otimes \mathbb{1}_P \quad \forall j \in (1, N_L), \quad (\text{II.105})$$

$$J_{j,C} \longrightarrow \tilde{J}_{j,\text{CP}} = J_{j,C} \otimes \mathbb{1}_P \quad \forall j \in (1, N_L), \quad (\text{II.106})$$

$$H_C \longrightarrow \tilde{H}_{\text{CP}} = H_C \otimes \mathbb{1}_P. \quad (\text{II.107})$$

This property can be motivated as follows: For every ticking clock specified by

$$(\rho_C^0, (\mathcal{M}_{\text{CR} \rightarrow \text{CR}}^t)_{t \geq 0}), \quad (\text{II.108})$$

there exists another ticking clock specified by

$$(|\Psi\rangle\langle\Psi|_{\text{CP}}^0, (\tilde{\mathcal{M}}_{\text{CPR} \rightarrow \text{CPR}}^t)_{t \geq 0}), \quad (\text{II.109})$$

where the initial state of the clockwork is given by the purification of  $\rho_C^0$  and P denotes the corresponding purifying system. The dynamics of this alternative ticking clock (Eq. (II.109)) are characterized by the ticking clock channels  $(\tilde{\mathcal{M}}_{\text{CPR} \rightarrow \text{CPR}}^t)_{t \geq 0}$  of the form given in Eq. (II.103), which act trivially on the purifying system. This second type of clock undergoes the same interactions with its environment. This is because the purifying system does not interact with the environment at all (see Eq. (II.105), (II.106), and (II.107)) and the dynamics of the clockwork C itself are identical for both clocks. Thus, the fundamental origin of irreversibility of the clock's dynamics – the non-unitary evolution of the clock – remains unchanged and any measure of irreversibility should be identical for these two clocks. This can be ensured for the first tick by the replacement of  $\rho_C^0$  by its purification  $|\Psi\rangle\langle\Psi|_{\text{CP}}^0$ , where the dynamics act trivially on the purifying system. To motivate the replacement of  $\rho_C^{(a,k-1)}$  by its purification  $|\Psi\rangle\langle\Psi|_{\text{CP}}^{(a,k-1)}$  for the assessment of the entropy production of the  $k$ th tick (as outlined above), we invoke our previous assumption that the entropy production of the  $k$ th tick of a ticking clock should be identical to the entropy production of the first tick of a ticking clock with the same dynamics, but which is initialized to the state  $\rho_C^{(a,k-1)}$  instead of  $\rho_C^0$  (see Section II.3). Note that this also guarantees the positivity of the two measures  $\Sigma_k^{(A)}$  (Eq. (II.97)) and  $\Sigma_k^{(B)}$  (Eq. (II.98)).

We can analyze the particular case of the thermodynamic ticking clock (see Section II.1) for a more physical motivation of this property. For the thermodynamic ticking clock, the

entropy production per tick can be attributed to the heat exchange between the two thermal baths that powers its clockwork. By purification of the initial state of the clockwork, we adopt a perspective of an observer that has complete knowledge of the initial state of the clockwork, i.e., an observer who also has access to the system that purifies the clockwork (which can be seen as an origin for the impurity of the original clockwork state). Clearly, adopting such a viewpoint does not alter the amount of heat that flows from the hot to the cold reservoir. This is because the heat flow is directly tied to the dynamics of the clockwork which remains the same in both perspectives.

We can further motivate this property by noting that the first measures in Eq. (II.95) and (II.96) were proposed based on an analysis of the environment E of the clockwork obtained by purifying the state of the clockwork before and after the  $k$ th tick as

$$\rho_C^{(b,k-1)} \longrightarrow |\Psi\rangle\langle\Psi|_{CE}^{(b,k-1)}, \quad (\text{II.110})$$

and

$$\rho_C^{(a,k)} \longrightarrow |\Psi\rangle\langle\Psi|_{CE}^{(a,k)}, \quad (\text{II.111})$$

respectively. Compare this to the second set of measures in Eq. (II.97) and (II.98) which were motivated by assessing the environment E' of the clockwork obtained by purifying the state of the clockwork before and after the  $k$ th tick as

$$\rho_{CP}^{(b,k-1)} \longrightarrow |\Psi\rangle\langle\Psi|_{CPE'}^{(b,k-1)}, \quad (\text{II.112})$$

and

$$\rho_{CP}^{(a,k)} \longrightarrow |\Psi\rangle\langle\Psi|_{CPE'}^{(a,k)}, \quad (\text{II.113})$$

respectively. These are obtained by purifying the state  $\rho_C^{(a,k-1)}$  first to yield  $|\Psi\rangle\langle\Psi|_{CP}^{(a,k-1)}$ . Based on this, one can observe that the first approach (Eq. (II.95) and (II.96)) assesses the change in entropy of the subsystems PE', whereas the second approach only assesses the change in entropy of the subsystem E'. This is because the entropy of any purifying system is identical to the entropy of the system which gets purified (see Section II.4.1). We know that the identification of the environment of a ticking clock with the subsystem E', as opposed to PE', is more faithful. This is because we can exclude that subsystem P is part of the relevant environment, as there will exist another clock that incorporates this system in its clockwork and undergoes the same dynamics. To probe the environment constituted by the subsystem labelled E', as opposed to both E' and P, we adopt the measures in Eq. (II.97) and (II.98) instead of Eq. (II.95) and (II.96).

*A priori*, it is unclear which of the two quantities,  $\Sigma_k^{(A)}$  or  $\Sigma_k^{(B)}$ , in Eq. (II.97) and (II.98)

is more appropriate for assessing the entropy production per tick of a ticking clock. Because we model the environment based on the clockwork alone, it is crucial to pick the appropriate clockwork states. This is illustrated by the fact that  $\Sigma_k^{(A)} = 0 \forall k \in \mathbb{N}_{>0}$  for reset clocks which reset to a pure state (Def. 5). An expression for the entropy production per tick of a ticking clock with such a property is undesired. Even if we take the expression as a minimal amount of entropy production per tick, this would result in a trivial relation between the minimal entropy production and the accuracy of ticking clocks. Intuitively, reset clocks that reset to a pure state are the most accurate class of ticking clocks. In particular, the ladder ticking clock (see Section I.1.1) and the quasi-ideal ticking clock (see Section I.1.2) fall in this category. For classical clocks, Theorem 1 formalizes this intuition. We note, however, that the dynamics of these clocks are not unitary, and therefore not fully reversible in general. This can be seen directly by noting that for such clocks  $S(\rho_{CP}^{(b,k-1)}) \neq 0 \forall k \in \mathbb{N}_{>0}$  in general, whereas entropy is conserved under unitary dynamics. Thus, the first measure given by  $\Sigma_k^{(A)}$  fails to assess the change in entropy of the environment or correlations based on the states of the clockwork alone. The reason for its failure can be understood by noting that  $\rho_C^{(a,k)} = \rho_C^{(a,0)} = \rho_C^0 \forall k \in \mathbb{N}$  for any pure state reset clock. An observer which only considers these states of the clockwork would ascribe the clock a trivial evolution. That is, given two identical states of the clockwork such an observer would assign the process connecting the two states a vanishing (minimal) change in the entropy of the environment because the same mapping between states can simply be achieved by an identity operation. What this approach fails to capture is the irreversibility of the dynamics of these clocks leading up to a tick event.

Hence, we adopt the second measure  $\Sigma_k^{(B)}$  in the following (Eq. (II.98)). This quantity is non-zero in general, even for reset clocks that reset to a pure state. Here, the environment of the clockwork is evaluated just before each tick as opposed to after. Intuitively, this precisely addresses the problem with the first measure  $\Sigma_k^{(A)}$  identified above. The transition from  $\rho_C^{(b,k-1)}$  to  $\rho_C^{(a,k)}$  involves the collapse of the clockwork state during the tick of the clock (see Eq. (II.47) and (II.50)), i.e., the advancement of its register, given by

$$\rho_C^{(k-1)}(t) \longrightarrow \frac{\sum_j J_j \rho_C^{(k-1)}(t) J_j^\dagger}{\text{tr} \left[ \sum_j J_j \rho_C^{(k-1)}(t) J_j^\dagger \right]}. \quad (\text{II.114})$$

By probing the state of the clockwork an instance before each tick, i.e., before the associated collapse of the clockwork state, we can faithfully assess the involvement of the environment in the evolution of the clockwork up to that point. In that sense, adopting the measure  $\Sigma_k^{(B)}$  over  $\Sigma_k^{(A)}$  can be viewed as a necessary ‘‘trick’’ to appropriately model the environment and its interactions with the clockwork when adopting the viewpoint of an observer that only has access to the observer-dependent states of the clockwork.

In the particular case of the thermodynamic ticking clock (see Section II.1), the ticking event is associated with the emission and subsequent detection of a photon and a collapse of the ladder to its ground state. The state of the clockwork an instance after this ticking event will be (approximately) equal to the initial state of the clockwork, whereas the state of the clockwork an instance before the tick is generally different. In particular, the population of the ladder is not all concentrated in its ground state (otherwise the probability of ticking would vanish). However, the amount of heat exchanged between the baths – and thus the entropy production per tick – remains the same, independent of whether it is assessed in an instance before or after the tick. By probing the state of the clockwork an instance after the tick event and comparing it to its initial state, an observer may draw false conclusions about the involvement of the environment. Instead, to properly assess the entropy production per tick as the heat exchanged between the thermal reservoirs one evaluates the state of the clockwork an instance before the completion of its cyclic process, i.e., an instance before the actual tick event takes place.

To conclude, in this section, we have motivated the following expression for the entropy production of the  $k$ th tick of a ticking clock

$$\Sigma_k = S(\rho_{\text{CP}}^{(b,k-1)}) \geq 0 \quad \forall k \in \mathbb{N}_{>0}, \quad (\text{II.115})$$

where  $\rho_{\text{CP}}^{(b,k-1)}$  is calculated according to Eq. (II.99). For this, we have postulated the following:

- The entropy production of the first tick of a ticking clock  $(\rho_C^0, (\mathcal{M}_{\text{CR} \rightarrow \text{CR}}^t)_{t \geq 0})$  should be identical to the entropy production of the first tick of the ticking clock

$$\left( |\Psi\rangle\langle\Psi|_{\text{CP}}^0, (\tilde{\mathcal{M}}_{\text{CPR} \rightarrow \text{CPR}}^t)_{t \geq 0} \right), \quad (\text{II.116})$$

where  $|\Psi\rangle\langle\Psi|_{\text{CP}}^0$  is the purification of  $\rho_C^0$  with purifying system P and the ticking clock channel of this second clock  $\tilde{\mathcal{M}}_{\text{CPR} \rightarrow \text{CPR}}^t = \mathcal{M}_{\text{CR} \rightarrow \text{CR}}^t \otimes \mathcal{I}_P$  acts trivially on P.

The measure  $\Sigma_k$  (Eq. (II.115)) is non-negative and its minimum value of zero can only be achieved by a pure state  $S(|\Psi\rangle\langle\Psi|_{\text{CP}}^{(b,k-1)}) = 0$ . Note that the state  $|\Psi\rangle\langle\Psi|_{\text{CP}}^{(a,k-1)}$  is pure by construction and thus has zero entropy. Because any unitary evolution leaves the entropy unchanged, when observing a state  $\rho_{\text{CP}}^{(b,k-1)}$  with non-zero entropy it is evident that it must have undergone a non-unitary, and thereby irreversible, evolution in the process. In particular, because  $|\Psi\rangle\langle\Psi|_{\text{CP}}^{(a,k-1)}$  is pure, we know that there cannot be any initial correlations with its environment. Because purity is conserved under unitary evolution, if the state  $\rho_{\text{CP}}^{(b,k)}$  is not pure, i.e., has non-zero entropy, it must necessarily share correlations with some other system – its environment E – during the process. If we purify the state  $\rho_{\text{CP}}^{(b,k-1)}$ , we find

$I_{\text{CP:E}}(|\Psi\rangle\langle\Psi|_{\text{CPE}}^{(\text{b},k-1)}) = 2S(\rho_{\text{CP}}^{(\text{b},k-1)}) = 2S(\rho_{\text{E}}^{(\text{b},k-1)})$ . Thus,  $\Sigma_k$  serves as a direct measure of the correlations which build up with its environment during the process leading up to the tick event, which is up to the instance just before the tick occurs. Looking back at Section II.2.1, we motivated the correlations between system and environment as the source of irreversibility of a process.

### II.5.2 Based on dilation of ticking channels

Having devised a first measure for the entropy production per tick of a ticking clock (Eq. (II.115)) based on the identification of an environment via the dilation of the relevant observer-dependent clockwork states, we here take an alternative approach based on modeling the environment via the dilation of the quantum channels connecting these clockwork states (see Section II.4.2). In particular, we may associate the two CPTP maps  $\mathcal{E}_{k-1}^{(\text{A})}$  and  $\mathcal{E}_{k-1}^{(\text{B})}$  ( $k \in \mathbb{N}_{>0}$ ) to the transitions between the relevant observer-dependent clockwork states

$$\rho_{\text{C}}^{(\text{a},k)} = \mathcal{E}_{k-1}^{(\text{A})}(\rho_{\text{C}}^{(\text{a},k-1)}), \quad (\text{II.117})$$

$$\rho_{\text{C}}^{(\text{b},k-1)} = \mathcal{E}_{k-1}^{(\text{B})}(\rho_{\text{C}}^{(\text{a},k-1)}). \quad (\text{II.118})$$

Based on the expressions for the observer-dependent clockwork states (see Section II.3), we can construct the Kraus operator representation of the quantum channel  $\mathcal{E}_{k-1}^{(\text{A})}$  (see Appendix B.4). The derivation of the relevant observer-dependent clockwork states does, however, not directly yield a Kraus operator representation for the channel  $\mathcal{E}_{k-1}^{(\text{B})}$ . Nevertheless, given that one can always find a quantum channel that maps between two valid quantum states, such a channel exists. The channel  $\mathcal{E}_{k-1}^{(\text{B})}$  may, however, be dependent on the particular input and output states. In specifying a ticking clock, one fixes the relevant observer-dependent clockwork states. While there will still be a remaining degree of freedom in the choice of the quantum channel  $\mathcal{E}_{k-1}^{(\text{B})}$ , we will ensure that the quantities which may eventually serve as measures for the entropy production per tick will be independent of this choice.

We dilate the quantum channels  $\mathcal{E}_{k-1}^{(\text{A})}$  and  $\mathcal{E}_{k-1}^{(\text{B})}$  according to Section II.4.2 to obtain

$$\rho_{\text{CE}}^{(\text{a},k)} = U_{k-1}^{(\text{A})}\rho_{\text{C}}^{(\text{a},k-1)} \otimes |0\rangle\langle 0|_{\text{E}}U_{k-1}^{(\text{A})\dagger}, \quad (\text{II.119})$$

$$\rho_{\text{CE}}^{(\text{b},k-1)} = U_{k-1}^{(\text{B})}\rho_{\text{C}}^{(\text{a},k-1)} \otimes |0\rangle\langle 0|_{\text{E}}U_{k-1}^{(\text{B})\dagger}. \quad (\text{II.120})$$

Thus, we naturally arrived at the setting in which the analysis of Section II.2.1 on entropy production as correlation between system and environment took place. That is, a system and environment which are initially uncorrelated and undergo a joint unitary evolution. In the following, we analyze the resulting states of clockwork and environment before and after

the application of the unitary channel according to Section II.2.1 to obtain expressions for the corresponding changes in environmental entropy and correlations between clockwork and environment. These are then identified as measures for the entropy production per tick of ticking clocks.

Before moving on, note that such a procedure assumes that the environment and the clockwork given by the state  $\rho_C^{(a,k-1)}$  are initially uncorrelated, see Eq. (II.119) and (II.120). This is common to the Stinespring dilation of any quantum channel [25, 69, 70]. Moreover, the product state assumption is also standard to many other common tasks in (quantum) information processing, such as error correction [25, 47]. In any case, it is certainly valid when the two systems did not previously interact, i.e., never had the possibility to get correlated in the first place. Thus, for the first tick of a ticking clock one can reasonably assume that the environment is not correlated to the initial state of the clockwork  $\rho_C^0$ . In fact, the assumption of vanishing correlations between system and environment is crucial for the derivation of the quantum Markovian master equations which underlies the dynamics of any ticking clock [26, 30, 31]. Imagine for a moment, that we do not assume product states for later ticks  $k > 1$ . Then, it may happen that even though the clock is a reset clock and the relevant observer-dependent clockwork states of the  $k$ th tick are equivalent to the clockwork states of the first tick, we do not get the same entropy production per tick in every tick. We did, however, postulate that the entropy per tick of a reset clock should be independent of the tick under consideration. In any case, we can justify the product state assumption for the later ticks  $k > 1$  by invoking our earlier statement that the entropy production of the  $k$ th tick of a clock should be identical to the entropy production of the first tick of a clock with the same clock dynamics  $(\mathcal{M}_{\text{CR} \rightarrow \text{CR}}^t)_{t \geq 0}$ , but which is initialized in the state  $\rho_C^{(a,k-1)}$ .

Analysing the quantum channel  $\mathcal{E}_{k-1}^{(A)}$ , we obtain

$$S(\rho_{\text{CE}}^{(a,k)}) = S(\rho_{\text{CE}}^{(a,k-1)}) = S(\rho_C^{(a,k-1)}), \quad (\text{II.121})$$

$$S(\rho_{\text{CE}}^{(a,k)}) = S(\rho_C^{(a,k)}) + S(\rho_E^{(a,k)}) - I(\rho_{\text{CE}}^{(a,k)}), \quad (\text{II.122})$$

$$S(\rho_E^{(a,k)}) - S(\rho_E^{(a,k-1)}) = S(\rho_C^{(a,k-1)}) - S(\rho_C^{(a,k)}) + I(\rho_{\text{CE}}^{(a,k)}) \geq 0, \quad (\text{II.123})$$

$$I(\rho_{\text{CE}}^{(a,k)}) = S(\rho_C^{(a,k)}) - S(\rho_C^{(a,k-1)}) + S(\rho_E^{(a,k)}) \geq 0. \quad (\text{II.124})$$

Similarly, for the quantum channel  $\mathcal{E}_{k-1}^{(B)}$  we have

$$S(\rho_{\text{CE}}^{(b,k-1)}) = S(\rho_{\text{CE}}^{(a,k-1)}) = S(\rho_C^{(a,k-1)}), \quad (\text{II.125})$$

$$S(\rho_{\text{CE}}^{(b,k-1)}) = S(\rho_C^{(b,k-1)}) + S(\rho_E^{(b,k-1)}) - I(\rho_{\text{CE}}^{(b,k-1)}), \quad (\text{II.126})$$

$$S(\rho_E^{(b,k-1)}) - S(\rho_E^{(a,k-1)}) = S(\rho_C^{(a,k-1)}) - S(\rho_C^{(b,k-1)}) + I(\rho_{CE}^{(b,k-1)}) \geq 0, \quad (\text{II.127})$$

$$I(\rho_{CE}^{(b,k-1)}) = S(\rho_C^{(b,k-1)}) - S(\rho_C^{(a,k-1)}) + S(\rho_E^{(b,k-1)}) \geq 0. \quad (\text{II.128})$$

We can make similar arguments as in Section II.5.1 to motivate that our measure for the entropy production of the first tick of a ticking clock ( $\rho_C^0, (\mathcal{M}_{CR \rightarrow CR}^t)_{t \geq 0}$ ) should be identical to the entropy production of the first tick of the ticking clock ( $|\Psi\rangle\langle\Psi|_{CP}^0, (\tilde{\mathcal{M}}_{CPR \rightarrow CPR}^t)_{t \geq 0}$ ), where  $\rho_{CP}^0 = |\Psi\rangle\langle\Psi|_{CP}^0$  is a pure state and P denotes the corresponding purifying system with dynamics given by  $\tilde{\mathcal{M}}_{CPR \rightarrow CPR}^t = \mathcal{M}_{CR \rightarrow CR}^t \otimes \mathcal{I}_P$ . That is, we can also motivate the replacement of  $\rho_C^{(a,k-1)}$  by  $|\Psi\rangle\langle\Psi|_{CP}^{(a,k-1)}$  in this approach. The corresponding modified quantum channels are then given as  $\tilde{\mathcal{E}}_{CP,k-1}^{(A/B)} = \mathcal{E}_{C,k-1}^{(A/B)} \otimes \mathcal{I}_P$ . We re-evaluate the change in environmental entropy and the correlations based on these channels and find

$$S(\rho_E^{(a,k)}) - S(\rho_E^{(a,k-1)}) = S(\rho_{CP}^{(a,k)}) \geq 0, \quad (\text{II.129})$$

$$I(\rho_{CP:E}^{(a,k)}) = 2S(\rho_{CP}^{(a,k)}) \propto S(\rho_{CP}^{(a,k)}) \geq 0, \quad (\text{II.130})$$

for the channel  $\tilde{\mathcal{E}}_{CP,k-1}^{(A)}$ , and

$$S(\rho_E^{(b,k-1)}) - S(\rho_E^{(a,k-1)}) = S(\rho_{CP}^{(a,k-1)}) - S(\rho_{CP}^{(b,k-1)}) + I_{CP:E}(\rho_{CPE}^{(b,k-1)}) = S(\rho_{CP}^{(b,k-1)}) \geq 0, \quad (\text{II.131})$$

$$I_{CP:E}(\rho_{CPE}^{(b,k-1)}) = 2S(\rho_{CP}^{(b,k-1)}) \propto S(\rho_{CP}^{(b,k-1)}) \geq 0, \quad (\text{II.132})$$

for the channel  $\tilde{\mathcal{E}}_{CP,k-1}^{(B)}$ .

Similar as in Section II.5.1, we note that  $\rho_{CP}^{(a,k)}$  corresponds to a pure state when reset clocks which reset to pure states are considered. Consequently, the quantities in Eq. (II.129) and (II.130) vanish for such clocks and we do not regard them as faithful measures of the entropy production per tick of ticking clocks. Instead, we rely on the expressions obtained by analyzing the quantum channel  $\tilde{\mathcal{E}}_{CP,k-1}^{(B)}$  given in Eq. (II.131) and (II.132). That is, we identify  $\Sigma_k = S(\rho_{CP}^{(b,k-1)})$  as a suitable measure for the entropy production of the  $k$ th tick of ticking clocks. This coincides with the measure identified in Section II.5.1 based on the dilation of the observer-dependent clockwork states, see Eq. (II.115).

The change in environmental entropy  $\Delta S_E^{(k)} = S(\rho_E^{(b,k-1)}) - S(\rho_E^{(a,k-1)})$  remains unchanged irrespective of whether the channel  $\tilde{\mathcal{E}}_{CP,k-1}^{(B)}$  or  $\mathcal{E}_{C,k-1}^{(B)}$  is considered. As such, it satisfies the assumption that the expression for the entropy production per tick should remain invariant under purification of the initial clockwork state. In particular, we have

$$\Delta S_E^{(k)} = S(\rho_{CP}^{(b,k-1)}) = S(\rho_C^{(a,k-1)}) - S(\rho_C^{(b,k-1)}) + I(\rho_{CE}^{(b,k-1)}) \geq S(\rho_C^{(a,k-1)}) - S(\rho_C^{(b,k-1)}), \quad (\text{II.133})$$

$$\Delta S_{\text{E}}^{(k)} \geq -\Delta S_{\text{S}}^{(k)}. \quad (\text{II.134})$$

Thus the change in entropy of the environment which coincides with our measure for the entropy production per tick satisfies Landauer's bound. In fact, it satisfies the improved equality version of the bound. Finally, note that for the correlations, we have  $I_{\text{CP:E}} \geq I_{\text{C:E}}$  due to the monotonicity of quantum mutual information [25, 69]. Here,

$$I_{\text{CP:E}}(\rho_{\text{CPE}}^{(\text{b},k-1)}) = 2 \left( I(\rho_{\text{CE}}^{(\text{b},k-1)}) + S(\rho_{\text{C}}^{(\text{a},k-1)}) - S(\rho_{\text{C}}^{(\text{b},k-1)}) \right) \geq 0, \quad (\text{II.135})$$

where  $I_{\text{CP:E}}(\rho_{\text{CPE}}^{(\text{b},k-1)}) = I(\rho_{\text{CE}}^{(\text{b},k-1)})$  in case of reset clocks which reset to a pure state.

### II.5.2.a Alternative ticking channels

In principle, one can also think of a quantum channel  $\mathcal{E}_{k-1}^{(\text{C})}$  which connects the states of the clockwork before and after a given tick as

$$\rho_{\text{CP}}^{(\text{a},k)} = \mathcal{E}_{k-1}^{(\text{C})}(\rho_{\text{CP}}^{(\text{b},k-1)}). \quad (\text{II.136})$$

Such an analysis is motivated as follows: through concatenation of the two channels  $\tilde{\mathcal{E}}_{k-1}^{(\text{B})}$  and  $\mathcal{E}_{k-1}^{(\text{C})}$ , one obtains a channel which maps  $|\Psi\rangle\langle\Psi|_{\text{CP}}^{(\text{a},k-1)} \rightarrow \rho_{\text{CP}}^{(\text{a},k)}$ . This may also yield a sensible measure for the entropy production of the  $k$ th tick. The splitting of the overall process into two steps may allow us to capture the collapse of the clockwork during the tick event explicitly. A similar type of analysis has been considered in Ref. [72] in the context of quantum error correction. There, one finds that the entropy production associated with both the noise process and restoration process is typically large, whereas the entropy production of the overall joint process is small.

Here, we already invoke the assumption that the initial state of the clockwork is purified beforehand as  $|\Psi\rangle\langle\Psi|_{\text{CP}}^{(\text{a},k-1)}$ . Thus, the channel  $\mathcal{E}_{k-1}^{(\text{C})}$  takes in the state  $\rho_{\text{CP}}^{(\text{b},k-1)}$ , as opposed to  $\rho_{\text{C}}^{(\text{b},k-1)}$  (see Eq. (II.136)). In fact, the measures for the entropy production which would arise from the analysis of the channel

$$\rho_{\text{C}}^{(\text{a},k)} = \mathcal{E}_{k-1}^{(\text{C}')}\left(\rho_{\text{C}}^{(\text{b},k-1)}\right) \quad (\text{II.137})$$

vanish when considering reset clocks with reset to a pure state.

Because the quantum channel takes as input the state  $\rho_{\text{CP}}^{(\text{b},k-1)}$  obtained from  $|\Psi\rangle\langle\Psi|_{\text{CP}}^{(\text{a},k-1)}$  by application of the quantum channel  $\tilde{\mathcal{E}}_{k-1}^{(\text{B})}$ , there exist correlations between clockwork and environment, as calculated in Eq. (II.132). Consequently, the assumption of an initial product state is now only valid if the quantum channel  $\mathcal{E}_{k-1}^{(\text{C})}$  is dilated using a separate, “second”

environment  $E'$  that has not previously interacted with the subsystems CP or the environment E. Dilation of the channel  $\mathcal{E}_{k-1}^{(C)}$  then results in

$$U_{k-1}^{(C)} \rho_{CP}^{(b,k-1)} \otimes |0\rangle\langle 0|_{E'} U_{k-1}^{(C)\dagger} = \rho_{CPE'}^{(a,k)}. \quad (\text{II.138})$$

Here,

$$S(\rho_{CPE'}^{(a,k)}) = S(\rho_{CP}^{(a,k)}) + S(\rho_{E'}^{(a,k)}) - I_{CP:E'}(\rho_{CPE'}^{(a,k)}) = S(\rho_{CPE'}^{(b,k-1)}) = S(\rho_{CP}^{(b,k-1)}), \quad (\text{II.139})$$

such that

$$S(\rho_{E'}^{(a,k)}) - S(\rho_{E'}^{(b,k-1)}) = S(\rho_{CP}^{(b,k-1)}) - S(\rho_{CP}^{(a,k)}) + I_{CP:E'}(\rho_{CPE'}^{(a,k)}), \quad (\text{II.140})$$

and

$$I_{CP:E'}(\rho_{CPE'}^{(a,k)}) = S(\rho_{CP}^{(a,k)}) - S(\rho_{CP}^{(b,k-1)}) + S(\rho_{E'}^{(a,k)}). \quad (\text{II.141})$$

If we consider the special case of reset clocks which reset to a pure state we obtain

$$S(\rho_{E'}^{(a,k)}) - S(\rho_{E'}^{(b,k-1)}) = S(\rho_{CP}^{(b,k-1)}), \quad (\text{II.142})$$

$$I_{CP:E'}(\rho_{CPE'}^{(a,k)}) = S(\rho_{CP}^{(b,k-1)}). \quad (\text{II.143})$$

That is, for this class of clocks the change in the entropy of the environment  $E'$  and the built-up correlations coincide with our previous measure  $\Sigma_k = S(\rho_{CP}^{(b,k-1)})$ .

Adding both the changes in the entropy of environment E and  $E'$  during the  $k$ th tick denoted by  $\Delta S_E^{(k)}$  and  $\Delta S_{E'}^{(k)}$ , respectively, we obtain

$$\Delta S_E^{(k)} + \Delta S_{E'}^{(k)} = 2S(\rho_{CP}^{(b,k-1)}) - S(\rho_{CP}^{(a,k)}) + I_{CP:E'}(\rho_{CPE'}^{(a,k)}), \quad (\text{II.144})$$

and adding their correlations we have

$$I_{CP:E}(\rho_{CPE}^{(b,k-1)}) + I_{CP:E'}(\rho_{CPE'}^{(a,k)}) = S(\rho_{CP}^{(b,k-1)}) + S(\rho_{CP}^{(a,k)}) + S(\rho_{E'}^{(a,k)}). \quad (\text{II.145})$$

For reset clocks that reset to a pure state these quantities reduce to

$$\Delta S_E^{(k)} + \Delta S_{E'}^{(k)} = 2S(\rho_{CP}^{(b,k-1)}), \quad (\text{II.146})$$

$$I_{CP:E}(\rho_{CPE}^{(b,k-1)}) + I_{CP:E'}(\rho_{CPE'}^{(a,k)}) = 2S(\rho_{CP}^{(b,k-1)}). \quad (\text{II.147})$$

Again, we recover our previous measure  $\Sigma_k = S(\rho_{CP}^{(b,k-1)})$  when considering reset clocks which reset to a pure state. The addition of the contribution of the two environments E

and  $E'$  is motivated by the fact that the environment  $E$  participates in the process mapping  $|\Psi\rangle\langle\Psi|_{CP}^{(a,k-1)} \rightarrow \rho_{CP}^{(b,k-1)}$ , whereas  $E'$  interacts with the clockwork during the tick event  $\rho_{CP}^{(b,k-1)} \rightarrow \rho_{CP}^{(a,k)}$ .

We can formalize this approach and analyze the transition of the clockwork from  $|\Psi\rangle\langle\Psi|_{CP}^{(a,k-1)} \rightarrow \rho_{CP}^{(a,k)}$  by splitting it into two discrete steps,  $|\Psi\rangle\langle\Psi|_{CP}^{(a,k-1)} \rightarrow \rho_{CP}^{(b,k-1)}$  and  $\rho_{CP}^{(b,k-1)} \rightarrow \rho_{CP}^{(a,k)}$ , as follows

$$U_{CE,k-1} \otimes \mathbb{1}_{PE'}(|\Psi\rangle\langle\Psi|_{CP}^{(a,k-1)} \otimes |0\rangle\langle 0|_E \otimes |0\rangle\langle 0|_{E'}) U_{CE,k-1}^\dagger \otimes \mathbb{1}_{PE'} \rightarrow |\Psi\rangle\langle\Psi|_{CE}^{(b,k-1)} \otimes |0\rangle\langle 0|_{E'}, \quad (II.148)$$

$$U_{CE',k-1} \otimes \mathbb{1}_{PE}(|\Psi\rangle\langle\Psi|_{CE}^{(b,k-1)} \otimes |0\rangle\langle 0|_{E'}) U_{CE',k-1}^\dagger \otimes \mathbb{1}_{PE} \rightarrow |\Psi\rangle\langle\Psi|_{CPEE'}^{(a,k)}. \quad (II.149)$$

Here,  $U_{CE,k-1}$  and  $U_{CE',k-1}$  are obtained from dilating the channels  $\mathcal{E}_{k-1}^{(A)}$  and  $\mathcal{E}_{k-1}^{(C')}$  which map  $\rho_C^{(a,k-1)} \rightarrow \rho_C^{(b,k-1)}$  and  $\rho_C^{(b,k-1)} \rightarrow \rho_C^{(a,k)}$ , respectively. We obtain

$$S(\rho_{EE'}^{(a,k)}) = S(\rho_{CP}^{(a,k)}), \quad (II.150)$$

$$I_{CP:EE'}(\rho_{CPEE'}^{(a,k)}) = 2S(\rho_{CP}^{(a,k)}). \quad (II.151)$$

Note that both these quantities vanish when considering reset clocks which reset to a pure state. However, we can identify that for such clocks

$$I(\rho_{EE'}^{(a,k)}) = 2S(\rho_{CP}^{(b,k-1)}). \quad (II.152)$$

Thus, when considering the intra-environmental correlations as an additional source of entropy production, we obtain a non-zero entropy production per tick even for such clocks. In fact, intra-environmental correlations have been verified to play a significant role in the entropy production of open quantum systems [63] and analysis of multi-step processes such as quantum error correction [72]. For general ticking clocks the intra-environmental correlations are given as

$$I(\rho_{EE'}^{(a,k)}) = S(\rho_{CP}^{(b,k-1)}) - S(\rho_{CP}^{(a,k)}) + S(\rho_{CPE}^{(a,k)}). \quad (II.153)$$

We then instead consider

$$I_{tot,k} = I_{CP:EE'}(\rho_{CPEE'}^{(a,k)}) + I(\rho_{EE'}^{(a,k)}) = S(\rho_{CP}^{(b,k-1)}) + S(\rho_{CP}^{(a,k)}) + S(\rho_{E'}^{(a,k)}) \quad (II.154)$$

as the relevant quantity measuring the total entropy production per tick. Using the triangle inequality (see Appendix A) we have

$$S(\rho_{E'}^{(a,k)}) = S(\rho_{CPE}^{(a,k)}) \geq |S(\rho_{CP}^{(a,k)}) - S(\rho_E^{(a,k)})| = |S(\rho_{CP}^{(a,k)}) - S(\rho_{CP}^{(b,k-1)})|. \quad (II.155)$$

Using Eq. (II.155) we can lower bound Eq. (II.154) as

$$I_{\text{tot},k} \geq 2\max\{S(\rho_{\text{CP}}^{(b,k-1)}, S(\rho_{\text{CP}}^{(a,k)}))\} \geq S(\rho_{\text{CP}}^{(b,k-1)}) + S(\rho_{\text{CP}}^{(a,k)}) \geq 2\min\{S(\rho_{\text{CP}}^{(b,k-1)}), S(\rho_{\text{CP}}^{(a,k)})\}. \quad (\text{II.156})$$

Therefore, we have

$$I_{\text{tot},k} \geq 2S(\rho_{\text{CP}}^{(b,k-1)}), \quad (\text{II.157})$$

where equality is achieved by reset clocks which reset to a pure state. For such clocks  $S(\rho_{\text{CP}}^{(b,k-1)}) = S(\rho_{\text{E}'}^{(a,k)})$  and  $S(\rho_{\text{E}'}^{(a,k)}) = 0$ . That is,  $I_{\text{CP:EE}'}(\rho_{\text{CPEE}'}^{(a,k)}) = 0$  and  $I(\rho_{\text{EE}'}^{(a,k)}) = I_{\text{CP:EE}'}(\rho_{\text{CPEE}'}^{(b,k-1)}) = 2S(\rho_{\text{CP}}^{(b,k-1)})$ . Therefore, the quantity  $S(\rho_{\text{CP}}^{(b,k-1)})$  emerges as an achievable lower bound. We observe that for reset clocks that reset to a pure state the correlations that have built up between the subsystems CP and E leading up to the  $k$ th tick are completely transferred from the subsystem CP to the additional environment  $\text{E}'$  during the tick event. This is akin to perfect quantum error correction [72], where the evolution leading up to the tick corresponds to a noise process and the tick event corresponds to a restoration process. In that sense, reset clocks that reset to a pure state are the most optimal class of ticking clocks.

### II.5.3 Based on the second law of thermodynamics

In a third approach, we take the expression for the entropy production per tick in Eq. (II.26) as a starting point

$$\Sigma^{(A)} = I(\rho'_{\text{CE}}) + S(\rho'_E \| \rho_E) = S(\rho'_C) - S(\rho_C) + S(\rho'_E) - S(\rho_E) + S(\rho'_E \| \rho_E), \quad (\text{II.158})$$

$$\Sigma^{(B)} = I(\rho'_{\text{CE}}) = S(\rho'_C) - S(\rho_C) + S(\rho'_E) - S(\rho_E). \quad (\text{II.159})$$

Here,  $\Sigma^{(A)}$  and  $\Sigma^{(B)}$  correspond to the two different choices for the definition of heat, where  $\Sigma^{(B)}$  neglects the contribution given by the quantum relative entropy. *A priori*, both expressions are viable options. We have seen that these expressions gain their operational meaning as the analogous of the second law of thermodynamics in a thermal setting, see Section II.2.1. In particular, under the assumption of the existence of a joint unitary evolution of clockwork and environment, we found that the expressions coincide with the entropy production per tick of the thermodynamic ticking clocks.

Here, one may additionally account for initial correlations by replacing  $I(\rho_{\text{CE}})$  with  $\Delta I_{\text{CE}} = I(\rho'_{\text{CE}}) - I(\rho_{\text{CE}})$ , as was done in previous works [45, 53, 56, 57]. By adopting this change, we can extend the applicability of Eq. (II.158) and (II.159) to the general case where the clockwork and environment may initially be correlated. Because the quantum mutual information vanishes for uncorrelated product states  $I(\rho_C \otimes \rho_E) = 0$ , the first term in Eq. (II.158) and (II.159) given by  $I(\rho'_{\text{CE}})$  faithfully captures the *novel* correlations between system and environment that arise

during the joint evolution if the two are initially uncorrelated. Lifting this assumption results in a quantum mutual information which is generally non-zero  $I(\rho_{CE}) \geq 0$ . Consequently,  $\Delta I_{CE}$  now appropriately captures the change in correlations, as opposed to  $I(\rho'_{CE})$ . Note that the second term  $S(\rho'_E \| \rho_E)$  in Eq. (II.158) remains unaffected by this change. Substituting  $I(\rho'_{CE})$  with  $\Delta I_{CE}$  in Eq. (II.158) and (II.159), we obtain

$$\Sigma^{(A)} = \Delta I_{CE} + S(\rho'_E \| \rho_E) = S(\rho_S) - S(\rho_C) + S(\rho'_E) - S(\rho_E) + S(\rho'_E \| \rho_E), \quad (\text{II.160})$$

$$\Sigma^{(B)} = \Delta I_{CE} = S(\rho'_C) - S(\rho_C) + S(\rho'_E) - S(\rho_E). \quad (\text{II.161})$$

Meaning, the right-hand side of the expressions for the entropy production remain the same when adopting this change. However, in the absence of initial correlations, the entropy in Eq. (II.158) and (II.159) is guaranteed to be non-negative. On the contrary  $\Delta I_{CE}$  can, in general, attain negative values. Thus, the entropy in both Eq. (II.160) and (II.161) may become negative in presence of initial correlations. It is well known, that initial correlations (classical or quantum) constitute a resource of work that can, for example, be leveraged to let heat flow from cold to hot manifesting itself as an apparent violation of the second law of thermodynamics and inversion of the arrow of time [45, 50, 53, 56, 57]. In terms of the entropy production, such cases are ascribed negative values.

Here, we model the environment as the purifying system of the relevant observer-dependent clockwork states (see Section II.4.1). Intuitively, when considering reset clocks we expect the contribution from the change in the entropy of the clockwork  $\Delta S_C = S(\rho'_C) - S(\rho_C)$  to vanish because it undergoes a cyclic process in each tick. This can be achieved by choosing

$$\Delta S_C^{(k)} = S(\rho_C^{(a,k)}) - S(\rho_C^{(a,k-1)}). \quad (\text{II.162})$$

Modeling the environment as the purifying system of the clockwork states  $\rho_C^{(a,k)}$  and  $\rho_C^{(a,k-1)}$ , we obtain

$$\Sigma_k^{(A)} = S(\rho_C^{(a,k)}) - S(\rho_C^{(a,k-1)}) + S(\rho_C^{(a,k)}) - S(\rho_C^{(a,k-1)}) + S(\rho_C^{(a,k)} \| \rho_C^{(a,k-1)}) \quad (\text{II.163})$$

and

$$\Sigma_k^{(B)} = S(\rho_C^{(a,k)}) - S(\rho_C^{(a,k-1)}) + S(\rho_C^{(a,k)}) - S(\rho_C^{(a,k-1)}) \quad (\text{II.164})$$

as measures for the entropy production for the  $k$ th tick of a ticking clock. Note that when considering reset clocks which reset to a pure state both quantities (Eq. (II.163) and (II.164)) vanish. Following the arguments of the previous sections, we can address this by evaluating

the environment an instance before the  $k$ th tick and obtain

$$\Sigma_k^{(A)} = S(\rho_C^{(a,k)}) - S(\rho_C^{(a,k-1)}) + S(\rho_C^{(b,k-1)}) - S(\rho_C^{(a,k-1)}) + S(\rho_C^{(b,k-1)} \parallel \rho_C^{(a,k-1)}), \quad (\text{II.165})$$

$$\Sigma_k^{(B)} = S(\rho_C^{(a,k)}) - S(\rho_C^{(a,k-1)}) + S(\rho_C^{(b,k-1)}) - S(\rho_C^{(a,k-1)}). \quad (\text{II.166})$$

Note that if  $\rho_C^{(a,k-1)}$  is pure, we have  $S(\rho_C^{(b,k-1)} \parallel \rho_C^{(a,k-1)}) \rightarrow \infty$  in general. This is because  $\rho_C^{(b,k-1)}$  is generally mixed and  $S(\rho \parallel \sigma) = 0$  if and only if  $\rho = \sigma$  (see Appendix A). Thus, we adopt the measure given by  $\Sigma_k^{(B)}$ . Ultimately, the choice between  $\Sigma_k^{(A)}$  and  $\Sigma_k^{(B)}$  boils down to the assumptions about whether the local state of the environment is accessible or not, i.e., the relevant definition of heat [53].

The relevant candidate for the entropy production per tick is then given by

$$\Sigma_k^{(B)} = S(\rho_C^{(a,k)}) - S(\rho_C^{(a,k-1)}) + S(\rho_C^{(b,k-1)}) - S(\rho_C^{(a,k-1)}) = \Delta S_C^{(k)} + \Delta S_E^{(k)}, \quad (\text{II.167})$$

where  $\Delta S_C^{(k)} = S(\rho_C^{(a,k)}) - S(\rho_C^{(a,k-1)})$  and  $\Delta S_E^{(k)} = S(\rho_C^{(b,k-1)}) - S(\rho_C^{(a,k-1)})$ . We require that the change in entropy of the environment  $\Delta S_E^{(k)}$  is invariant under purification of the clockwork state  $\rho_C^{(a,k-1)}$ . Following the analysis in Section II.5.2, we choose  $\Delta S_E^{(k)} = S(\rho_{CP}^{(b,k-1)}) - S(|\Psi\rangle\langle\Psi|_{CP}^{(a,k-1)}) = S(\rho_{CP}^{(b,k-1)}) \geq 0$ . The expression for the entropy production is then given by

$$\Sigma_k^{(B)} = S(\rho_C^{(a,k)}) - S(\rho_C^{(a,k-1)}) + S(\rho_{CP}^{(b,k-1)}) = \Delta S_C^{(k)} + \Delta S_E^{(k)}. \quad (\text{II.168})$$

For reset clocks  $\Delta S_C^{(k)} = 0 \forall k \in \mathbb{N}_{>0}$ , and Eq. (II.168) reduces to

$$\Sigma_k^{(B)} = S(\rho_{CP}^{(b,k-1)}), \quad (\text{II.169})$$

which corresponds to the familiar expression of the entropy production per tick obtained in the previous sections. Note that we did not adjust the expression for the change in the entropy of the clockwork  $\Delta S_C^{(k)}$ . This may be motivated by the fact that it can be faithfully assessed by an observer who has access only to the states of the clockwork. However, we argued earlier that we expect the overall measure for the entropy production per tick to be invariant under purification of the clockwork state  $\rho_C^{(a,k-1)}$ . This discrepancy points to the fact that  $\Sigma_k^{(B)}$  (Eq. (II.168)) is not a well-suited measure for the entropy production per tick. Additionally, we note that  $\Sigma_k^{(B)}$  can assume negative values. Instead, if we also modify  $\Delta S_C^{(k)}$  accordingly, we obtain

$$\Sigma_k^{(B)} = S(\rho_{CP}^{(a,k)}) + S(\rho_{CP}^{(b,k-1)}) \geq S(\rho_{CP}^{(b,k-1)}) \geq 0. \quad (\text{II.170})$$

Not only does this change restore non-negativity of the measure, the quantity  $S(\rho_{CP}^{(b,k-1)})$  emerges as a lower bound. Moreover, reset clocks that reset to a pure state achieve equality in Eq. (II.170).

### II.5.4 Summary

To summarize the results obtained in Section II.5, we constructed the clock's environment by going to the church of the larger Hilbert space (see Section II.4) and identified the entropy production per tick of the ticking clock as the emerging correlations between the clock and environment, or equivalently, the change in entropy of the environment. We excluded several expressions for the entropy production per tick which emerged in the process by imposing the following condition:

- The entropy production of the first tick of a ticking clock specified by  $(\rho_C^0, (\mathcal{M}_{CR \rightarrow CR}^t)_{t \geq 0})$  should be invariant under purification of the initial state of the clockwork. That is, it should be identical to the entropy production of the first tick of the ticking clock  $(|\Psi\rangle\langle\Psi|_{CP}^0, (\tilde{\mathcal{M}}_{CPR \rightarrow CPR}^t)_{t \geq 0})$ , where  $|\Psi\rangle\langle\Psi|_{CP}^0$  is the purification of  $\rho_C^0$  with purifying system P and  $\tilde{\mathcal{M}}_{CPR \rightarrow CPR}^t = \mathcal{M}_{CR \rightarrow CR}^t \otimes \mathcal{I}_P \forall t \geq 0$ .

Based on the dilation of the observer-dependent clockwork states (see Section II.5.1) and the dilation of the corresponding ticking channels (see Section II.5.2) we obtained the following, well-motivated measure for the entropy production for the  $k$ th tick of a ticking clock

$$\Sigma_k = S(\rho_{CP}^{(b,k-1)}). \quad (\text{II.171})$$

In all other approaches in Section II.5.2.a and II.5.3, the measure in Eq. (II.171) emerges when considering the particular case of reset clocks which reset to pure states. Moreover, in some instances Eq. (II.171) also takes on the role of a lower bound. In the following, we thus refer to Eq. II.171 as the entropy production for the  $k$ th tick of a ticking clock.

## II.6 Re-analysis of thermodynamic ticking clock

Let us re-analyze the thermodynamic ticking clock (see Section II.1) in view of the measure for entropy production per tick of a (general) ticking clock derived in Section II.5. Looking at the representation of the thermodynamic ticking clock as given by Proposition 1, we see that the no-tick operators  $\{L_j\}$  characterize the interaction of the engine qubits within the clockwork with the thermal baths, whereas the tick operators  $\{J_j\}$  characterize the interaction of the ladder within the clockwork with the photon field. The Hermitian operator  $H$  describes the unitary part of the evolution of the clockwork, in particular the interaction of the ladder with the engine qubits. In Chapter I, we mentioned that any ticking clock written in the form of Proposition 1 can be realized via joint unitary evolution with an infinite-dimensional environment based on a time-independent Hamiltonian under appropriate limits, such as the weak-coupling or singular coupling limit.

Consider a ticking clock written in the form of Proposition 1 with an initial state of the clockwork  $\rho_C^0$ , a set of no-tick operators  $\{L_j\}$  and tick operators  $\{J_j\}$ , as well as a Hermitian operator  $H$ . We can construct another valid ticking clock by setting  $J_j = 0 \forall j$  and  $H = 0$ . Without considering the explicit limits (and thus informally), we can construct a Hamiltonian  $H_{\text{tot}}$  governing the joint evolution of this clock and an infinite-dimensional environment with an initial state given by  $\rho_C^0 \otimes \rho_E^0$ . Subsequently, we construct a novel ticking clock by “inclusion” of the environment into the clockwork. That is, we choose the initial state of the clockwork as  $\rho_C^0 \otimes \rho_E^0$  with vanishing no-tick operators  $L_j = 0 \forall j$ , tick operators  $J'_j = J_{C,j} \otimes \mathbb{1}_E$  which act trivially on the environment E, and a Hermitian operator  $H' = H_C \otimes \mathbb{1}_E + H_{CE,\text{tot}}$ , where  $H_C$  corresponds to the initial choice for the Hermitian operator. This corresponds to a valid ticking clock, albeit potentially with a clockwork of dimension  $d \rightarrow \infty$ . Intuitively, what we accomplished is to account for the action of the no-tick operators  $\{L_j\}$  by explicitly constructing an environment that yields the appropriate clock dynamics when undergoing a joint unitary evolution. Because this new ticking clock has vanishing no-tick operators  $L_j = 0 \forall j$ , we can write (see Appendix B.5 for a proof)

$$\tilde{\rho}_{CE}^{(0)}(t) = e^{-iH't-t/2\sum_j J_j'^\dagger J'_j} \rho_C^0 \otimes \rho_E^0 e^{iH't-t/2\sum_j J_j'^\dagger J'_j}. \quad (\text{II.172})$$

Based on this construction, we are guaranteed that  $\tilde{\rho}_C^{(0)}(t) = \text{tr}_E [\tilde{\rho}_{CE}^{(0)}(t)]$  coincides with the state of the clockwork of the original clock. The evolution specified by Eq. (II.172) is intuitive: the clockwork undergoes joint unitary evolution with its environment E and at each point in time a certain amount of probability is removed from the clockwork state due to the ticking process characterized by the tick operators  $\{J_j\}$ . In the context of the thermodynamic ticking clock, the unitary part of the dynamics corresponds to the unitary interaction of the thermal baths with the clockwork which drives the ladder out of equilibrium with respect to the photon field, whereas the spontaneous (stochastic) photon emission constitutes the ticking process. It is the heat exchange during the unitary interaction between clockwork and environment which constitutes the entropy production per tick in this case.

Analysing the states of clockwork and environment an instance before and after the first tick as described in Section II.3, we obtain

$$\rho_{CE}^{(b,0)} = \int_0^\infty P^{(0 \rightarrow 1)}(t) \rho_{CE}^{(0)}(t) dt \quad (\text{II.173})$$

$$\rho_{CE}^{(a,1)} = \int_0^\infty P^{(0 \rightarrow 1)}(t) \frac{\sum_j J'_j \rho_{CE}^{(0)}(t) J_j'^\dagger}{\text{tr} [\sum_j J'_j \rho_{CE}^{(0)}(t) J_j'^\dagger]} dt. \quad (\text{II.174})$$

Because the tick operators  $\{J'_j\}$  act trivially on the environment, we have

$$\text{tr}_C \left[ \frac{\sum_j J'_j \rho_{CE}^{(0)}(t) J'^\dagger_j}{\text{tr} \left[ \sum_j J'_j \rho_{CE}^{(0)}(t) J'^\dagger_j \right]} \right] = \text{tr}_C \left[ \rho_{CE}^{(0)}(t) \right] = \rho_E^{(0)}(t), \quad (\text{II.175})$$

and thus  $\rho_E^{(b,0)} = \rho_E^{(a,1)}$ . That is, the state of the environment is identical when evaluated an instance before and after the tick, i.e., before or after the application of the tick operators. In the thermodynamic ticking clock, the state of the environment is associated with the heat exchanged per tick. This analysis thus confirms the intuition that the heat exchanged per tick can be evaluated in an instance before or after a given tick. Given that this type of analysis also applies to any clock other than the thermodynamic ticking clock, we show that the state of the environment with which we associate an entropy production per tick is the same an instance before or after each tick. The state of the clockwork does, however, change due to the action of the tick operators. This is the reason why it is necessary to investigate the state of the clockwork just before a given tick to appropriately gauge its corresponding environment, as opposed to an instance after the tick. Furthermore, we observe that the environment with which we associate an entropy production per tick corresponds to the system which generates the clockwork dynamics as specified by the set of no-tick operators  $\{L_j\}$ , whereas the environment associated with the tick generation is related to the set of operators  $\{J_j\}$ . This reflects the splitting of the inner working of a ticking clock into a process that pushes the clockwork out of equilibrium and a stochastic, effectively irreversible process given by an out-of-equilibrium system evolving towards equilibrium, respectively [11].

Let us purify the initial state of clockwork and environment  $\rho_C^0 \otimes \rho_E^0$  to obtain the pure state  $|\Psi\rangle\langle\Psi|_{CP}^0 \otimes |0\rangle\langle 0|_{EE'}^0$ , where P is the purifying system of the clockwork C and E' is the purifying system of the environment E. Moreover, we extend the dynamics of the ticking clock to act trivially on the purifying systems by choosing

$$J'_{CE,j} \longrightarrow J'_{CE,j} \otimes \mathbb{1}_{PE'} \quad \forall j, \quad H'_{CE} \longrightarrow H'_{CE} \otimes \mathbb{1}_{PE'}. \quad (\text{II.176})$$

Again, this constitutes a valid ticking clock with a representation given in Proposition 1. With

$$A(t) = e^{-iH't - t/2 \sum_j J'^\dagger_j J'_j}, \quad (\text{II.177})$$

we can write the evolution given in Eq. (II.172) as

$$|\tilde{\Psi}\rangle\langle\tilde{\Psi}|_{CPPE'}^{(0)}(t) = A(t)|\Psi\rangle\langle\Psi|_{CP}^0 \otimes |0\rangle\langle 0|_{EE'}^0 A^\dagger(t). \quad (\text{II.178})$$

Here,  $|\tilde{\Psi}\rangle\langle\tilde{\Psi}|_{CPPE'}^{(0)}(t)$  corresponds to an unnormalized pure state. Thus, based on the Schmidt

decomposition (see Section II.4.1) we are guaranteed that  $S(\rho_{\text{CP}}^{(0)}(t)) = S(\rho_{\text{EE}'}^{(0)}(t))$ , where  $\rho_{\text{CP}}^{(0)}(t) = \text{tr}_{\text{EE}'} [\langle \Psi | \Psi |_{\text{CPEE}'}^{(0)}(t)]$  and  $\rho_{\text{EE}'}^{(0)}(t) = \text{tr}_{\text{CP}} [\langle \Psi | \Psi |_{\text{CPEE}'}^{(0)}(t)]$ . So we can compute

$$S(\rho_{\text{CP}}^{(b,0)}) = S \left( \int_0^\infty P^{(0 \rightarrow 1)}(t) \rho_{\text{CP}}^{(0)}(t) dt \right), \quad (\text{II.179})$$

and

$$S(\rho_{\text{EE}'}^{(b,0)}) = S \left( \int_0^\infty P^{(0 \rightarrow 1)}(t) \rho_{\text{EE}'}^{(0)}(t) dt \right). \quad (\text{II.180})$$

Note that  $\Sigma_1 = S(\rho_{\text{CP}}^{(b,0)})$ . While we have  $S(\rho_{\text{CP}}^{(0)}(t)) = S(\rho_{\text{EE}'}^{(0)}(t))$ , we are not guaranteed that  $S(\rho_{\text{CP}}^{(b,0)}) = S(\rho_{\text{EE}'}^{(b,0)})$  in general. This can be seen by the fact that the state

$$\rho_{\text{CPEE}'}^{(b,0)} = \int_0^\infty P^{(0 \rightarrow 1)}(t) |\Psi\rangle\langle\Psi|_{\text{CPEE}'}^{(0)}(t) dt \quad (\text{II.181})$$

is not pure in general, whereas  $|\Psi\rangle\langle\Psi|_{\text{CPEE}'}^{(0)}(t)$  is. We can, however, purify the state given in Eq. (II.181) using the purifying system  $E''$  to get  $|\Psi\rangle\langle\Psi|_{\text{CPEE}'E''}^{(b,0)}$ . Based on this, we note that our measure for the entropy production per tick (Eq. (II.171)) assesses the entropy of the subsystems  $\text{EE}'E''$ , as opposed to the subsystem  $\text{EE}'$  alone. This difference arises from the conditioning on the observer's knowledge, i.e., the integration over time. One can, however, show that

$$S(\rho_{\text{CP}}^{(b,0)}) = S \left( \int_0^\infty P^{(0 \rightarrow 1)}(t) \rho_{\text{CP}}^{(0)}(t) dt \right) \geq \int_0^\infty P^{(0 \rightarrow 1)}(t) S(\rho_{\text{CP}}^{(0)}(t)) dt \quad (\text{II.182})$$

$$= \int_0^\infty P^{(0 \rightarrow 1)}(t) S(\rho_{\text{EE}'}^{(0)}(t)) dt \geq \int_0^\infty P^{(0 \rightarrow 1)}(t) (|S(\rho_E^{(0)}(t)) - S(\rho_E^0)|) dt, \quad (\text{II.183})$$

where for the first inequality we made use of the concavity of the von Neumann entropy and for the second inequality we use the triangle inequality to write  $S(\rho_{\text{EE}'}^{(0)}(t)) \geq |S(\rho_E^{(0)}(t)) - S(\rho_E^0)| \forall t \geq 0$ . Here,  $S(\rho_{\text{EE}'}^{(0)}(t)) = S(\rho_E^0)$  because the dynamics act trivially on the purifying system  $E'$ . So our measure for the entropy production  $\Sigma_1$  can be lower bounded by the mean magnitude of the change in entropy of the environment  $E$  within the first tick, where the environment  $E$  generates the dynamics of the clockwork as specified by the no-tick generators  $\{L_j\}$  via a unitary interaction. Similarly, we have

$$S(\rho_E^{(b,0)}) - S(\rho_E^0) \geq \int_0^\infty P^{(0 \rightarrow 1)}(t) (S(\rho_E^{(0)}(t)) - S(\rho_E^0)) dt, \quad (\text{II.184})$$

where  $\rho_E^{(b,0)} = \text{tr}_{\text{CPEE}'} [\rho_{\text{CPEE}'}^{(b,0)}]$  (see Eq. (II.181)).

Figure II.7 compares the entropy production given by our measure in Eq. (II.171) and  $\Sigma_1^{\text{th}} = \beta_c Q_c - \beta_h Q_h$ , which was identified as the relevant measure in the context of the thermal

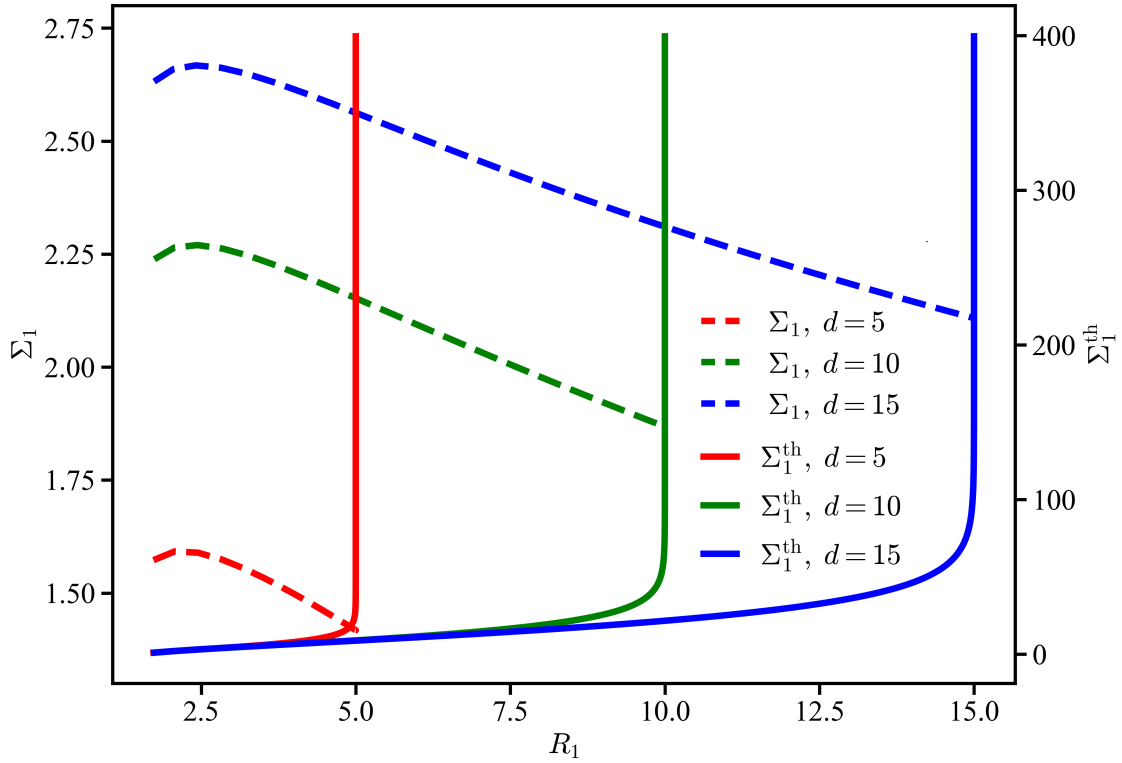


Figure II.7: Entropy production for the first tick given by our measure  $\Sigma_1$  (Eq. (II.171), dashed lines, y-scale on the left-hand side) and  $\Sigma_1^{\text{th}} = \beta_c Q_c - \beta_h Q_h$  (solid lines, y-scale on the right-hand side) as a function of the accuracy  $R_1$  for thermodynamic ticking clocks treated in the biased random walk approximation (Eq. (II.13)) with varying ladder dimension  $d$ . The numerical simulations are performed as outlined in Fig. II.2 with the same choices of the remaining parameters.

environment of thermodynamic ticking clocks (see Section II.1), for various thermodynamic ticking clocks in the weak-coupling limit. Note that  $\Sigma_1^{\text{th}}$  does not involve explicit conditioning of the state of the environment on the observation of a tick. Instead, the conditioning is done implicitly. The measure  $\Sigma_1^{\text{th}}$  increases steadily with increasing accuracy  $R_1$  of the thermodynamic ticking clocks and diverges as the accuracy approaches its classically-allowed limit of  $R = d$ , i.e., as the thermodynamic ticking clock approaches an optimal ladder clock with a ladder of dimension  $d$ . In contrast, our entropy measure may decrease with increasing accuracy for a fixed ladder dimension  $d$  and is strictly bounded from above by  $2 \ln(d_C)$ , where  $d_C$  is the dimension of the clockwork Hilbert space (see Appendix A). Nevertheless, both expressions for the entropy production per tick are strictly non-negative and seem to exhibit a lower bound at a given accuracy that increases with increasing accuracy. Note that despite the drastic difference in scale, our measure for the entropy production does not constitute a lower

bound to  $\Sigma_1^{\text{th}}$ . As outlined above, ultimately the differences between the two measures can be explained by the fact that they assess the change in entropy in different (sub-)systems and rely on a different conditioning of the entropy production on the observation of a tick. This comes at the benefit of our measure being independent of the particular physical implementation of a ticking clock specified by  $(\rho_C^0, (\mathcal{M}_{\text{CR} \rightarrow \text{CR}}^t)_{t \geq 0})$ .



## Chapter III

# Relationship between accuracy and entropy production of ticking clocks

In this chapter, we are concerned with investigating the relationship between the accuracy of ticking clocks in our model (see Chapter I) and their entropy production per tick (see Chapter II). The existence of a fundamental trade-off between these quantities has been investigated in several recent works for a restricted class of (thermodynamic) ticking clocks [11, 18–20] (see Section II.1). In particular, all these works find that there exists a minimal amount of irreversible entropy production per tick, or equivalently, a minimal amount of energy dissipation per tick, which increases with increasing accuracy of these clocks. The precise relationship between the accuracy and these quantities does, however, vary. As such, these works identified the entropy production per tick, or equivalently, the dissipated heat per tick, of ticking clocks as a fundamental resource for measuring time. Thereby, they establish a connection between the arrow of time and the irreversibility of the ticking clock governed by the second law of thermodynamics.

The question that remains is whether this connection is specific to the ticking clocks studied in these works or a general property of ticking clocks – and thus a fundamental aspect of measuring time. To tackle this question, we have motivated an expression for the entropy per tick of a ticking clock treated in the axiomatic framework put forwards in Chapter I. One can verify that the ticking clocks studied in Refs. [11, 18] are, in fact, special classes of ticking clocks of the type introduced Chapter I. Our measure for the irreversible entropy per tick quantifies the irreversibility of the underlying clockwork dynamics arising from its interaction with the environment and is not restricted to any particular implementation, i.e., clockwork environment. From an information-theoretic perspective, a clock is a system that emits information about time [14]. Our expression for the entropy production per tick of a ticking clock quantifies the correlations which build up between the clockwork and its environment, and

can thus be seen as a measure for the shared information between system and environment, or equivalently, the information about the system which leaks into the environment. The finding and characterization of a minimal entropy production per tick which increases with the accuracy of ticking clocks would thus shed light on the minimal information-theoretic resources required to measure time.

### III.1 Quantum ticking clocks

We start with an investigation of the relationship between the accuracy of general quantum ticking clocks and their entropy production per tick. In Section III.2, we will then restrict our analysis to the set of classical ticking clocks (Def. 4).

#### III.1.1 Zero temporal information at vanishing entropy production per tick

Remember that the accuracy  $R_1$  of the first tick of a reset clock corresponds to the number of ticks that the clock generates on average before the next tick has a standard deviation equal to the mean time between ticks (see Section I.2). Consequently, if  $R_1 < 1$  our uncertainty in the mean time between ticks is larger than the time interval itself and we effectively do not gain any information about time from such a clock. On the contrary, a useful clock is characterized by  $R_1 > 1$ , where we get more (certain) information about time with increasing accuracy. A ticking clock with  $R_1 = 1$  can thus be interpreted as a clock that yields no information about time at all. Here, we show by explicit construction that a ticking clock with  $R_1 = 1$  must not produce any amount of entropy per tick.

Consider the special class of ticking clocks for which

$$\sum_{j=1}^{N_L} J_j^\dagger J_j = \lambda \mathbb{1}, \quad \lambda > 0, \quad L_j = 0 \quad \forall j \in (1, N_L), \quad (\text{III.1})$$

with an arbitrary Hermitian operator  $H$ . Because the no-tick operators all vanish, we can write (see Appendix B.5 for proof)

$$\tilde{\rho}_C^{(k-1)}(t) = e^{-\lambda t} e^{-iHt} \rho_C^{(a,k-1)} e^{iHt} \quad \forall k \in \mathbb{N}_{>0}, \forall t \geq 0. \quad (\text{III.2})$$

We have

$$P^{(k-1 \rightarrow k)}(t) = \text{tr} \left[ \sum_j J_j^\dagger J_j \tilde{\rho}_C^{(k-1)}(t) \right] = \lambda \text{tr} \left[ \tilde{\rho}_C^{(k-1)}(t) \right] = \lambda e^{-\lambda t}, \quad (\text{III.3})$$

with

$$\int_0^\infty \lambda e^{-\lambda t} dt = 1, \quad (\text{III.4})$$

$$\mu = \int_0^\infty t \lambda e^{-\lambda t} dt = 1/\lambda, \quad (\text{III.5})$$

$$\sigma^2 = \int_0^\infty (t - \mu)^2 \lambda e^{-\lambda t} dt = 1/\lambda^2. \quad (\text{III.6})$$

Given that  $P^{(0 \rightarrow 1)}(t)$  coincides with the delay function of the first tick, we have  $R_1 = \mu^2/\sigma^2 = 1$ . To assess the entropy production per tick of this class of clocks, we calculate

$$\rho_C^{(b,k-1)} = \int_0^\infty P^{(k-1 \rightarrow k)}(t) \rho_C^{(k-1)}(t) dt = \int_0^\infty \lambda e^{-\lambda t} e^{-iHt} \rho_C^{(a,k-1)} e^{iHt} dt, \quad (\text{III.7})$$

and

$$\rho_C^{(a,k)} = \int_0^\infty \sum_j J_j \tilde{\rho}_C^{(k-1)}(t) J_j^\dagger dt = \int_0^\infty e^{-\lambda t} \sum_j J_j e^{-iHt} \rho_C^{(a,k-1)} e^{iHt} J_j^\dagger. \quad (\text{III.8})$$

We choose  $J_j = \sqrt{\lambda/N_L} \mathbb{1} \forall j \in (1, N_L)$ , which renders these clocks reset clocks and yields

$$\rho_C^{(a,k)} = \int_0^\infty \lambda e^{-\lambda t} e^{-iHt} \rho_C^{(a,k-1)} e^{iHt} dt = \rho_C^{(b,k-1)}. \quad (\text{III.9})$$

If we set  $H = 0$ , we additionally have  $\rho_C^{(a,k)} = \rho_C^{(b,k-1)} = \rho_C^{(a,k-1)}$ . Thus,  $\Sigma_k = \Sigma_1$  and  $R_k = kR_1 = k$  for all  $k \in \mathbb{N}_{>0}$ . Now, we choose the initial state to be a pure state  $\rho_C^0 = |\Psi\rangle\langle\Psi|_C^0$  which makes these reset clocks that reset to a pure state. We have  $\rho_C^{(a,k)} = \rho_C^{(b,k)} = |\Psi\rangle\langle\Psi|_C^0 \forall k \in \mathbb{N}$  and all corresponding entropies vanish, resulting in  $\Sigma_k = \Sigma_1 = 0$ .

Note that this clock is classical, because the clockwork remains incoherent throughout its dynamics. One can check that its classical representation (see Corollary 1) is given by the choice

$$\vec{v}_C^0 = \vec{e}_0, \quad \mathcal{N} = -\lambda \mathbb{1}, \quad \mathcal{T} = \lambda \mathbb{1}. \quad (\text{III.10})$$

Thus, we demonstrated that one can always find a reset clock with a clockwork of arbitrary dimension that resets to a pure state for which  $R_k = kR_1 = k$  and  $\Sigma_k = 0 \forall k \in \mathbb{N}_{>0}$ . The delay function of the first tick  $\tau^{(1)}(t) = \lambda e^{-\lambda t}$  is given by a simple Poisson distribution which reflects the fact that the clockwork only undergoes a trivial evolution and exhibits Poissonian tick statistics. The entropy production per tick is fundamentally linked to the non-unitary dynamics generated by the no-tick operators  $\{L_j\}_{j=0}^{N_L}$ . The ticking clocks considered here do not exhibit such dynamics and thus have a vanishing minimal entropy production per tick.

In the quantum case with  $\rho_C^0 = |\Psi\rangle\langle\Psi|_C^0$  we can, for example, also consider the choice

$$J_j = \sqrt{\lambda/d} |\Psi\rangle\langle\Psi_j|_C \quad \forall j \in (1, d), \quad L_j = 0 \quad \forall j \in (1, d), \quad (\text{III.11})$$

with  $\{|\Psi_j\rangle_C\}_{j=1}^d$  some orthonormal basis of  $\mathcal{H}_C$ . Then,

$$\sum_j J_j \rho_C J_j^\dagger = \lambda |\Psi\rangle\langle\Psi|_C^0 \propto |\Psi\rangle\langle\Psi|_C^0, \quad (\text{III.12})$$

and

$$\sum_{j=1}^d J_j^\dagger J_j = \sum_{j=1}^d \lambda/d |\Psi_j\rangle\langle\Psi_j|_C = \lambda \mathbb{1}, \quad (\text{III.13})$$

such that these clocks are reset clocks that reset to a pure state and achieve  $R_k = kR_1 = k$ . But now let us choose  $H \neq 0$ , then

$$\rho_C^{(b,k-1)} = \rho_C^{(b,0)} = \int_0^\infty \lambda e^{-\lambda t} e^{-iHt} |\Psi\rangle\langle\Psi|_C^0 e^{iHt} dt, \quad (\text{III.14})$$

and  $\rho_C^{(a,k)} = |\Psi\rangle\langle\Psi|_C^0$ . With  $H \neq 0$ , we have  $\Sigma_k = \Sigma_1 = S(\rho_C^{(b,0)}) \neq 0$  in general, whereas the choice  $H = 0$  yields  $\Sigma_k = 0$ . However, for any choice of  $H$  this class of clocks still only achieves an accuracy  $R_k = kR_1 = k$ , because the delay functions governing the accuracy of the clock are independent of  $H$ . This example illustrates the point that a large entropy production per tick does not necessarily imply a large accuracy. The clock can produce entropy without “using” it as a resource to improve its accuracy. In general, we will find many clocks at a given accuracy that produce more than the conjectured minimal amount of entropy per tick. To conclude, this motivates the idea of a minimal amount of entropy per tick at a given accuracy, rather than a direct correspondence between the irreversible entropy production per tick and the accuracy of ticking clocks.

### III.1.2 Infinite temporal information at vanishing entropy production

In the case of general quantum ticking clocks, we are able to show that one can achieve  $\Sigma_k \rightarrow 0$  in the limit of infinite accuracy  $R_1 \rightarrow \infty$ , where  $R_k = kR_1$ . This is in contrast to the previous conjecture that any ticking clock must produce a minimal amount of entropy per tick at a given accuracy which increases with increasing accuracy.

To show this, consider the class of reset clocks which reset to a pure state  $\rho_C^0 = |\Psi\rangle\langle\Psi|_C^0$  with vanishing no-tick operators  $L_j = 0 \forall j \in (1, N_L)$ . With this choice  $\rho_C^{(b,k)} = \rho_C^{(b,0)}$ , and  $\rho_C^{(a,k)} = |\Psi\rangle\langle\Psi|_C^0$ , as well as  $R_k = kR_1$  and  $\Sigma_k = \Sigma_1$ . Because the no-tick operators all vanish, we can write (see Appendix B.5 for proof)

$$\tilde{\rho}_C^{(0)}(t) = e^{-iHt - t/2 \sum_j J_j^\dagger J_j} |\Psi\rangle\langle\Psi|_C^0 e^{iHt - t/2 \sum_j J_j^\dagger J_j}, \quad (\text{III.15})$$

where

$$\rho_C^{(b,1)} = \int_0^\infty P^{(0 \rightarrow 1)}(t) \rho_C^{(0)}(t) dt. \quad (\text{III.16})$$

Let us write

$$e^{-iHt-t/2\sum_j J_j^\dagger J_j} |\Psi\rangle\langle\Psi|_C^0 e^{iHt-t/2\sum_j J_j^\dagger J_j} = A(t)|\Psi\rangle\langle\Psi|_C^0 A^\dagger(t) = |\tilde{\Psi}\rangle\langle\tilde{\Psi}|_C(t), \quad (\text{III.17})$$

where  $|\tilde{\Psi}\rangle\langle\tilde{\Psi}|_C(t)$  corresponds to an unnormalized pure state. In the limit  $R \rightarrow \infty$ , we have  $P^{(0 \rightarrow 1)}(t) \rightarrow \delta(t - \mu)$ , and thus

$$\rho_C^{(b,1)} = \int_0^\infty \delta(t - \mu) |\Psi\rangle\langle\Psi|_C(t) dt = |\Psi\rangle\langle\Psi|_C(\mu). \quad (\text{III.18})$$

This results in  $\Sigma_k = S(\rho_C^{(b,1)}) = S(|\Psi\rangle\langle\Psi|_C(\mu)) = 0$ . Thus, in the infinite accuracy limit, such clocks can achieve zero entropy production per tick. Note that this proof relies on the assumption that there exists a ticking clock of this form which is capable of achieving the infinite accuracy limit  $R_1 \rightarrow \infty$ . We can show by explicit construction that there exists such a ticking clock: the quasi-ideal quantum clock [14, 15] discussed in Section I.1.2 is a reset clock that resets to a pure state with  $L_j = 0 \forall j \in (1, N_L)$  that has been proven to achieve an accuracy  $R_1 \geq d^{2-\epsilon} + o(d^{2-\epsilon})$  at large  $d$  for any arbitrary  $\epsilon > 0$ . Hence, we obtain the result outlined above in the limit  $d \rightarrow \infty$  when considering such a quasi-ideal ticking clock.

This result can be understood as follows: the above proof exploits the fact that these ticking clocks have vanishing no-tick operators  $L_j = 0 \forall j \in (1, N_L)$ . Meaning, the particular interaction between clockwork and environment which we have ascribed to be the underlying source of entropy production vanishes. These ticking clocks only interact with an environment as part of the tick-generating process, which is characterized by the set of tick operators  $\{J_j\}_{j=1}^{N_L}$ . Note that this interaction is fundamental to any ticking clock, because ticking clocks for which  $J_j = 0 \forall j \in (1, N_L)$  cannot produce any ticks. On the contrary, looking at the quasi-ideal clock, for example, we see that the interaction characterized by the no-tick operators  $\{L_j\}_{j=1}^{N_L}$  is not essential to achieve high accuracy. The question that remains is how physical such ticking clocks are, and thus, how physical the result of a vanishing entropy production per tick in the infinite accuracy limit is.

A ticking clock with vanishing no-tick operators entirely relies on unitary dynamics of the clockwork generated by the Hermitian operator  $H$  during its evolution leading up to a tick. In particular, its only interaction with an environment is during the inevitable tick-generating process. Consider, for example, a macroscopic pendulum clock [20]. In the absence of any dissipation, i.e., interaction with its environment (except during the inevitable readout of the pendulum position), and for small oscillations, the pendulum dynamics are properly de-

scribed by Hamilton's equations of motion: the pendulum will oscillate at constant amplitude and frequency. Consequently, this pendulum clock achieves infinite accuracy by our measure. Moreover, because the pendulum has a well-defined position at each point, i.e., is always in a definite state throughout its evolution, it would also produce zero entropy when naively applying our measure. This is in close analogy to the quasi-ideal ticking clocks which achieve zero entropy production with coherent internal dynamics at infinite accuracy.

We know, however, that any physical realization of this ticking clock, i.e., any macroscopic pendulum clock, will eventually stop oscillating due to internal friction, collisions with air molecules, or other (unwanted) interactions with its environment. Instead, any sustained oscillation requires some sort of external driving which provides the necessary work to counteract the energy lost due to dissipation. In the case of the pendulum clock, one is able to achieve sustained oscillation in the form of limit cycles. Reaching a large accuracy requires a large driving force which, in turn, necessitates a larger heat dissipation according to the fluctuation-dissipation theorem [76, 77]. Note that heat dissipation can be seen as a source of entropy production. The dynamics of such a clock in the presence of dissipation necessarily involve some non-zero no-tick operators  $L_j \neq 0$  that characterize this inevitable interaction of the clock with its environment.

The example of a pendulum clock illustrates the fundamental necessity of ticking clocks with non-zero no-tick operators when trying to model physically realizable, macroscopic clocks. We remind ourselves that the above proof relies on taking the limit  $d \rightarrow \infty$  to reach infinite accuracy, which we expect to be a general feature independent of whether a quasi-ideal ticking clock is considered. In the limit of large system size, the appearance of decoherence phenomena becomes unavoidable [26, 77–79]. In general, macroscopic systems will never be isolated from their environments and the loss of quantum coherence arises due to an inevitable interaction with the environment and the correlations that arise in the process. These correlations lead to the emergence of classical dynamics characterized by vanishing quantum coherence and diagonal density matrices. In fact, it is widely believed that classical physics arises from quantum mechanics due to naturally occurring decoherence [80, 81]. In the context of our ticking clock model, such dynamics are accounted for by the class of classical ticking clocks. In particular, when approaching the limit  $d \rightarrow \infty$ , and thus the  $R \rightarrow \infty$  limit, this will be the relevant class of ticking clocks that is currently physically realizable. One can only speculate how far technological advancements will push the limits on the size of quantum systems which can still be controlled in a coherent manner [82]. Instead of considering ticking clocks with partially coherent dynamics, we will restrict ourselves to the class of classical ticking clocks which exhibit completely incoherent dynamics in the following.

For classical ticking clocks the above proof does not apply, because one may always choose  $H = 0$  for such clocks. The particular case of vanishing no-tick operators then corresponds to a diagonal no-tick generator  $\mathcal{N}$ . Such clocks can be shown to achieve a maximal accuracy of  $R_k = kR_1 = k$  (see Appendix B.6 for a proof). As such, for classical ticking clocks the interaction with the environment characterized by the no-tick operators  $\{L_j\}_{j=1}^{N_L}$  becomes essential to achieve high accuracy. Given that we identified this interaction as the key source of entropy production, we expect these clocks to exhibit a fundamental trade-off between their irreversible entropy production and accuracy.

Before moving to the classical case, we note that the above proof exposes another related issue. We can follow the construction scheme in Section II.6 to obtain

$$\tilde{\rho_{CE}}^{t,0} = e^{-iH't-t/2\sum_j J_j^\dagger J_j} \rho_C^0 \otimes \rho_E^0 e^{iH't-t/2\sum_j J_j^\dagger J_j}. \quad (\text{III.19})$$

from an arbitrary ticking clock with  $L_j \neq 0 \forall j \in \{1, 2, \dots, N_L\}$ . Thus, starting from any arbitrary ticking clock we can construct a ticking clock for which  $L_j = 0 \forall j \in \{1, 2, \dots, N_L\}$  by including the corresponding (possibly) infinite-dimensional environment in the clockwork. Considering the specific example of the thermodynamic ticking clock, this would correspond to the inclusion of the two heat baths in the clockwork itself. Clearly, such situations are unphysical. However, note that the dynamics on subsystem C of this new clockwork given by CE remain unchanged. Thereby, the accuracy of the clock remains unchanged. Thus, while we expect to be able to construct such ticking clocks at any accuracy in the limit  $d \rightarrow \infty$ , zero entropy production can still only be achieved in the limit  $P^{(0 \rightarrow 1)}(t) \rightarrow \delta(t - \mu)$ , i.e.,  $R \rightarrow \infty$ .

One can exclude the clocks arising from such a construction scheme by restricting the clockwork dimension to be finite. Moreover, one can introduce the notion of a “minimal” clockwork which enforces any dynamics that can be generated by an appropriate interaction with the environment to be implemented in such a manner, rather than via inclusion of the environment into the clockwork itself:

- Consider a ticking clock  $(\rho_C^0, (\mathcal{M}_{CR \rightarrow CR}^t)_{t \geq 0})$  which achieves a certain accuracy  $\{R_k\}_{k \in \mathbb{N}_{>0}}$ . We define its minimal implementation as the ticking clock specified by

$$(\rho_{C_{\min}}^0, (\mathcal{M}_{C_{\min}R \rightarrow C_{\min}R}^t)_{t \geq 0}) \quad (\text{III.20})$$

which achieves the same accuracy, where

$$\mathcal{M}_{C_{\min}R \rightarrow C_{\min}R}^t(\rho_{C_{\min}R}^0) = \text{tr}_{C'}(\mathcal{M}_{CR \rightarrow CR}^t(\rho_{CR}^0)) \forall t \geq 0. \quad (\text{III.21})$$

The bipartition  $\mathcal{H}_C = \mathcal{H}_{C_{\min}} \otimes \mathcal{H}_{C'}$  is chosen such that  $\dim(\mathcal{H}_{C_{\min}})$  is minimal.

Note that this guarantees that the two clocks yield the same dynamics on the subsystem  $C_{\min}$  of the clockwork  $C$  itself which is responsible for the tick generation, i.e., can be identified as the source of timing. Ultimately, one would then be concerned with finding the relation between the entropy production per tick and accuracy given the minimal implementation of each clock.

### III.2 Classical ticking clocks

In this section, we will analyze the relation between the entropy production per tick and accuracy for classical ticking clocks (Def. 4). In classical notation, the relevant observer-dependent clockwork states (see Section II.3) can be expressed as

$$\vec{v}_C^{(b,k-1)} = \int_0^\infty \|\mathcal{T}e^{\mathcal{N}t}\vec{v}_C^{(a,k-1)}\| \frac{e^{\mathcal{N}t}\vec{v}_C^{(a,k-1)}}{\|e^{\mathcal{N}t}\vec{v}_C^{(a,k-1)}\|} dt, \quad (\text{III.22})$$

$$\vec{v}_C^{(a,k)} = \int_0^\infty \|\mathcal{T}e^{\mathcal{N}t}\vec{v}_C^{(a,k-1)}\| \frac{\mathcal{T}e^{\mathcal{N}t}\vec{v}_C^{(a,k-1)}}{\|\mathcal{T}e^{\mathcal{N}t}\vec{v}_C^{(a,k-1)}\|} dt = \int_0^\infty \mathcal{T}e^{\mathcal{N}t}\vec{v}_C^{(a,k-1)} dt, \quad (\text{III.23})$$

where  $\vec{v}_C^{(a,0)} = \vec{v}_C^0$  (see Appendix B.7 for a proof). The entropy of a clockwork state is then calculated as

$$S(\vec{v}) = \sum_i -v_i \ln(v_i), \quad (\text{III.24})$$

where  $S(\vec{v})$  denotes the Shannon entropy and  $\vec{v} = \sum_i v_i \vec{e}_i$  with  $\{\vec{e}_i\}_{i=0}^{d-1}$  some orthonormal basis of  $\mathbb{R}^d$ .

Remember that our measure for the entropy production per tick devised Section II.5 satisfies the following property: given a ticking clock  $(\rho_C^0, (\mathcal{M}_{\text{CR} \rightarrow \text{CR}}^t)_{t \geq 0})$ , the entropy production of its  $k$ th tick  $\Sigma_k$  corresponds to the entropy production of the first tick  $\Sigma_1$  of the ticking clock given by  $(|\Psi\rangle\langle\Psi|_{\text{CP}}^{(a,k-1)}, (\tilde{\mathcal{M}}_{\text{CPR} \rightarrow \text{CPR}}^t)_{t \geq 0})$ , which we will call its “conditional” clock of the  $k$ th tick. Hence, the entropy production of any ticking clock can be investigated by looking at the entropy production of the first tick of its conditional clocks. Note that the accuracy of the first tick  $R_1$  of the conditional clock is identical to the accuracy of the first tick of the clock given by  $(\rho_C^{(a,k-1)}, (\mathcal{M}_{\text{CR} \rightarrow \text{CR}}^t)_{t \geq 0})$ . This is because the accuracy is assessed based on the dynamics of subsystem  $C$  alone, i.e., the tick operators act trivially on the purifying system  $P$ . For a reset clock all conditional clocks are identical, which results in  $\Sigma_k = \Sigma_1 \forall k \in \mathbb{N}_{>0}$ . The conditional clocks are simply a special class of ticking clocks whose initial clockwork is in a pure state:  $(|\Psi\rangle\langle\Psi|_C^0, (\mathcal{M}_{\text{CR} \rightarrow \text{CR}}^t)_{t \geq 0})$ . To start our investigation of the relation between the entropy production per tick and accuracy of all classical ticking clocks, we thus analyze the first tick of classical ticking clocks that are initialized in a pure state and the resulting relation

between  $\Sigma_1$  and  $R_1$ .

### III.2.1 Analysis of first tick

The entropy production of the  $k$ th tick of a classical ticking clock is in general given by  $\Sigma_k = S(\vec{v}_{\text{CP}}^{(b,k-1)})$ . Because we restrict our analysis to the first tick ( $k = 1$ ) of classical ticking clocks that are initialized in a pure state, the relevant quantities to investigate are  $\Sigma_1 = S(\vec{v}_{\text{C}}^{(b,0)})$  and  $R_1$ . In the following, w.l.o.g. we choose  $\vec{v}_{\text{C}}^0 = \vec{e}_0 = (1, 0, \dots, 0)^T$ .

Note that  $P^{(0 \rightarrow 1)}(t)$ , and thus  $R_1$ , as well as  $\vec{v}_{\text{C}}^{(b,0)}$  are independent of the choice of the no-tick generator  $\mathcal{T}$ . We can show this by rewriting  $P^{(0 \rightarrow 1)}(t)$  as

$$P^{(0 \rightarrow 1)}(t) = \|\mathcal{T}e^{\mathcal{N}t}\vec{v}^0\| = \sum_{ij} v_{\text{C},i}^0 (e^{\mathcal{N}t})_{ji} \|\vec{\mathcal{T}}_j\|, \quad (\text{III.25})$$

where  $\vec{\mathcal{T}}_j$  denotes the vector given by the  $j$ th column of  $\mathcal{T}$ . By Corollary 1, this column sum is guaranteed to satisfy

$$\|\vec{\mathcal{T}}_j\| = \sum_{i=0}^{d-1} \mathcal{T}_{ij} = - \sum_{i=0}^{d-1} \mathcal{N}_{ij} \geq 0. \quad (\text{III.26})$$

Using Eq. (III.26) we can rewrite Eq. (III.25) as

$$P^{(0 \rightarrow 1)}(t) = \sum_{ij} v_{\text{C},i}^0 (e^{\mathcal{N}t})_{ji} \left( - \sum_k \mathcal{N}_{kj} \right). \quad (\text{III.27})$$

Looking at Eq. (III.27), we see that  $P^{(0 \rightarrow 1)}(t)$  is independent of the choice of  $\mathcal{T}$ . Moreover, we have

$$\vec{v}_{\text{C}}^{(b,0)} = \int_0^\infty P^{(0 \rightarrow 1)}(t) \frac{e^{\mathcal{N}t} \vec{v}_{\text{C}}^0}{\|e^{\mathcal{N}t} \vec{v}_{\text{C}}^0\|} dt, \quad (\text{III.28})$$

thereby  $\Sigma_1 = S(\vec{v}_{\text{C}}^{(b,0)})$  is also independent of  $\mathcal{T}$ .

Therefore, for any valid no-tick generator  $\mathcal{N}$  satisfying  $\sum_{i=0}^{d-1} \mathcal{N}_{ij} \leq 0 \forall j$  we can construct a valid tick generator  $\mathcal{T}$  such that  $\sum_{k=0}^{d-1} \mathcal{T}_{kj} + \mathcal{N}_{kj} = 0 \forall j$  without affecting  $\Sigma_1$  or  $R_1$ . In particular, the choice of  $\mathcal{N}$  only restricts the column sums of  $\mathcal{T}$  given by

$$s_j = \|\vec{\mathcal{T}}_j\| = \sum_{i=0}^{d-1} \mathcal{T}_{ij} = - \sum_{i=0}^{d-1} \mathcal{N}_{ij} \geq 0. \quad (\text{III.29})$$

The set of valid tick generators compatible with the no-tick generator  $\mathcal{N}$  is given by all tick generators  $\mathcal{T}$  whose column sums satisfy Eq. III.29. This includes the following choice

$$\mathcal{T}_r = (s_1 \vec{v}_{\text{C},r}, s_2 \vec{v}_{\text{C},r}, \dots, s_d \vec{v}_{\text{C},r}), \quad (\text{III.30})$$

where  $\vec{v}_{C,r}$  is an arbitrary normalized state vector and corresponds to the reset state of  $\mathcal{T}_r$ . For any arbitrary normalized state vector  $\vec{v}_C$ , we have

$$\mathcal{T}_r \vec{v}_C = \sum_i v_{C,i} s_i \vec{v}_{C,r} \propto \vec{v}_{C,r}. \quad (\text{III.31})$$

Any classical ticking clock initialized in a state  $\vec{v}_{C,r}$  with a tick generator  $\mathcal{T}_r$  of the form in Eq. (III.30) corresponds to a reset clock.

So when restricting our analysis to  $\Sigma_1$  and  $R_1$  of classical ticking clocks initialized in a pure state, the set of no-tick generators  $\mathcal{N}$  satisfying  $\sum_{i=0}^{d-1} \mathcal{N}_{ij} \leq 0 \forall j$  constitutes our remaining degrees of freedom. Furthermore, for each choice of  $\mathcal{N}$  which results in some given values of  $\Sigma_1$  and  $R_1$ , we can choose  $\mathcal{T} = \mathcal{T}_r$  with  $\vec{v}_{C,r} = \vec{e}_0$  and thus render the clock a reset clock for which  $\Sigma_k = \Sigma_1$  and  $R_k = kR_1$ . Note that there is an additional invariance under scaling:  $R_1$  and  $\vec{v}_C^{(b,0)}$  remain unchanged under rescaling of  $\mathcal{N}$  and  $\mathcal{T}$  by a positive constant  $a > 0$  as

$$\mathcal{N}' = a\mathcal{N}, \quad \mathcal{T}' = a\mathcal{T}. \quad (\text{III.32})$$

This can be shown by considering

$$P^{(0 \rightarrow 1)}(t) = \|\mathcal{T} e^{\mathcal{N} t} \vec{v}_C^0\|, \quad P^{(0 \rightarrow 1)'}(t) = \|\mathcal{T}' e^{\mathcal{N}' t} \vec{v}_C^0\|, \quad (\text{III.33})$$

for which

$$\mu' = \int_0^\infty t P^{(0 \rightarrow 1)'}(t) dt = \int_0^\infty at \|\mathcal{T} e^{\mathcal{N} at} \vec{v}_C^{(a,k-1)}\| dt = 1/a \int_0^\infty t' \|\mathcal{T} e^{\mathcal{N} t'} \vec{v}_C^{(a,k-1)}\| dt' = \mu/a, \quad (\text{III.34})$$

where we substitute  $at = t'$ . And

$$\sigma'^2 = \int_0^\infty (t - \mu')^2 P^{(0 \rightarrow 1)'}(t) dt = \int_0^\infty a(t - \mu/a)^2 \|\mathcal{T} e^{\mathcal{N} at} \vec{v}_C^{(a,k-1)}\| dt' \quad (\text{III.35})$$

$$= \int_0^\infty (t'/a - \mu/a)^2 \|\mathcal{T} e^{\mathcal{N} at} \vec{v}_C^{(a,k-1)}\| dt' = \sigma^2/a^2. \quad (\text{III.36})$$

Thus, the accuracy  $R'_1 = \mu'^2/\sigma'^2 = \mu^2/\sigma^2 = R_1$  remains unchanged. Similarly, we can show that

$$\vec{v}_C^{(b,k-1)'} = \int_0^\infty a \|\mathcal{T} e^{\mathcal{N} at} \vec{v}_C^{(a,k-1)}\| \frac{e^{\mathcal{N} at} \vec{v}_C^{(a,k-1)}}{\|e^{\mathcal{N} at} \vec{v}_C^{(a,k-1)}\|} dt \quad (\text{III.37})$$

$$= \int_0^\infty \|\mathcal{T} e^{\mathcal{N} t'} \vec{v}_C^{(a,k-1)}\| \frac{e^{\mathcal{N} t'} \vec{v}_C^{(a,k-1)}}{\|e^{\mathcal{N} t'} \vec{v}_C^{(a,k-1)}\|} dt' = \vec{v}_C^{(b,k-1)}. \quad (\text{III.38})$$

Hence, the entropy production  $\Sigma_1$  also remains unchanged. We will make use of this freedom

in scale of the generators  $\mathcal{N}$  and  $\mathcal{T}$  shortly.

### III.2.1.a Qubit clockwork

We start with an analysis of classical ticking clocks with a clockwork of dimension  $d = 2$ , that is a clockwork given by a qubit. Using the results obtained above, we can restrict our investigation to the set of allowed no-tick generators parametrized as

$$\mathcal{N} = \begin{pmatrix} -a & b \\ c & -d \end{pmatrix}, \quad (\text{III.39})$$

where  $1 \geq a \geq c \geq 0, 1 \geq d \geq b \geq 0$ . Here, we made use of the freedom in scale  $\mathcal{N} = a\mathcal{N}'$  by choosing  $a = \max_{ij}\{\mathcal{N}_{ij}\}$  to restrict all parameters to the unit interval. Here,  $\mathcal{N}'$  corresponds to the no-tick generator before rescaling. The initial state of the clockwork is  $\vec{v}_C^0 = \vec{e}_0 = (1, 0)^T$ . Without affecting  $\Sigma_1$  and  $R_1$ , we can choose a tick generator  $\mathcal{T}$  of the form

$$\mathcal{T} = \begin{pmatrix} a - c & d - b \\ 0 & 0 \end{pmatrix}. \quad (\text{III.40})$$

This renders this set of ticking clocks reset clocks with a pure initial state. In particular, they achieve  $\Sigma_k = \Sigma_1$  and  $R_k = R_1$ . Moreover, any such clock is completely specified by the set of parameters in Eq. (III.39) given by  $\vec{p} = (a, b, c, d)$ .

Solving for  $R_1$  analytically as a function of the free parameters  $\vec{p}$  of the no-tick generator  $\mathcal{N}$  (Eq. (III.39)), we find

$$R_1 = \frac{(c + d)^2}{(2c(a + b) - c) + d^2}. \quad (\text{III.41})$$

To get an analytical expression for  $\Sigma_1$  as a function of  $\vec{p}$ , we first search for an expression for  $v_{C,0}^{(b,0)}$ . The entropy production per tick  $\Sigma_1$  is then given by

$$\Sigma_1 = -v_{C,0}^{(b,0)} \ln(v_{C,0}^{(b,0)}) - (1 - v_{C,0}^{(b,0)}) \ln(1 - v_{C,0}^{(b,0)}). \quad (\text{III.42})$$

We find

$$v_{C,0}^{(b,0)} = \frac{{}_2F_1[1, \beta - 1/2, \beta + 1/2, \gamma]\delta}{\alpha(a - \alpha + d)(-a + 2c + \alpha + d)} + \frac{{}_2F_1[1, 3/2 + \beta, 5/2 + \beta, -\gamma]\delta}{\alpha(-a + 2c + \alpha + d)(a + 3\alpha + d)} \quad (\text{III.43})$$

$$- \frac{{}_2F_1[1, 1/2 + \beta, 3/2 + \beta, -\gamma](4c(-a^2 + c(-2b + d) + a(c + d)))}{\alpha(a + \alpha + d)(-a + 2c + \alpha + d)}, \quad (\text{III.44})$$

where  $\alpha = \sqrt{4bc + (a - d)^2}$ ,  $\beta = \frac{a+d}{2\alpha}$ ,  $\gamma = \frac{a-2c+\alpha-d}{-a+2c+\alpha+d}$ ,  $\delta = (2c(-a^2 + \alpha(a - c) + c(-2b + d) + a(c + d)))$ , and  ${}_2F_1[a, b; c; z]$  denotes the ordinary hypergeometric function [83].

With the analytical expressions for  $\Sigma_1$  and  $R_1$  as a function of the matrix elements of the tick generator  $\mathcal{N}$  in Eq. (III.41) and (III.42), respectively, we can efficiently explore the relation between these two quantities by sampling them over the parameter space defined by  $\mathcal{S} = \{\vec{p} = (a, b, c, d) | 1 \geq a \geq c \geq 0, 1 \geq d \geq b \geq 0\}$ . For a 4-dimensional parameter space, such a direct sampling is still computationally feasible. Figure III.1 shows  $\Sigma_1$  as a function of  $R_1$  obtained by direct random sampling of the parameter space  $\mathcal{S}$ . This sampling is unbiased, meaning that each part of the entire parameter space in a uniform fashion and we start to observe convergence of the plot at the chosen sample size. Therefore, this constitutes a faithful characterization of the relation between  $\Sigma_1$  and  $R_1$  for the class of clocks under consideration.

Looking at Fig. III.1, we can confirm the existence of a minimal entropy production  $\Sigma_{1,\min}$  at a given accuracy  $R_1$  which increases with increasing accuracy. Furthermore, we re-confirm our analytical result presented in Section III.1.1 that  $R_1 = 1$  can be achieved at  $\Sigma_1 = 0$  even in the classical case. We observe that at a given accuracy  $R_1$  there exists various ticking clocks which exhibit an entropy production  $\Sigma_1$  larger than the minimal amount

$$\ln(2) \geq \Sigma_1 \geq \Sigma_{1,\min}, \quad (\text{III.45})$$

where the upper bound is given by  $\ln(2)$ , the maximal achievable Shannon entropy for a state living in a two-dimensional vector space  $S((1/2, 1/2)^T) = \ln(2)$  (see Appendix A). Again, this confirms that while a large accuracy necessitates a large entropy production, the inverse is not true. Intuitively, the entropy production (quantifying the interaction of the clockwork with the environment) serves as a resource that can, but must not necessarily, be used to improve the accuracy of the clock by giving rise to an altered dynamic of the clockwork. The accuracy of the sampled ticking clocks ranges from  $R_1 = 1$  to  $R_1 = 2$ . This is in agreement with Ref. [14], which proved that the maximal achievable accuracy of classical ticking clocks with a clockwork of dimension  $d$  is  $R_1 = d$ , where  $d = 2$  in our case. In particular, this maximal accuracy can be achieved by the ladder ticking clock discussed in Section I.1.1. Note that the ladder ticking clock is a classical reset clock with a pure initial state of the clockwork and thus belongs to the class of clocks we considered here. In particular, the ladder ticking clock with a qubit clockwork is given by the choice  $\vec{p}_{\text{ladder}} = (a, b, c, d) = (1, 0, 1, 1)$ . In fact, we observe that the ladder clock in  $d = 2$  seems to achieve  $\Sigma_{1,\min}$  at  $R_1 = 2$  (see red crosses in Fig. III.1).

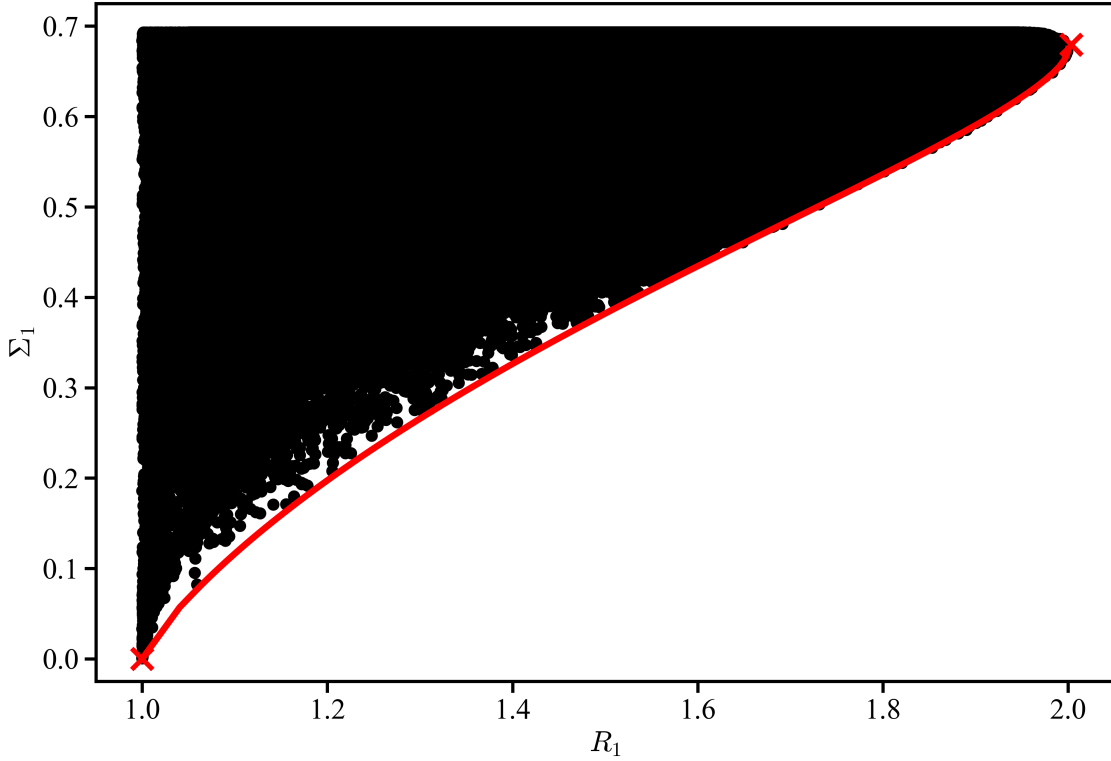


Figure III.1: Entropy production of the first tick  $\Sigma_1$  as a function of the accuracy of the first tick  $R_1$  for classical reset ticking clocks with a qubit clockwork that is initialized in a pure state. Data points in black are obtained by direct random sampling ( $\approx 3.1 \times 10^6$  samples) of the analytical expressions given in Eq. (III.41) and (III.42) over the relevant parameter space  $\mathcal{S} = \{\vec{p} = (a, b, c, d) | 1 \geq a \geq c \geq 0, 1 \geq d \geq b \geq 0\}$ . The red line corresponds to the minimum entropy production per tick  $\Sigma_{1,\min}$  at a given accuracy for such clocks. The optimal clock in  $d = 2$  which achieves this lower bound is characterized by the no-tick generator given in Eq. (III.52). The red crosses mark the entropy production per tick of ladder ticking clocks with clockworks of various dimensions  $d = R_1$  (see Appendix B.8 for the expressions of the accuracy and entropy production of ladder ticking clocks).

Next, given that there seems to exist a minimal entropy production  $\Sigma_{1,\min}$  at a given accuracy  $R_1$  (see black data points in Fig. III.1) we are interested in finding this lower bound and the ticking clocks which achieve it. In a first step, we try to find the lower bound and the corresponding clocks analytically. This task can be written in the standard form of a

continuous optimization problem as

$$\underset{\mathcal{N}}{\text{minimize}} \quad \Sigma_1 = S \left( \int_0^\infty P^{(0 \rightarrow 1)}(t) \frac{e^{\mathcal{N}t} \vec{e}_0}{\|e^{\mathcal{N}t} \vec{e}_0\|} dt \right) \quad (\text{III.46a})$$

$$\text{subject to} \quad R_1 = \mu_1^2 / \sigma_1^2 = \text{const.} \geq 1, \quad (\text{III.46b})$$

$$P^{(0 \rightarrow 1)}(t) = - \sum_{ij} \mathcal{N}_{ij} (e^{\mathcal{N}t})_{j0}, \quad (\text{III.46c})$$

$$\mu_1 = \int_0^\infty t P^{(0 \rightarrow 1)}(t) dt, \quad (\text{III.46d})$$

$$\sigma_1^2 = \int_0^\infty (t - \mu_1)^2 P^{(0 \rightarrow 1)}(t) dt, \quad (\text{III.46e})$$

$$\sum_i \mathcal{N}_{ij} \leq 0 \quad \forall j, \quad (\text{III.46f})$$

$$1 \leq \mathcal{N}_{ij} \leq 0, \quad \text{for } i = j, \quad (\text{III.46g})$$

$$1 \geq \mathcal{N}_{ij} \geq 0, \quad \text{for } i \neq j. \quad (\text{III.46h})$$

The optimization as specified by Eq. (III.46) is then carried out at each accuracy  $d \geq R_1 \geq 1$ . Because we expect the lower bound of  $\Sigma_{1,\min}$  to increase with increasing accuracy, we can also formulate the problem differently by replacing Eq. (III.46b) with

$$R_1 = \mu_1^2 / \sigma_1^2 \geq \text{const.} \geq 1. \quad (\text{III.47})$$

Alternatively, we can also remove the degree of freedom in the scale of  $\mathcal{N}$  by setting a particular matrix element to a constant. This is achieved by the choice  $a = 1/\mathcal{N}_{ij}$ , where  $\mathcal{N} = a\mathcal{N}'$  with  $\mathcal{N}'$  as the no-tick generator before rescaling. Here, w.l.o.g. we will choose  $\mathcal{N}_{d-1,d-1} = -1$  to formulate the analogous optimization problem with Eq. (III.46g) and (III.46h) replaced by

$$\mathcal{N}_{d-1,d-1} = -1, \quad (\text{III.48})$$

$$\mathcal{N}_{ij} \leq 0, \quad \text{for } i = j, \quad (\text{III.49})$$

$$\mathcal{N}_{ij} \geq 0, \quad \text{for } i \neq j. \quad (\text{III.50})$$

The task specified in Eq. (III.46) corresponds to a nonlinear constrained optimization problem with both equality and inequality constraints and a differentiable objective function  $\Sigma_1$  [84, 85]. In general, optimization problems are hard to solve. There are, however, important classes of problems for which algorithms exist that can yield a solution reliably and efficiently even when optimizing over a large number of parameters subject to many constraints. These include the class of linear, least-squares, as well as convex problems. Given that our objective function  $\Sigma_1$  is not linear and also not written as a sum of squares of terms of the form  $\vec{a}_i^T \vec{p} + b_i$ , the problem at hand does not fall into the class of linear or least-squares problems. A general

convex optimization problem can be written in the following form

$$\underset{\vec{x}}{\text{minimize}} \quad f(\vec{x}) \quad (\text{III.51a})$$

$$\text{subject to} \quad g_i(\vec{x}) \leq 0 \quad \forall i \in (1, l), \quad (\text{III.51b})$$

$$h_i(\vec{x}) = 0, \quad \forall i \in (1, m). \quad (\text{III.51c})$$

where  $\vec{x} \in \mathbb{R}^n$  is the optimization variable, the objective function  $f : \mathbb{R}^n \rightarrow \mathbb{R}$  is convex, the inequality-constraint functions  $g_i : \mathbb{R}^n \rightarrow \mathbb{R}$  are convex  $\forall i \in (1, l)$ , and the equality-constraint functions  $h_i : \mathbb{R}^n \rightarrow \mathbb{R}$  are affine, i.e.,  $h_i(\vec{x}) = \vec{a}_i^T \vec{x} + b_i \quad \forall i \in (1, m)$ . For a convex optimization task, each local minimum of the objective function is guaranteed to be a global minimum. This significantly simplifies the problem of finding a global minimum, because one can rely on local optimization algorithms. Moreover, the properties of the constraint functions guarantee that the set of viable optimization parameters is a convex set. Note that the problem of minimizing a concave objective function  $f$  can simply be re-formulated as a minimization problem for the convex function  $-f$ .

Based on the analytical expression for  $\Sigma_1$  (Eq. (III.42)), we can verify that it is neither a convex nor a concave function of the matrix elements of  $\mathcal{N}$ , similarly for  $R_1$  (Eq. (III.41)). The accuracy  $R_1$  is also not an affine function. Therefore, we conclude that the optimization problem outlined above (Eq. (III.46)) is not convex (concave) and thus cannot be simplified by exploiting the beneficial properties of convexity. Unfortunately, there do not exist any efficient methods for solving nonlinear constrained optimization problems which fall outside these categories [84, 85]. Even problems with under 10 parameters can be highly challenging and become computationally intractable at a larger number of parameters. In general, one can distinguish between two different approaches to finding a solution: local and global optimization. In local optimization we search the feasible region of the parameter space for solutions that are locally optimal, meaning that these solutions minimize the objective function when compared to the set of all other feasible points in its vicinity. However, having found a solution that is optimal locally we are not guaranteed that it also corresponds to the global minimum of the objective function. This is because the latter may have multiple local minima (in contrast to convex objective functions). On the contrary, in global optimization strategies, we seek to find the global minimum. Clearly, these methods will be computationally demanding in comparison and become intractable at a large number of parameters.

Firstly, note that one possible global optimization method is simple sampling of the parameter space [84, 85]. Given a dense enough coverage of the parameter space, one can guarantee to have found the global minimum. Clearly, this approach is computationally demanding and inefficient. Straightforward extensions of this approach are random search algorithms. These

are based on generating a set of random starting points and subsequently using local optimization method from each of the starting points to find local minima. The best guess for the global minimum is then given by the lowest-lying local minimum discovered in the process. Such a random search is faster but suffers from the same issues as direct sampling when a large parameter space needs to be searched. For the optimization task at hand, sequential least-squares programming (SLSQP) has been proven to be successful as a local optimization method to use for random search. In particular, the algorithm uses gradient information and is capable of dealing with nonlinear optimization problems with both inequality and equality constraints [86, 87]. Here, we use the implementation provided by the NLOpt library [88]. SLSQP is akin to sequential quadratic programming [89] (SQP), where the quadratic programming subproblem is replaced by a linear least-squares subproblem under appropriate matrix factorization. In sequential quadratic programming, one solves a sequence of simplified optimization subproblems, where the simplification arises via a quadratic approximation of the objective function and a linearization of the constraint functions.

A global optimization method that has also been proven effective in solving our problem at hand is the direct search method called Nelder–Mead [90]. The method relies on the construction of a simplex, a particular polytope with  $d + 1$  vertices spanning  $d$  dimensions, where the objective function is evaluated at its vertices. Based on these evaluations, new test points are constructed that then replace the old vertices. This is done iteratively, such that the simplex eventually shrinks and a desired termination condition is met. Note that the method does not take in any gradient information. It has, however, been proven to work well in practice for problems with few local minima. Here, we use the implementation of the Nelder-Mead algorithm provided in Mathematica [91]. Note that we have run tests using all suitable algorithms available both in the SciPy [92] and NLOpt [88] library for nonlinear optimization, as well as in Mathematica [91] and found the above-mentioned methods to be most suited for the task at hand. Finally, note that given an analytical expression of the objective function and the constraint functions, one can also think of finding an exact solution analytically. A common, general approach is cylindrical algebraic decomposition [93–95]. This does, however, require both the objective and constraints to be real algebraic functions. This is not the case here, because our objective function involves the ordinary hypergeometric function [83] which can only be expressed algebraically in special cases [96].

Using the approaches to solve the optimization task (Eq. (III.46)) described above, we find the ticking clocks with the following no-tick generator  $\mathcal{N}$  to be both locally and globally optimal

$$\mathcal{N} = \begin{pmatrix} -a & 0 \\ a & -1 \end{pmatrix}, \quad (\text{III.52})$$

where  $a \geq 1$ . That is, we find that these clocks achieve  $\Sigma_{1,\min}$  at a given accuracy  $R_1$  over all clocks under consideration. In Fig. III.1, we plot the entropy production  $\Sigma_{1,\min}(a)$  and accuracy  $R_1(a)$  of these optimal clocks for  $a \geq 1$  in red. Based on the direct sampling of the relevant parameter space, we can reconfirm the optimality of these clocks.

We can obtain analytical expressions for the entropy production per tick  $\Sigma_{1,\min}$  and its accuracy  $R_1$  of these optimal clocks as a function of the free parameter  $a$  from Eq. (III.41) and (III.42) with the choice  $\vec{p} = (a, b, c, d) = (a, 0, a, -1)$ . Here, we do not show the analytical expression for the entropy production per tick explicitly. The accuracy of these clocks is given by

$$R_1(a) = \frac{(1+a)^2}{1+a^2} \quad \forall a \geq 1. \quad (\text{III.53})$$

Solving for  $a \geq 1$ , we obtain

$$a(R_1) = \frac{1}{R_1 - 1} + \sqrt{\frac{1}{(R_1 - 1)^2} - 1}. \quad (\text{III.54})$$

Substituting the parameter  $a(R_1)$  (Eq. (III.54)) in the expression given in Eq. (III.42), we can obtain an analytical expression for the minimal entropy production as a function of the accuracy  $\Sigma_{1,\min}(R_1)$ , see red line in Fig. III.1. For the choice  $a = 1$ , the no-tick generator in Eq. (III.52) coincides with the no-tick generator of a ladder clock with a qubit clockwork (Eq. (I.54)). Whereas in the limit  $a \rightarrow \infty$ , we approach  $R_1 = 1$  and  $\Sigma_1 = 0$ . As an event generator, we can w.l.o.g. choose

$$\mathcal{T} = \begin{pmatrix} 0 & 1 \\ 0 & 0 \end{pmatrix}. \quad (\text{III.55})$$

This renders these clocks reset clocks with a pure initial state of the clockwork that achieve  $\Sigma_k = \Sigma_{1,\min}$  at  $R_k = kR_1$ . Hence, the ladder clock with a qubit clockwork is a ticking clock achieving  $\Sigma_{1,\min}(R_1 = 2)$  and is optimal in that regard.

### III.2.1.b Clockworks of dimension $d > 2$

After this analysis of clocks with a qubit clockwork, we extend our investigation to clocks with clockworks of larger dimension  $d > 2$ . *A priori*, one may expect that these clocks can be analyzed in the same manner as outlined above. Indeed, one can use a parametrization of the no-tick and tick generators analogous to Eq. (III.39) and (III.40). Moreover, the minimization task specified in Eq. (III.46) remains the same, albeit for no-tick generators of larger dimension. However, the increased dimension and the resulting increase in free parameters cause problems. In particular, we were not able to obtain an analytical expression for the entropy production per tick  $\Sigma_1$  as a function of the free parameters of the no-tick generators for  $d > 2$ . This

is because we were not able to find an analytical expression for the integrals involved in calculating

$$\bar{v}_C^{(b,0)} = \int_0^\infty P^{(0 \rightarrow 1)}(t) \frac{e^{\mathcal{N}t} \vec{e}_0}{\|e^{\mathcal{N}t} \vec{e}_0\|} dt. \quad (\text{III.56})$$

Nevertheless, one can solve the corresponding integrals numerically.

Starting with  $d = 3$ , in a first step we again attempt at a direct exhaustive sampling of the parameter space. Random, unbiased sampling of the entire parameter space becomes less efficient due to the increased number of free parameters at  $d > 2$ . Specifically, one has difficulties in randomly sampling highly accurate clocks. The results obtained via direct, unbiased sampling are depicted in Fig. III.2. These results demonstrate that such an approach fails at covering parts of the plot at high accuracy  $2 \leq R_1 \leq 3$ . Intuitively, this issue arises from the fact that most clocks are not accurate, i.e., accurate clocks require a more carefully tuned no-tick generator  $\mathcal{N}$ . Thus, when sampling  $\mathcal{N}$  uniformly only a small portion of the samples will fall into the small part of the parameter space populated by highly accurate clocks. To resolve these issues, we need to bias our sampling towards more accurate clocks.

We found that an efficient way to achieve such biasing is by using the global optimization technique called simulated annealing to maximize  $R_1$  subject to the constraints on  $\mathcal{N}$  as given in Eq. (III.46). In fact, using this method we are eventually able to sample clocks which achieve the maximal achievable accuracy of  $R_1 = d$ . The method is based on an adaptation of the Metropolis-Hastings algorithm [97]. Here, we briefly explain the working principle behind the method. Further details can be found in Refs. [98–100]. At the core of the method lies a parameter  $T$  which takes the role of a temperature. Having initialized the method at a no-tick generator  $\mathcal{N}$  associated with a particular accuracy  $R_1$  and large temperature  $T$ , we obtain a new trial generator  $\mathcal{N}'$  by addition of a perturbation  $\Delta\mathcal{N}$  which is sampled from a “visiting” distribution that is itself a function of  $T$ . In particular, the probability of sampling perturbations of large magnitude  $|\Delta\mathcal{N}|$  from the visiting distribution decreases with decreasing  $T$ . Next, one computes the accuracy  $R'_1$  associated with the trial generator  $\mathcal{N}'$ . If  $\Delta R_1 = R'_1 - R_1 > 0$ , the algorithm takes  $\mathcal{N}'$  as a new starting point, otherwise, the algorithm remains at the current starting point with a certain “rejection” probability characterized by a distribution which is dependent on  $T$  and  $\Delta R_1$ . The rejection probability increases with decreasing  $T$  and decreasing  $\Delta R_1$ . Subsequently, the process is repeated. When running the algorithm,  $T(n)$  is readjusted in each step to decrease with the total number of previous iterations  $n \in \mathbb{N}$ . There are various implementations of this scheme that differ in their choices of visiting distributions, distributions governing the rejection, as well as schedulers for the temperature parameter  $T$ . Here, we use the default implementation of dual annealing in SciPy with random initialization, but without any local optimization step and stopping criteria [92].

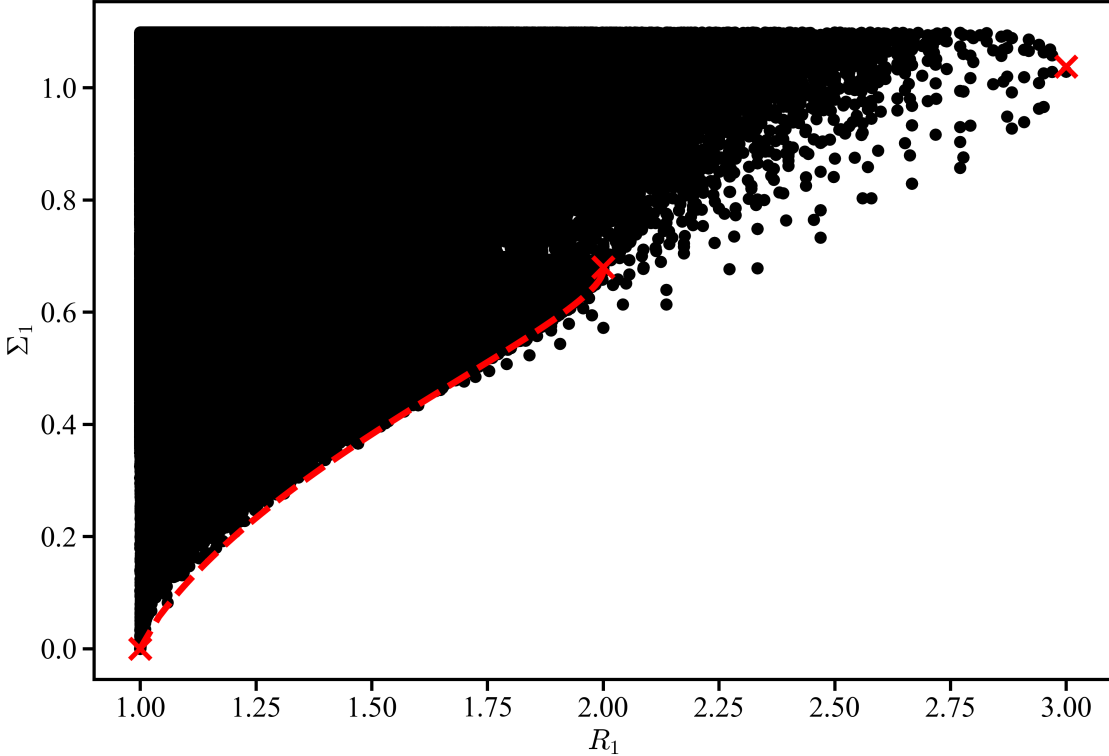


Figure III.2: Entropy production of the first tick  $\Sigma_1$  as a function of the accuracy of the first tick  $R_1$  for classical reset ticking clocks with a clockwork of dimension  $d = 3$  which is initialized in a pure state. Data points in black are obtained by direct random sampling ( $\approx 1.3 \times 10^6$  samples) of the no-tick generator in  $d = 3$ , as well as direct sampling of the latter over a grid with 11 grid points per entry of the no-tick generator ( $\approx 1.4 \times 10^6$  samples). Additionally, we re-plot all the data points from Fig. III.1 because they also constitute valid ticking clocks when considering a clockwork of larger dimension. The red dashed line corresponds to the minimum entropy production per tick  $\Sigma_{1,\min}$  at a given accuracy for clocks with a qubit clockwork, see Fig. III.1, which is achieved by clocks of the form given in Eq. (III.52). The red crosses mark the entropy production per tick of ladder ticking clocks with clockworks of various dimensions  $d = R_1$  (see Appendix B.8).

Finally, note that we have run tests using all algorithms available in both the SciPy [92] and NLOpt [88] library for nonlinear optimization and found this scheme based on simulated annealing to be most suited for the task at hand.

Once we performed sampling using simulated annealing as outlined above, we use the sampled no-tick generators as starting points for a second step: given an initial choice of no-tick generator  $\mathcal{N}$  we add to it a small perturbation  $\Delta\mathcal{N}$  that is generated in a random fashion to

obtain  $\mathcal{N}'$  and evaluate its accuracy  $R'_1$  and entropy production  $\Sigma'_1$ . Next, one either (a) takes  $\mathcal{N}'$  as a new starting point regardless of the computed accuracy  $R'_1$ , or (b) takes  $\mathcal{N}'$  as a new starting point only if it yields a higher accuracy  $\Delta R_1 = R'_1 - R_1 > 0$ , and otherwise  $\mathcal{N}$  remains as a starting point. Subsequently, the process is repeated. Here, we implemented and applied this scheme both with options (a) and (b) for choosing the subsequent starting point. This approach helped substantially in reaching full coverage of the parameter space, particularly at high accuracy  $R_1$ . Finally, we also apply this scheme to randomly generated starting points, as opposed to points generated via simulated annealing, with option (b). Figure III.3 shows a plot of  $\Sigma_1$  against  $R_1$  of sampled clocks with a clockwork of dimension  $d = 3$  obtained using all the above-mentioned sampling methods.

Note that the black data points shown in Fig. III.3 hint at the existence of a minimal entropy production per tick  $\Sigma_{1,\min}$  which increases with increasing accuracy  $R_1$ , even for clocks with a clockwork of dimension  $d = 3$ . We attempt to find  $\Sigma_{1,\min}$  for such clocks. To start, we make a naive ansatz and extend the class of clocks which were found to be optimal for  $d = 2$  to  $d > 2$  as follows

$$\mathcal{N}_{\text{qopt}} = \begin{pmatrix} -a & 0 & 0 & \cdots & 0 & 0 & 0 \\ a & -a & 0 & \cdots & 0 & 0 & 0 \\ 0 & a & a & \cdots & 0 & 0 & 0 \\ \vdots & \vdots & \vdots & \ddots & \vdots & \vdots & \vdots \\ 0 & 0 & 0 & \cdots & a & -a & 0 \\ 0 & 0 & 0 & \cdots & 0 & a & -1 \end{pmatrix}, \quad (\text{III.57})$$

where  $a \geq 1$ . We will call this class of clocks quasi-optimal. The analytical expression for the accuracy of the quasi-optimal clocks with a clockwork of dimension  $d \geq 2$  is

$$R_{1,\text{qopt}} = \frac{((d-1)+a)^2}{(d-1)+a^2}. \quad (\text{III.58})$$

These clocks attain the maximal achievable accuracy of  $R_1 = d$  for the choice  $a = 1$ . In this case, these clocks have identical no-tick generators (Eq. (III.57)) as ladder ticking clocks (Eq. (I.54)). And in the limit  $a \rightarrow \infty$ , these clocks approach  $R_1 = 1$ . We do not, however, find an analytical expression for the entropy production per tick  $\Sigma_{1,\text{qopt}}$  of the quasi-optimal clocks for  $d > 2$  due to the reasons outlined above. In Fig. III.3 we show  $\Sigma_{1,\text{qopt}}$  as a function of  $R_1$  for  $d = 3$  in green, where  $\Sigma_{1,\text{qopt}}$  is calculated numerically for a given choice of  $a$ . While these clocks achieve a low entropy production at a given accuracy, we identify several clocks that achieve a lower entropy production at the same accuracy (see Fig. III.3). In conclusion, quasi-ideal clocks cannot reach  $\Sigma_{1,\min}(R_1)$  in  $d = 3$ , whereas they were indeed optimal in  $d = 2$ .

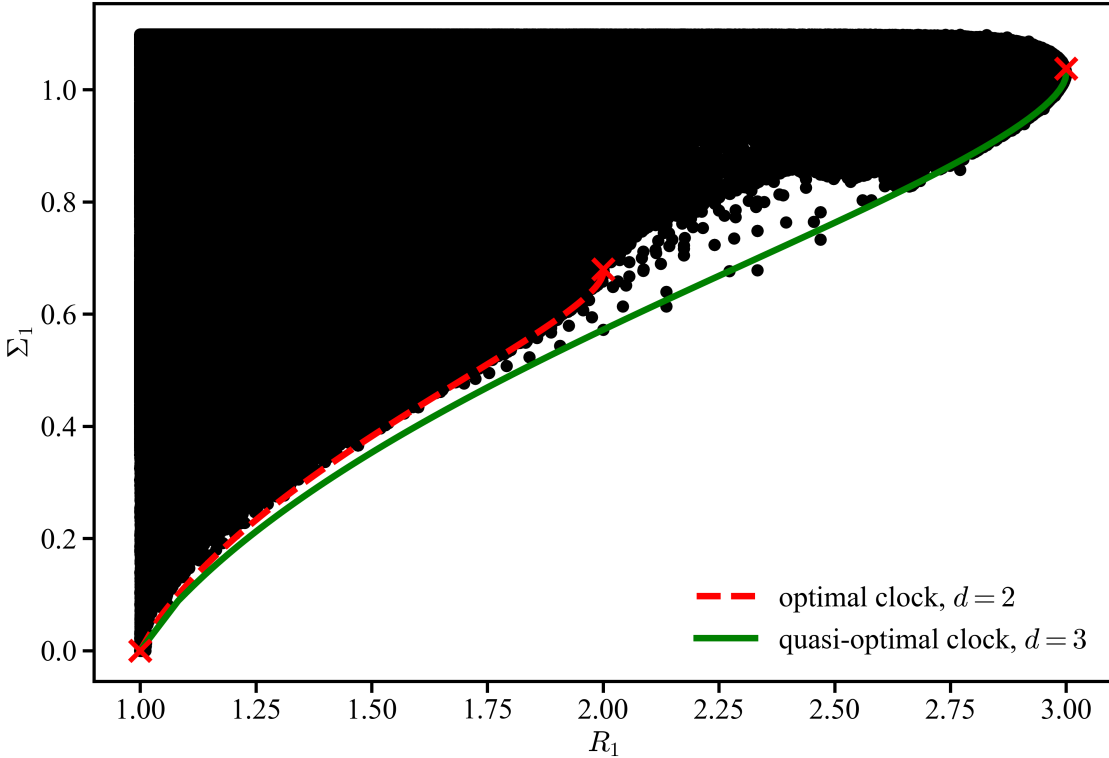


Figure III.3: Entropy production of the first tick  $\Sigma_1$  as a function of the accuracy of the first tick  $R_1$  for classical reset ticking clocks with a clockwork of dimension  $d = 3$  which is initialized in a pure state. Data points in black ( $\approx 1.0 \times 10^6$  samples) are obtained by biased sampling of the no-tick generator in  $d = 3$  using simulated annealing, as well as related random biased sampling strategies (see main text). Additionally, we re-plot all the data points from Fig. III.1 and Fig. III.2. The red dashed line corresponds to the minimum entropy production per tick  $\Sigma_{1,\min}$  at a given accuracy for clocks with a qubit clockwork, see Fig. III.1, achieved by an optimal clock of the form given in Eq. (III.52). The green line corresponds to  $\Sigma_{1,\text{opt}}(R_1)$  for the quasi-optimal ticking clock with a clockwork of dimension  $d = 3$ , see Eq. (III.57). The red crosses mark the entropy production per tick of ladder ticking clocks with clockworks of various dimensions  $d = R_1$  (see Appendix B.8).

To find  $\Sigma_{1,\min}(R_1)$  in  $d = 3$  and the clocks which achieve it, we apply nonlinear optimization methods, here SLSQP, to minimize  $\Sigma_1$  similar as in  $d = 2$  (see Eq. (III.46)). For a given choice of  $R_1$ , the optimization method yields the particular no-tick generator  $\mathcal{N}_{\text{opt}}$  achieving  $\Sigma_{1,\min}$  at  $R_1$ . We find that clocks achieving  $\Sigma_{1,\min}(R_1)$  all have a no-tick generator of the following form

$$\mathcal{N}_{\text{opt}} = \begin{pmatrix} -a_1 & 0 & 0 \\ a_1 & -a_2 & 0 \\ 0 & a_2 & -1 \end{pmatrix}, \quad (\text{III.59})$$

with  $a_1, a_2 \geq 0$  and  $a_1 \neq a_2$  in general. We call this class of clocks optimal. Note that from running the optimization algorithm we do not obtain an analytical expression for the functional relationship of  $a_1$  and  $a_2$ . In Fig. III.4 we show  $\Sigma_1$  as a function of  $R_1$  for various different clocks in  $d = 3$  which is a refined version of Fig. III.3. The additional points are obtained by random sampling of clocks with a no-tick generator of the form given in Eq.(III.59), as well as points obtained by resampling these points using the schemes described above. Clocks of the form given in Eq. (III.59) are found to achieve  $\Sigma_{1,\min}(R_1)$  in  $d = 3$ . In particular, they achieve a slightly lower entropy production at a given accuracy compared to the quasi-optimal clocks of the form given in Eq. (III.57), i.e., clocks of the form as in Eq. (III.59) but restricted to  $a = a_1 = a_2$ ,  $a \geq 1$ . Finally, note that the class of clocks as specified by Eq. (III.59) still corresponds to an intuitive extension of the optimal clocks in  $d = 2$ .

Figure III.5 show the relation between  $\Sigma_1$  and  $R_1$  for various different clocks with clockworks of dimension  $d = 4$ . These plots are generated following the same procedure as for Fig. III.4. Again, the minimal entropy production per tick at a given accuracy is achieved by the optimal class of clocks with a no-tick generator of dimension  $d = 4$  of the form

$$\mathcal{N}_{\text{opt}} = \begin{pmatrix} -a_1 & 0 & 0 & \cdots & 0 & 0 & 0 \\ a_1 & -a_2 & 0 & \cdots & 0 & 0 & 0 \\ 0 & a_2 & -a_3 & \cdots & 0 & 0 & 0 \\ \vdots & \vdots & \vdots & \ddots & \vdots & \vdots & \vdots \\ 0 & 0 & 0 & \cdots & 0 & -a_{d-1} & 0 \\ 0 & 0 & 0 & \cdots & 0 & a_{d-1} & -1 \end{pmatrix} \quad (\text{III.60})$$

with  $a_1, a_2, \dots, a_{d-1} \geq 0$ , where  $a_1 \neq a_2 \neq \dots \neq a_{d-1}$  in general. We observe that the minimal entropy production per tick at a given accuracy decreases slightly with increasing dimension of the clockwork  $d$ . Because clocks with clockworks of larger dimension can always reproduce the results of clocks with clockworks of smaller dimension by acting trivially on a particular subspace, the minimal entropy production per tick at a given accuracy can only decrease when increasing  $d$ . Ultimately, we are interested in the minimal entropy production per tick at a given accuracy irrespective of the clockwork dimension, i.e., in the limit  $d \rightarrow \infty$ .

We stop our analysis at  $d = 4$ , but based on the results obtained for clockworks of dimension  $d = 2, 3, 4$  we make the following conjecture: For the first tick of classical ticking clocks with a pure initial clockwork state, there exists a fundamental trade-off between entropy production  $\Sigma_1$  and accuracy  $R_1$ . In particular, there exists a minimal entropy production per tick  $\Sigma_{1,\min}(R_1)$  which increases with increasing accuracy. At a fixed dimension of the clockwork  $d$ , the no-tick generators of the clocks which achieve this lower bound are of the form given in

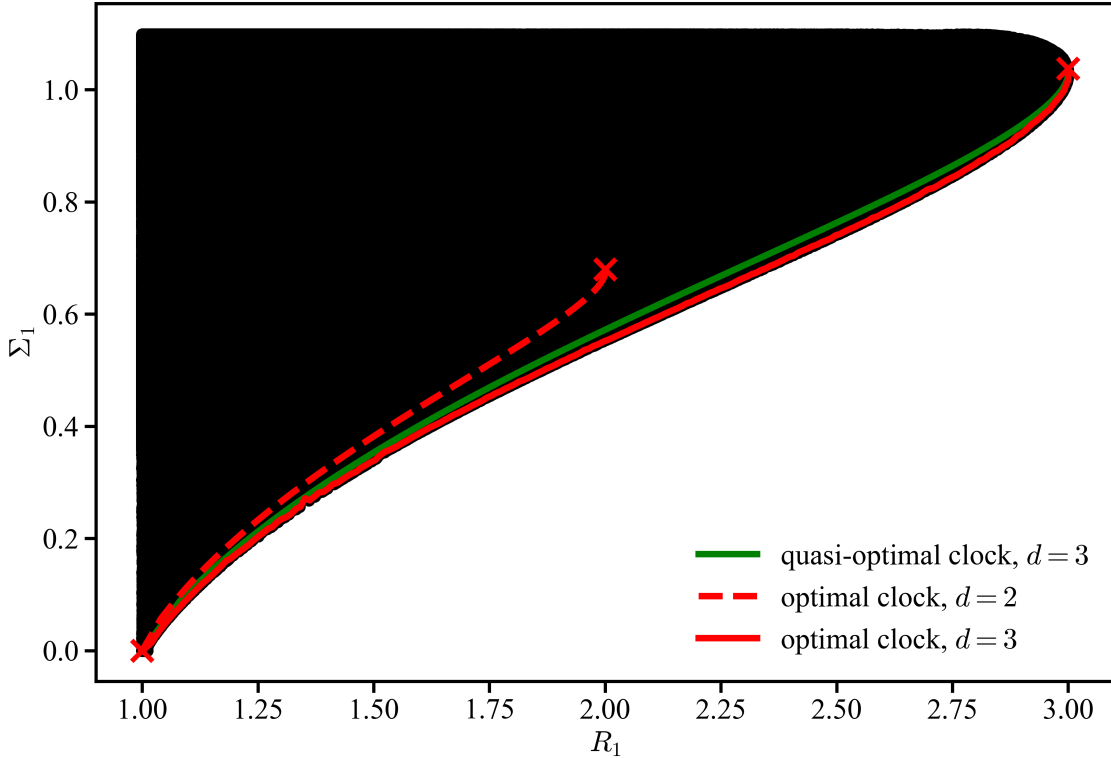


Figure III.4: Entropy production of the first tick  $\Sigma_1$  as a function of the accuracy of the first tick  $R_1$  for classical reset ticking clocks with a clockwork of dimension  $d = 3$  which is initialized in a pure state. Data points in black ( $\approx 0.3 \times 10^6$ ) are obtained by random sampling and re-sampling of the no-tick generators of the (optimal) form given in Eq. (III.59) (see main text). Additionally, we re-plot all the data points from Fig. III.1, III.2, and III.3. The red dashed line corresponds to the minimum entropy production per tick  $\Sigma_{1,\min}$  at a given accuracy for clocks with a qubit clockwork, see Fig. III.1, achieved by an optimal clock. The green line corresponds to  $\Sigma_{1,\text{qopt}}(R_1)$  for the quasi-optimal ticking clock with a clockwork of dimension  $d = 3$ , see Eq. (III.57). Here, the red line corresponds to the minimal entropy production  $\Sigma_{1,\min}(R_1)$  for clocks with a clockwork of dimension  $d = 3$  achieved by optimal clocks of the form given in Eq. (III.59). The red crosses mark the entropy production per tick of ladder ticking clocks with clockworks of various dimensions  $d = R_1$  (see Appendix B.8).

Eq. (III.60). An increased clockwork dimension  $d$  generally yields a lower value of  $\Sigma_{1,\min}(R_1)$  at each  $R_1$ . Thus, lifting the restriction of fixed clockwork dimension  $d$ , we expect the minimal entropy production per tick  $\Sigma_{1,\min}(R_1)$  to be achieved by clocks of the form in Eq. (III.60) with  $d \rightarrow \infty$ . Consequently, because classical internal Hamiltonian dynamics can be recovered in this limit, we expect that such clocks must also produce a non-zero amount of entropy per tick. Remember that a naive application of our measure to clocks that evolve according

to Hamiltonian dynamics and thus have a well-defined position at each point, i.e., is always in a definite state throughout their evolution, yields zero entropy production per tick (see Section III.1.2). Intuitively, the non-zero entropy production obtained here can be associated with a large number of microscopic degrees of freedom of such clocks that are not explicitly considered in the “coarse-grained” picture where classical Hamiltonian dynamics emerge.

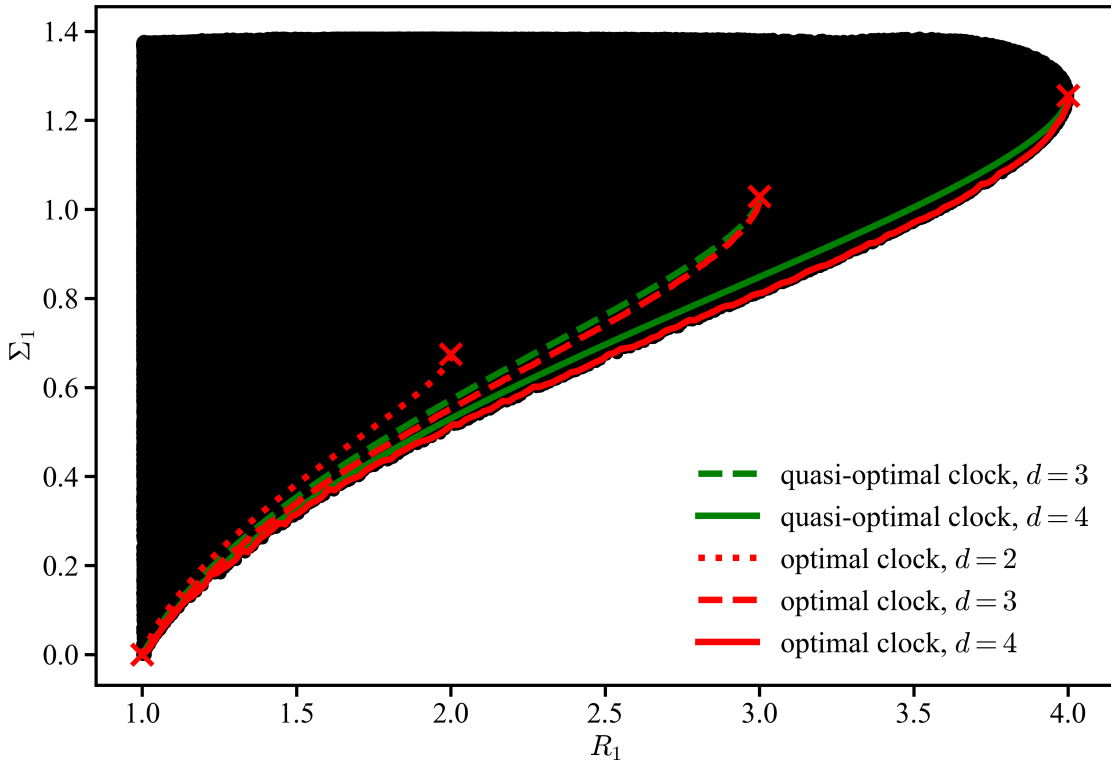


Figure III.5: Entropy production of the first tick  $\Sigma_1$  as a function of the accuracy of the first tick  $R_1$  for classical reset ticking clocks with a clockwork of dimension  $d = 4$  which is initialized in a pure state. Data points in black ( $\approx 1.1 \times 10^6$  samples) are obtained using sampling strategies analogous to Fig. III.4 with no-tick generators in  $d = 4$  (see main text). Additionally, we re-plot all the data points from Fig. III.1, III.2, III.3 and III.4. The entropy production of quasi-optimal ticking clocks (Eq. (III.57)) is depicted in green, whereas the entropy production of optimal ticking clocks (Eq. (III.60)) is shown in red. The red crosses mark the entropy production per tick of ladder ticking clocks with clockworks of various dimensions  $d = R_1$  (see Appendix B.8). Here, the minimal entropy production per tick  $\Sigma_{1,\min}$  at a given accuracy in  $d = 4$  is achieved by optimal ticking clocks of the form given in Eq. (III.60).

### III.2.2 Implications for later ticks of arbitrary classical ticking clocks

We have successfully investigated the relationship between  $\Sigma_1$  and  $R_1$  of classical ticking clocks that are initialized in a pure state. Recall that this analysis was motivated by the fact that the entropy production of the  $k$ th tick  $\Sigma_k$  of a ticking clock corresponds to the entropy production of the first tick of its conditional clock of the  $k$ th tick, where conditional clocks are simply a special class of ticking clocks that are initialized in a pure state. Thus, we have effectively investigated the relationship between  $\Sigma_1$  and  $R_1$  of all conditional clocks lying at the heart of every ticking clock. Meaning, a ticking clock can simply be seen as a particular sequence of conditional clocks. Now, what conclusions about the relationship between  $\{\Sigma_k\}_{k \in \mathbb{N}_{>0}}$  and  $\{R_k\}_{k \in \mathbb{N}_{>0}}$  for any type of classical ticking clock can we draw from these results?

First off, for any clock with a pure initial clockwork state that achieves a given  $\Sigma_1$  and  $R_1$  in its first tick, we have shown that we can construct another clock with a pure initial clockwork state with a suitable choice of tick generator  $\mathcal{T}$  that achieves  $\Sigma_k = \Sigma_1$  and  $R_k = kR_1$ , where  $\Sigma_1$  and  $R_1$  remain unchanged. In particular, this type of construction applies to any clock investigated in Section III.2.1. That is, to every conditional clock, there exists a ticking clock that realizes an infinite sequence of this conditional clock. Remember that for reset clocks that reset to a pure clockwork state all measures considered in Section II.5 coincide. For the optimal conditional clocks that achieve  $\Sigma_{1,\min}(R_1)$ , which we identified in the previous section, there thus exists a ticking clock that realizes an infinite sequence of this optimal conditional clock with  $\Sigma_k = \Sigma_{1,\min}$  and  $R_k = kR_1$ . We call this class of ticking clocks optimal in the following. Intuitively, we expect these to be the ticking clocks that produce the minimal entropy production per tick at a given accuracy, i.e., the clocks which are most efficient at converting the resource of entropy into temporal information. Specifically, for any optimal clock one cannot find any other classical ticking clock that produces less entropy per tick but is equally or more accurate. In the following, we will explore whether this statement is true. We have stated how to compare clocks based on their accuracy in Section I.2. Here, we define a similar notion for the entropy production per tick:

- ticking clock A produces an equal amount of entropy per tick as ticking clock B if and only if  $\Sigma_k^A = \Sigma_k^B \forall k \in \mathbb{N}_{>0}$ ,
- ticking clock A produces strictly less entropy per tick than ticking clock B if and only if  $\Sigma_k^A < \Sigma_k^B \forall k \in \mathbb{N}_{>0}$ ,
- ticking clock A produces less entropy per tick than ticking clock B if and only if  $\Sigma_k^A \leq \Sigma_k^B \forall k \in \mathbb{N}_{>0}$ , but the two clocks do not produce an equal amount of entropy per tick.

First, let us show that there exists no other reset clock which is more optimal. A reset clock necessarily has  $\Sigma_k = \Sigma_1 \forall k \in \mathbb{N}_{>0}$  and  $R_k = kR_1 \forall k \in \mathbb{N}_{>0}$ . Therefore, an equal or higher

accuracy can only be achieved by  $R_1 \geq R_{1,\text{opt}}$ , where  $R_{1,\text{opt}}$  denotes the accuracy of the corresponding optimal clock, and a lower entropy production necessitates  $\Sigma_1(R_1) < \Sigma_{1,\min}(R_{1,\text{opt}})$ , respectively. By construction of the optimal class of ticking clocks, if  $R_1 = R_{1,\text{opt}}$  we have  $\Sigma_1(R_1) \geq \Sigma_{1,\min}(R_{1,\text{opt}})$ . Moreover, we assume that  $\Sigma_1(R_1^A) \geq \Sigma_1(R_1^B)$  if  $R_1^A > R_1^B$ , i.e., we assume that the minimal entropy production per tick increases monotonically with increasing accuracy. Thus, if  $R_1 > R_{1,\text{opt}}$  we have  $\Sigma_1(R_1) \geq \Sigma_{1,\min}(R_1) \geq \Sigma_{1,\min}(R_{1,\text{opt}})$ . Therefore, we showed that no other reset clock can produce less entropy per tick at equal or higher accuracy than the optimal class of ticking clocks. Note that we did not make the assumption that the reset clocks start with an initial state of the clockwork that is pure. This result is intuitive and can be interpreted as follows: any reset clock realizes a sequence of identical conditional clocks with a fixed entropy production and accuracy for their first tick. So for a reset clock to produce less entropy, its (unique) conditional clock would need to produce less entropy. However, this necessitates a lower accuracy of the conditional clock. This is directly linked to the overall accuracy  $R_k = kR_1$ , where  $R_1$  is the accuracy of the first tick of its conditional clock.

Let us entertain the possibility of a more optimal non-reset ticking clock. To that end, we note that reset clocks, in particular reset clocks which reset to a pure clockwork state, are the most accurate type of classical clocks. This statement was formalized in Theorem 1. That is, for every classical clock there exists a reset clock that resets to a pure clockwork state with the same clockwork dimension that upper bounds its accuracy, i.e., achieves a higher accuracy. One can construct such a clock from the original clock by making a suitable choice of the initial pure state of the clockwork and changing the tick generator  $\mathcal{T}$  to reset to that state. That is, to maximize the accuracy one constructs a ticking clock that realizes an infinite sequence of the conditional clock which yields the maximal accuracy for its first tick. We can build on this intuition by proving the following statement: if a non-reset clock were to achieve a lower entropy production than the optimal class of (reset) clocks, it would have to do so by incorporating conditional clocks into its sequence that are less accurate than the (unique) conditional clock of the corresponding optimal reset clock. Consider such a non-reset clock with entropy production  $\{\Sigma_k\}_{k \in \mathbb{N}_{>0}}$  and accuracy  $\{R_k\}_{k \in \mathbb{N}_{>0}}$ . There exists an optimal clock which achieves  $\Sigma_k = \Sigma_{1,\min}(R_{1,\text{opt}})$  at  $R_{k,\text{opt}} = kR_{1,\text{opt}}$ , where  $R_1 = R_{1,\text{opt}}$ . If the non-reset clock produces less entropy per tick it must have  $\Sigma_k \leq \Sigma_{1,\min}(R_1) \forall k \in \mathbb{N}_{>0}$ . This necessitates  $R_1^{(c,k)} \leq R_1 \forall k \in \mathbb{N}_{>0}$ , where  $R_1^{(c,k)}$  denotes the accuracy  $R_1$  of the conditional clock of its  $k$ th tick, where  $R_1 = R_1^{(c,1)}$ . This follows from the fact, that if  $R_1^{(c,k)} > R_1$  then by construction  $\Sigma_k(R_1^{(c,k)}) \geq \Sigma_{1,\min}(R_1^{(c,k)}) \geq \Sigma_{1,\min}(R_1) = \Sigma_{1,\min}(R_{1,\text{opt}})$ . That is, a lower entropy production in the  $k$ th tick compared to the optimal clock would necessitate a lower accuracy  $R_1^{(c,k)} < R_1 = R_{1,\text{opt}}$  of the conditional clock of its  $k$ th tick compared to the optimal conditional clock.

The irregularity of the tick events of non-reset clocks also comes at an entropic cost. Consider a non-reset clock with entropy production  $\{\Sigma_k\}_{k \in \mathbb{N}_{>0}}$  and accuracy  $\{R_k\}_{k \in \mathbb{N}_{>0}}$ . Using the construction scheme in Theorem 1, we can always find a reset clock with a pure initial clock-work state that upper bounds its accuracy  $R'_k = kR'_1 \geq R_k \forall k \in \mathbb{N}_{>0}$  with possibly different entropy production  $\{\Sigma'_k\}_{k \in \mathbb{N}_{>0}}$ . Now, we can replace this reset clock with one of optimal entropy production  $\Sigma'_k = \Sigma_{1,\min}(R'_1) \forall k \in \mathbb{N}_{>0}$  at the same accuracy  $R'_k = kR'_1 \geq R_k \forall k \in \mathbb{N}_{>0}$ . This can always be done because the class of optimal reset clocks spans the entire range of achievable accuracies  $R_1$ . Similarly, we can always find an optimal reset clock which lower bounds the accuracy of the non-reset clock  $R''_k = kR''_1 \leq R_k \forall k \in \mathbb{N}_{>0}$  with optimal entropy production  $\Sigma''_k = \Sigma_{1,\min}(R''_1) \forall k \in \mathbb{N}_{>0}$ . Because  $R''_1 \leq R'_1$ , we have  $\Sigma_{1,\min}(R''_1) \leq \Sigma_{1,\min}(R'_1)$  and thus  $\Sigma''_k \leq \Sigma'_k \forall k \in \mathbb{N}_{>0}$ . So for every non-reset clock whose accuracy and entropy production vary for the different ticks, i.e.,  $R_k \neq kR_1$  and  $\Sigma_k \neq \Sigma_1$ , we can find optimal reset clocks which lower and upper bound the accuracy of the non-reset clock while achieving optimal entropy production. The tick events of these clocks are independent and identically distributed, i.e., these clocks deliver temporal information in the most regular fashion. Here, the reset clock which upper bounds the accuracy necessarily produces more entropy per tick compared to the reset clock which constitutes a lower bound to the accuracy of the non-reset clock. Finally, note that one can also construct optimal reset clocks for any arbitrary accuracy  $R'''_1$  in between the two bounds, such that  $R'_k = kR'_1 \geq R'''_k = kR'''_1 \geq R''_k = kR''_1 \forall k \in \mathbb{N}_{>0}$ , whose entropy production is also bounded from above and below as  $\Sigma''_k \leq \Sigma'''_k \leq \Sigma'_k \forall k \in \mathbb{N}_{>0}$ .

Let us investigate the particular case of non-reset clocks further. For this, we analyse the sequence of states  $\{\vec{v}_C^{(a,k)}\}_{k \in \mathbb{N}}$  through which such a ticking clock cycles. The state of the clockwork after the  $k$ th tick  $\vec{v}_C^{(a,k)}$  can be computed as

$$\vec{v}_C^{(a,k)} = \int_0^\infty \mathcal{T} e^{\mathcal{N}t} \vec{v}_C^{(a,k-1)} dt, \quad (\text{III.61})$$

where  $\vec{v}_C^{(a,0)} = \vec{v}_C^0$  by definition. Using  $\vec{v}_C^{(a,k-1)} = \sum_i v_{C,i}^{(a,k-1)} \vec{e}_i$  we can write Eq. (III.61) as

$$\vec{v}_C^{(a,k)} = \sum_i v_{C,i}^{(a,k-1)} \int_0^\infty \mathcal{T} e^{\mathcal{N}t} \vec{e}_i dt. \quad (\text{III.62})$$

We denote  $\vec{v}_{C,i}^{(a)} = \int_0^\infty \mathcal{T} e^{\mathcal{N}t} \vec{e}_i dt$  and thus

$$\vec{v}_C^{(a,k)} = \left( \vec{v}_{C,0}^{(a)}, \vec{v}_{C,1}^{(a)}, \dots, \vec{v}_{C,d-1}^{(a)} \right) \vec{v}^{(a,k-1)}. \quad (\text{III.63})$$

Note that  $\vec{v}^{(a,k-1)}$  are normalized state vectors and

$$\mathcal{P} = \left( \vec{v}_{C,0}^{(a)}, \vec{v}_{C,1}^{(a)}, \dots, \vec{v}_{C,d-1}^{(a)} \right) \quad (\text{III.64})$$

is a valid left stochastic matrix, i.e., a real square matrix with unit column sum. Thus, the sequence of states  $\{\vec{v}_C^{(a,k)}\}_{k \in \mathbb{N}_0}$  is governed by a Markov chain where  $\vec{v}_C^{(a,k)}$  is computed from  $\vec{v}_C^{(a,k-1)}$  via Eq. (III.63) and does not depend on  $\vec{v}_C^{(a,n)}$  with  $n < k - 1$ . The transition matrix of the Markov chain is given in Eq. (III.64). Given that we deal with discrete events – the ticks – it is a discrete-time Markov chain. Moreover, it has a finite state space whose dimension is given by the Hilbert space dimension of the clockwork. Because the transition matrix (Eq. (III.64)) is independent of the tick under consideration, the Markov chain is also time-homogeneous. Therefore, the sequence of states  $\{\vec{v}_C^{(a,k)}\}_{k \in \mathbb{N}_0}$  is governed by a discrete-time, time-homogeneous Markov chain with a finite state space whose transition matrix is stated in Eq. (III.64).

There are many known results for these classes of Markov chains which we will briefly explore [101–103]. First, we restrict ourselves to the case of a two-dimensional state space, i.e., a qubit clockwork. We can parametrize the transition matrix (Eq. (III.64)) as

$$\mathcal{P} = \begin{pmatrix} a & 1-b \\ 1-a & b \end{pmatrix}, \quad (\text{III.65})$$

where  $1 \geq a, b \geq 0$ . This Markov chain has a limiting transition matrix given by [103]

$$\lim_{k \rightarrow \infty} \mathcal{P}^k = \mathcal{P}_{\lim} = \frac{1}{a+b} \begin{pmatrix} a & a \\ b & b \end{pmatrix}, \quad (\text{III.66})$$

for all valid  $(a, b)$  except for the choice  $(a, b) = (0, 0)$ . Thus, for any valid initial state of the clockwork  $\vec{v}_C^0$ , we have

$$\lim_{k \rightarrow \infty} \vec{v}_C^{(a,k)} = \vec{v}_C^{(a,\lim)} = \lim_{k \rightarrow \infty} \mathcal{P}^k \vec{v}_C^0 = \mathcal{P}_{\lim} \vec{v}_C^0 = \frac{1}{a+b} (a, b)^T. \quad (\text{III.67})$$

Note that the limiting transition matrix  $\mathcal{P}_{\lim}$  is itself a valid transition matrix for which

$$\mathcal{P}_{\lim} = \lim_{k \rightarrow \infty} \mathcal{P}^k = \lim_{l \rightarrow \infty} \mathcal{P}^{l+1} = \mathcal{P} \mathcal{P}_{\lim}, \quad (\text{III.68})$$

such that

$$\vec{v}_C^{(a,\lim)} = \mathcal{P}_{\lim} \vec{v}_C^0 = \mathcal{P} \mathcal{P}_{\lim} \vec{v}_C^0 = \mathcal{P} \vec{v}_C^{(a,\lim)}. \quad (\text{III.69})$$

Therefore, there exists a valid Markov chain with transition matrix  $\mathcal{P}_{\lim}$  which remains in the same state throughout, i.e., is stationary, if initialized in  $\vec{v}_C^0 = \vec{v}_C^{(a,\lim)}$ . In the case where  $(a, b) = (0, 0)$ , the transition matrix is given by

$$\mathcal{P} = \begin{pmatrix} 0 & 1 \\ 1 & 0 \end{pmatrix}, \quad (\text{III.70})$$

where  $\mathcal{P}^2 = \mathbb{1}$ . For any initial state  $\vec{v}_C^0 = (x, 1-x)^T$  ( $1 \geq x \leq 0$ ) one thus obtains

$$\vec{v}_C^{(a,k)} = \begin{cases} (x, 1-x)^T, & \text{for even } k, \\ (1-x, x)^T, & \text{for odd } k. \end{cases} \quad (\text{III.71})$$

A ticking clock with such a transition matrix would therefore cycle between the same two states and exhibit oscillatory behavior, whereas all other choices of transition matrices – and thus ticking clocks – would eventually settle to a fixed state  $\vec{v}_C^{(a,\lim)}$ . The question remains what transition matrices can be realized by ticking clocks. In particular, does there exist a ticking clock that exhibits such oscillatory behavior?

To answer this question, we parametrize the generators of any arbitrary classical ticking clocks with a qubit clockwork as

$$\mathcal{N} = \begin{pmatrix} -a & b \\ c & -d \end{pmatrix} \quad \mathcal{T} = \begin{pmatrix} e & f \\ a - c - e & d - b - f \end{pmatrix}, \quad (\text{III.72})$$

where  $1 \leq a, b, c, d, e, f \leq 0$  with  $a - c - e \geq 0$  and  $d - b - f \geq 0$ . We solve for the transition matrix  $\mathcal{P}$  (Eq. (III.64)) explicitly and obtain

$$\mathcal{P} = \begin{pmatrix} \frac{af+be}{ad-bc} & \frac{de+cf}{ad-bc} \\ 1 - \frac{af+be}{ad-bc} & 1 - \frac{de+cf}{ad-bc} \end{pmatrix}. \quad (\text{III.73})$$

Thus, the following choice of generators

$$\mathcal{N} = \begin{pmatrix} -a & 0 \\ 0 & -d \end{pmatrix}, \quad \mathcal{T} = \begin{pmatrix} 0 & d \\ a & 0 \end{pmatrix}, \quad (\text{III.74})$$

where  $1 \geq a, d \geq 0$ , yields the oscillatory behavior governed by the transition matrix

$$\mathcal{P} = \begin{pmatrix} 0 & 1 \\ 1 & 0 \end{pmatrix}. \quad (\text{III.75})$$

Note that this clock's accuracy is upper bounded by  $R_k = k \forall k \in \mathbb{N}_{>0}$  (see Appendix B.6 for a proof). So similar to general Markov chains with a two-dimensional state space, we can observe that all ticking clocks with a qubit clockwork fall into two classes: clocks which are guaranteed to reach a fixed state  $\vec{v}_C^{(a,\lim)}$  after many ticks  $\lim_{k \rightarrow \infty} \vec{v}_C^{(a,k)} = \vec{v}_C^{(a,\lim)}$ , or clocks which exhibit oscillatory behavior and cycle between two fixed states indefinitely (see Eq. (III.71)).

Note that the conditional clocks for the  $i$ th and  $j$ th tick of a given ticking clock will be identical if the corresponding states  $\vec{v}_C^{(a,i)}$  and  $\vec{v}_C^{(a,j)}$  are identical. Thus, the entropy production

for these two ticks of the ticking clock will be identical  $\Sigma_i = \Sigma_j$ . The results above imply that the first class of ticking clocks with a qubit clockwork settles to a fixed conditional clock in the limit of many ticks and thus settles to produce a fixed entropy per tick  $\Sigma_{\text{lim}} = \lim_{k \rightarrow \infty} \Sigma_k$  after many ticks. Note that for any ticking clock of this class there exists another ticking clock with the same ticking clock channels but whose clockwork is initialized in  $\vec{v}_C^0 = \vec{v}_C^{(a,\text{lim})}$ , for which  $\vec{v}_C^{(a,k)} = \vec{v}_C^{(a,\text{lim})} \forall k \in \mathbb{N}_0$ . That is, for every ticking clock which reaches a limiting behavior after many ticks there exists another ticking clock that achieves this limiting behavior from the first tick onwards. In particular, this clock is comprised of identical conditional clocks and will thus have  $\Sigma_k = \Sigma_{\text{lim}} \forall k \in \mathbb{N}_0$ , where  $\Sigma_{\text{lim}}$  is the limiting entropy production of the original clock. Such a clock can operationally be constructed from the original one by letting it tick many times and reach its limiting behavior. On the contrary, there exists a second class of ticking clocks that cycle between two, possibly distinct, conditional clocks whose entropy production shows the same oscillatory behavior. These clocks produce an equal amount of entropy in all even ( $\Sigma_2$ ) and odd ticks ( $\Sigma_1$ ).

Following standard results from Markov chain literature [101–103], we can divide all possible ticking clocks with clockworks of arbitrary dimension  $d > 2$  into three types of classes:

1. reset clocks or non-reset clocks which are initialized in the stationary distribution such that  $\mathcal{P}\vec{v}_C^0 = \vec{v}_C^0$ ,
2. non-reset clocks (which do not belong to class 1) for which  $\lim_{k \rightarrow \infty} \mathcal{P}^k \vec{v}_C^0$  converges to a fixed state in the limit of many ticks  $\vec{v}_C^{(a,\text{lim})}$ , where  $\vec{v}^{(a,\text{lim})}$  may depend on the choice of  $\vec{v}_C^0$ ,
3. non-reset clocks which show periodic behavior in the limit of many ticks, i.e., they cycle between  $p$  different states  $\lim_{k \rightarrow \infty} \{\mathcal{P}^{pk} \vec{v}_C^0, \mathcal{P}^{pk+1} \vec{v}_C^0, \dots, \mathcal{P}^{pk+(p-1)} \vec{v}_C^0\}$ , where  $p$  is their period.

Based on our previous discussion, we note that this classification places restrictions on the entropy production per tick of ticking clocks, see Fig. III.6. Let us first discuss the ticking clocks which belong either to class 1 or 2: ticking clocks of class 1 will realize an infinite sequence of the same conditional clock, whereas a ticking clock of class 2 approaches a fixed conditional clock in the limit of many ticks. As such, they will either already produce a fixed amount of entropy per tick (class 1) or approach a fixed entropy production per tick in the limit of many ticks (class 2). Moreover, any clock of class 2 has an analog in class 1 with the same generators but a different, well-chosen initial state  $\vec{v}_C^0 = \vec{v}_C^{(a,\text{lim})}$ . This analogous clock in class 1 can be constructed operationally from the clock of class 2 by letting it tick many times and reach its long-term behavior. Subsequently, the clock is handed to another observer who starts counting ticks from zero onwards and assigns the state of the clockwork of the

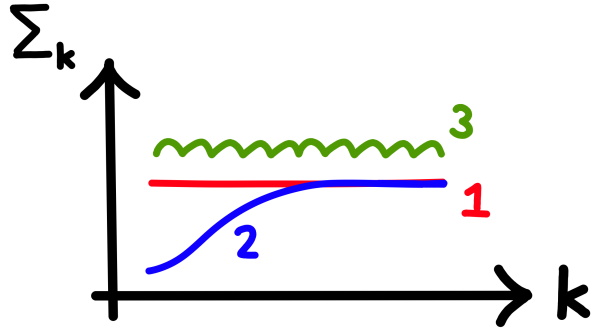


Figure III.6: Illustration of all three possible behaviors of the entropy production per tick  $\Sigma_k$  of ticking clocks in the limit of many ticks, i.e.,  $k \rightarrow \infty$ . Ticking clocks of class 1 are characterized by a constant entropy production  $\Sigma_k = \Sigma_1 \forall k \in \mathbb{N}_{>0}$ , whereas ticking clocks of class 2 approach a constant entropy production  $\Sigma_{\lim}$  in the limit of many ticks. Ticking clocks of class 3 will inevitably exhibit an oscillatory entropy production in the limit of many ticks. However, their entropy production may also already show oscillations from the first tick onwards.

handed clock as an initial state. Next, let us analyze clocks belonging to class 3 in a similar manner. Ticking clocks of class 3 will cycle between  $d$ , possibly different, conditional clocks in the limit of many ticks. As such, they will approach a cyclic pattern of entropy production which repeats itself every  $d$  ticks. For any such ticking clock we can find a clock that realizes this oscillatory behavior starting from the first tick onwards. This clock can be operationally constructed, as outlined above in the case of clocks belonging to class 2.

While we have analyzed all *potential* behaviors of ticking clocks in the limit of many ticks, one may still ask whether there exist ticking clocks that achieve all these behaviors. In particular, do there exist clocks with higher dimensional clockworks  $d > 2$  that can show oscillatory behavior in their entropy production? We can show that there exist such clocks by explicit construction. An example of such a clock in  $d = 3$  with a period  $p = 3$  is given by the following choice of generators

$$\mathcal{N} = \begin{pmatrix} -a & 0 & 0 \\ 0 & -b & 0 \\ 0 & 0 & -c \end{pmatrix}, \quad \mathcal{T} = \begin{pmatrix} 0 & 0 & c \\ a & 0 & 0 \\ 0 & b & 0 \end{pmatrix}, \quad (\text{III.76})$$

where  $a, b, c \geq 0$ . This results in

$$\mathcal{P}^{3k+1} = \begin{pmatrix} 0 & 0 & 1 \\ 1 & 0 & 0 \\ 0 & 1 & 0 \end{pmatrix}, \quad \mathcal{P}^{3k+2} = \begin{pmatrix} 0 & 1 & 0 \\ 0 & 0 & 1 \\ 1 & 0 & 0 \end{pmatrix}, \quad \mathcal{P}^{3k+3} = \begin{pmatrix} 1 & 0 & 0 \\ 0 & 1 & 0 \\ 0 & 0 & 1 \end{pmatrix} \forall k \in \mathbb{N}. \quad (\text{III.77})$$

Note that this clock's accuracy is upper bounded by  $R_k = k \forall k \in \mathbb{N}_{>0}$  (see Appendix B.6 for a proof). Another example of a clock that shows oscillatory behavior but necessarily cycles between states  $\vec{v}_C^{(a,k)}$  of different entropy with a period  $p = 2$  is given by the following choice of generators

$$\mathcal{N} = \begin{pmatrix} -a & 0 & 0 \\ 0 & -b & 0 \\ 0 & 0 & -c \end{pmatrix}, \quad \mathcal{T} = \begin{pmatrix} 0 & b & c \\ a\alpha & 0 & 0 \\ a(1-\alpha) & 0 & 0 \end{pmatrix}, \quad (\text{III.78})$$

where  $a, b, c \geq 0$  and  $1 \geq \alpha \geq 0$ . This clock's accuracy is also upper bounded by  $R_k = k \forall k \in \mathbb{N}_{>0}$  (see Appendix B.6 for a proof). We then have

$$\mathcal{P}^{2k+1} = \begin{pmatrix} 0 & 1 & 1 \\ \alpha & 0 & 0 \\ 1-\alpha & 0 & 0 \end{pmatrix}, \quad \mathcal{P}^{2k+2} = \begin{pmatrix} 1 & 0 & 0 \\ 0 & \alpha & \alpha \\ 0 & 1-\alpha & 1-\alpha \end{pmatrix} \forall k \in \mathbb{N}. \quad (\text{III.79})$$

Let us parametrize the initial clockwork state as  $\vec{v}_C^0 = (x, y, 1-x-y)^T$ , where  $1 \geq x, y \geq 0$ ,  $1 \geq x+y$ . Thus, we have

$$\vec{v}_C^{(a,k)} = \begin{cases} (1-x, \alpha x, (1-\alpha)x)^T, & \text{for odd } k, \\ (x, \alpha(1-x), (1-\alpha)(1-x))^T, & \text{for even } k. \end{cases} \quad (\text{III.80})$$

We can, for example, construct a clock that swaps between states of different entropy by the choice  $\vec{v}_C^0 = (1, 0, 0)^T$ . This results in  $\vec{v}_C^{(a,k)} = (0, \alpha, (1-\alpha))^T$  for odd  $k$  and  $\vec{v}_C^{(a,k)} = (1, 0, 0)^T$  for even  $k$ . Consequently, the clock will exhibit an oscillatory behavior in its entropy production.

# Conclusion and outlook

In this work, we successfully motivated an information-theoretic measure for the entropy production  $\Sigma_k$  of the  $k$ th tick of a ticking clock from first principles. Our expression quantifies the degree of correlations that build up between the clock and its environment during each tick. As such, it measures the amount of information that the clock exchanges with its outside world. This viewpoint is further strengthened by the fact that  $\Sigma_k$  gains operational meaning in quantum cryptographic protocols, where it serves as an upper bound on the amount of information that an eavesdropper can potentially acquire when the quantum channel governing the ticking process is used to transmit information. It is precisely this exchange of information that we can identify as an origin of irreversibility of the dynamics of ticking clocks. Crucially, this information content is appropriately conditioned on the knowledge of a typical observer which utilizes the ticking clock to gain information about time. Moreover, the measure applies to any ticking clock modeled in the framework proposed in Ref. [16] irrespective of the physical realization of the clock, i.e., the nature of its environment. This aspect allowed us to go beyond the investigations of previous works, which were largely restricted to a thermodynamic setting.

Next, we analyzed the relationship between the entropy production per tick and the accuracy of the most general class of quantum ticking clocks. We proved analytically by explicit construction that there exist quantum ticking clocks that operate at a vanishing entropy production per tick while being infinitely accurate. Thus, for this general class of ticking clocks, we showed that the minimal amount of entropy that needs to be produced in each tick to achieve a given accuracy vanishes in the infinite accuracy limit. On the contrary, we were not able to construct classical ticking clocks that are capable of achieving this limit. This result can be understood when taking note of the fact, that the clocks which achieve a vanishing entropy production per tick as their accuracy approaches infinity rely on coherent unitary clockwork dynamics leading up to each tick. Furthermore, the dimension of their clockwork is also required to approach infinity. Hence, to realize such clocks in a lab one would need a large (macroscopic) quantum system with coherent dynamics. It remains to be seen at what rate quantum computing technology and the field of quantum control advance in the upcoming years [104, 105], and thus whether this regime can be approached in practice. If so, this would

constitute a drastic quantum-over-classical advantage in the task of timekeeping: a quantum ticking clock would be capable of achieving a similar or higher accuracy while utilizing fewer information-theoretic resources in each tick.

Restricting our analysis to classical ticking clocks, we numerically confirmed the existence of a fundamental trade-off between the entropy production per tick and the accuracy of clocks with a clockwork of dimension  $d < 5$ . That is, to achieve a certain accuracy all such ticking clocks must produce a minimal amount of entropy per tick which increases with increasing accuracy. Moreover, we found a set of optimal ticking clocks that achieve this lower bound. Their generators take on a simple, sparse form. Thus, we successfully characterized the minimal information-theoretic resources required for these clocks to achieve a certain level of accuracy. In contrast to quantum ticking clocks which may exhibit coherent dynamics, the dynamics of classical ticking clocks are – by construction – completely incoherent and stochastic. These results further underpin the fact of our measure for the entropy production per tick quantifies the exchanged information between the clock and its outside. This is because in quantum mechanics noise arises due to information exchange with the outside, as can be seen from the quantum Fano inequality (see Eq. (II.94)). As such, classical ticking clocks must rely on an interaction with the environment leading up to each tick to achieve high accuracy. Our results show that there exists a minimal interaction “strength” at a given accuracy which must necessarily increase with increasing accuracy. In the future, it would be interesting to investigate the relation between the entropy production per tick and the accuracy of quantum ticking clocks with a limited clockwork dimension and contrast it to the results obtained for classical ticking clocks. As such, one may find a quantum-over-classical advantage even for low-dimensional clockworks.

We found that the minimal entropy production per tick of classical ticking clocks at a given accuracy decreases with increasing clockwork dimension  $d$ . Ultimately, we are interested in the lower bound which emerges in the  $d \rightarrow \infty$  limit. Here, we have conjectured that there exists such a lower bound that increases with increasing accuracy and that the optimal clocks which achieve it have a no-tick generator of the form given in Eq. (III.60). A major task that remains for future works is to leverage these numerical insights and analyze the minimal entropy production per tick in the  $d \rightarrow \infty$  limit analytically.

Finally, note that our ticking clock model assumes a perfect coupling of the clockwork to the register. That is, the ticking clocks do not tick backward and do not skip a tick. As pointed out previously, one can w.l.o.g. assume such a coupling for any valid clockwork. Nevertheless, it would be of interest to investigate the entropy that needs to be produced in order to implement such an ideal register that replaces an attentive observer. That is, analyze

the entropic cost associated with moving from a non-ideal to an ideal register, i.e., the tick-counting process. This would serve as an additional source of entropy production in ticking clocks described by our ticking clock model in addition to the entropy production per tick.



# Acknowledgement

I thank Mischa Woods for his excellent supervision. During the course of my thesis, I benefited substantially from his advice when presenting current problems and new results. I would also like to express my gratitude to Christoph Bruder for the stimulating discussions and encouraging words, as well as for granting me access to run numerical simulations at sciCORE (scicore.unibas.ch) scientific computing core facility at University of Basel. I thank Nilanjana Datta and Robert Salzmann for laying the foundation for this project during their discussions together with Mischa Woods prior to the start of my master's thesis. Moreover, I am very grateful to Renato Renner for giving me the opportunity to conduct my master's thesis in his group. I thank Patrick Potts for his valuable feedback on the manuscript. Lastly, I would like to express my gratitude to my friends and family for supporting me throughout the course of this thesis.



## Appendix A

# Quantum information and entropy

Here, we provide a brief overview of quantum information-theoretic quantities utilized in this work, such as the von Neumann entropy, quantum mutual information, or quantum relative entropy, and their properties. For more details, see Refs. [25, 69, 70, 106].

**Von Neumann entropy:** The von Neumann entropy  $S(\rho)$  of a density matrix  $\rho$  acting on states in a Hilbert space  $\mathcal{H}$  of dimension  $d = \dim(\mathcal{H})$  is given by

$$S(\rho) = -\text{tr} [\rho \ln(\rho)] = \sum_{i=0}^{d-1} -\lambda_i \ln(\lambda_i) \geq 0, \quad (\text{A.1})$$

where the eigendecomposition of the density matrix is  $\rho = \sum_{i=0}^{d-1} \lambda_i |i\rangle\langle i|$  with eigenvalues  $\{\lambda_i\}_{i=0}^{d-1}$  and eigenbasis  $\{|i\rangle\}_{i=0}^{d-1}$ . In the following, we list a few useful properties of the von Neumann entropy:

- The von Neumann entropy of a pure state is zero  $S(|\Psi\rangle\langle\Psi|) = 0$ .
- For a Hilbert space  $\mathcal{H}$  of fixed dimension  $d = \dim(\mathcal{H})$ , the von Neumann entropy is upper bounded by  $\ln(d)$  which is achieved by the maximally mixed state  $\rho = \mathbb{1}/d$ .
- The von Neumann entropy is invariant under unitary transformation  $S(U\rho U^\dagger) = S(\rho)$ . This follows from the fact that  $\rho' = U\rho U^\dagger = \sum_{i=0}^{d-1} \lambda_i U|i\rangle\langle i|U^\dagger = \sum_{i=0}^{d-1} \lambda_i |i'\rangle\langle i'|$ , where  $\{|i'\rangle\}_{i'=0}^{d-1}$  is another orthonormal basis of  $\mathcal{H}$ . The density matrix  $\rho'$  has the same eigenvalues as  $\rho$ , and thus the same von Neumann entropy.
- The von Neumann entropy is subadditive, that is  $S(\rho_{AB}) \leq S(\rho_A) + S(\rho_B)$ . Note that if the joint state is a product state  $\rho_{AB} = \rho_A \otimes \rho_B$  we achieve equality, because  $S(\rho_A \otimes \rho_B) = S(\rho_A) + S(\rho_B)$ .

- The von Neumann entropy obeys a triangle inequality

$$|S(\rho_A) - S(\rho_B)| \leq S(\rho_{AB}) \leq S(\rho_A) + S(\rho_B), \quad (\text{A.2})$$

where the right-hand side follows from subadditivity.

- The von Neumann entropy is concave and thus satisfies

$$S\left(\sum_i p_i \rho_i\right) \leq \sum_i p_i S(\rho_i), \quad (\text{A.3})$$

where  $\{p_i\}_{i=1}^N$ ,  $N \in \mathbb{N}_{>0}$  is a normalized probability distribution and  $\{\rho_i\}_{i=1}^N$  are a set of density matrices. That is, we have  $\sum_i p_i = 1$  and  $p_i \geq 0 \forall i$ .

**Quantum mutual information:** Consider density matrices  $\rho_{AB}$  acting on a bipartite Hilbert space  $\mathcal{H}_{AB} = \mathcal{H}_A \otimes \mathcal{H}_B$ . The quantum mutual information  $I_{A:B}(\rho_{AB})$  is then given by

$$I_{A:B}(\rho_{AB}) = S(\rho_A) + S(\rho_B) - S(\rho_{AB}) \geq 0, \quad (\text{A.4})$$

where  $S$  denotes the von Neumann entropy and  $\rho_{A/B} = \text{tr}_{B/A}[\rho_{AB}]$  denotes the reduced state of system A/B, respectively. For brevity, we write  $I_{A:B}(\rho_{AB}) = I(\rho_{AB})$  when it is clear with respect to what bipartition of the Hilbert space the quantum mutual information is computed.

**Quantum relative entropy:** The quantum relative entropy  $S(\rho\|\sigma)$  of the density matrix  $\rho$  with respect to the density matrix  $\sigma$  is given by

$$S(\rho\|\sigma) = -\text{tr}[\rho \ln(\sigma)] - S(\rho) \geq 0. \quad (\text{A.5})$$

Here, both density matrices act on states in a Hilbert space  $\mathcal{H}$ . We have  $S(\rho\|\sigma) = \infty$  when  $\text{supp}(\rho) \cap \ker(\sigma) \neq 0$ , where  $\text{supp}(\rho)$  denotes the support of  $\rho$  and  $\ker(\sigma)$  is the kernel of  $\sigma$ . Thus, given that  $\sigma$  is a pure state  $\sigma = |\Psi\rangle\langle\Psi|$  then  $S(\rho\|\sigma) \neq \infty$  if and only if  $\sigma = \rho$ .

## Appendix B

# Additional proofs

### B.1 Delay functions and accuracy of ticking clocks

In this section, we prove that for reset ticking clocks the delay function of the  $k$ th tick is given by a convolution of  $k$  delay functions of the first tick, which yields  $R_k = kR_1 \forall k \in \mathbb{N}_{>0}$ . Based on the implicit clockwork representation given in Lemma 1, one can write the dynamics of a ticking clock as follows

$$\frac{d}{dt} \tilde{\rho}_C^{(k)}(t) = \begin{cases} \mathcal{C}_{(1,0)}(\tilde{\rho}_C^{(0)}(t)), & \text{for } k = 0 \\ \mathcal{C}_{(1,0)}(\tilde{\rho}_C^{(k)}(t)) + \mathcal{C}_{(2,0)}(\tilde{\rho}_C^{(k-1)}(t)), & \text{for } k \neq 0 \end{cases}, \quad (\text{B.1})$$

with initial conditions

$$\tilde{\rho}_C^{(k)}(0) = \begin{cases} \rho_C^0, & \text{for } k = 0 \\ 0, & \text{for } k \neq 0 \end{cases}, \quad (\text{B.2})$$

where  $\tilde{\rho}_C^{(k)} = \text{tr}_R [\rho_C |k\rangle\langle k|_R]$ ,  $k \in \mathbb{N}$ . Here, we made use of the fact that we consider ticking clocks with registers in the limit  $N_T \rightarrow \infty$ , where the distinction between cut-off registers and periodic registers becomes irrelevant. This can be seen as the quantum analog of the representation given in Corollary 1 for classical ticking clocks.

The solution for the clockwork states in the first two tick subspaces,  $k = 0$  and  $k = 1$ , are

$$\tilde{\rho}_C^{(0)}(t) = e^{t\mathcal{C}_{(1,0)}}(\rho_C^0), \quad (\text{B.3})$$

and

$$\tilde{\rho}_C^{(1)}(t) = \int_0^\infty e^{(t-t')\mathcal{C}_{(1,0)}} \circ \mathcal{C}_{(2,0)} \circ e^{t'\mathcal{C}_{(1,0)}}(\rho_C^0) dt'. \quad (\text{B.4})$$

If the clock is a reset clock, we have  $\mathcal{C}_{(2,0)} \circ e^{t'\mathcal{C}_{(1,0)}}(\rho_C^0) \propto \rho_C^0$  because  $\mathcal{C}_{(2,0)}(\rho_C) \propto \rho_C^0 \forall \rho_C$ .

Given that  $\tau^{(k)}(t) = \text{tr} \left[ \mathcal{C}_{(2,0)}(\tilde{\rho}_C^{(k-1)}(t)) \right]$ , we can write

$$\mathcal{C}_{(2,0)} \circ e^{t' \mathcal{C}_{(1,0)}}(\rho_C^0) = \tau^{(1)}(t') \rho_C^0, \quad (\text{B.5})$$

and

$$\tau^{(2)}(t) = \text{tr} \left[ \mathcal{C}_{(2,0)} \left( \int_0^\infty e^{(t-t')\mathcal{C}_{(1,0)}} \circ \mathcal{C}_{(2,0)} \circ e^{t'\mathcal{C}_{(1,0)}}(\rho_C^0) dt' \right) \right] \quad (\text{B.6})$$

$$= \int_0^\infty \text{tr} \left[ \mathcal{C}_{(2,0)} \left( e^{(t-t')\mathcal{C}_{(1,0)}}(\rho_C^0) \tau^{(1)}(t') dt' \right) \right] \quad (\text{B.7})$$

$$= \int_0^\infty \tau^{(1)}(t-t') \tau^{(1)}(t') dt' = (\tau^{(1)} * \tau^{(1)})(t). \quad (\text{B.8})$$

The proof for  $\tau^{(k)}(t)$  with  $k > 2$  then follows by induction. For classical ticking clocks, one can obtain analogous expressions by making the following substitutions

$$\rho_C \longleftrightarrow \vec{v}_C, \quad \mathcal{C}_{(1,0)} \longleftrightarrow \mathcal{N}, \quad \mathcal{C}_{(2,0)} \longleftrightarrow \mathcal{T}, \quad \text{tr}[\cdot] \longleftrightarrow \|\cdot\|, \quad (\text{B.9})$$

i.e., one replaces Eq. (B.1) and (B.2) by the analogous expressions given in Corollary 1.

Given the tick delay functions  $\{\tau^{(k)}(t)\}_{k \in \mathbb{N}_{>0}}$  of a ticking clock, its accuracy  $\{R_k\}_{k \in \mathbb{N}_{>0}}$  is completely specified. Note that the tick delay functions are normalized probability densities. We compute the expected time  $\mu_k$  and the variance  $\sigma_k^2$  of the  $k$ th tick as

$$\mu_k = \int_0^\infty \tau^{(k)}(t) t dt, \quad (\text{B.10})$$

$$\sigma_k^2 = \int_0^\infty \tau^{(k)}(t) (t - \mu_k)^2 dt, \quad (\text{B.11})$$

where the accuracy of the  $k$ th tick is then given by  $R_k = \mu_k^2 / \sigma_k^2$ . Consider the case where the delay function of the  $k$ th tick is given by a convolution of  $k$  tick delay functions of the first tick

$$\begin{aligned} \tau^{(k)}(t) &= \int_0^\infty dt_{k-1} \cdots \int_0^\infty dt_2 \int_0^\infty dt_1 \tau^{(1)}(t_1) \tau^{(1)}(t_2 - t_1) \tau^{(1)}(t_3 - t_2) \cdots \tau^{(1)}(t - t_{k-1}) \\ &\quad (\text{B.12}) \end{aligned}$$

$$= \underbrace{(\tau^{(1)} * \tau^{(1)} * \cdots * \tau^{(1)})(t)}_{k \text{ times}}. \quad (\text{B.13})$$

One can calculate the moments of this delay function through direct integration as

$$\mu_k = k \mu_1, \quad (\text{B.14})$$

$$\langle t^2 \rangle_k = k\langle t^2 \rangle_1 + k(k-1)\mu_1^2, \quad (\text{B.15})$$

$$\sigma_k = \sqrt{k}\sigma_1, \quad (\text{B.16})$$

and thus  $R_k = \mu_k^2/\sigma_k^2 = k\mu_1^2/\sigma_1^2 = kR_1$ .

## B.2 Entropy production as correlation between system and environment

Here, we provide the additional proofs for the expressions stated in Section II.2.1 on entropy production as correlation between system and environment.

**Thermal environment:** We start from Eq. (II.20), which states

$$\Delta S_S + \Delta S_E = I(\rho'_{SE}) \geq 0. \quad (\text{B.17})$$

We consider the special case where the environment is initially in a thermal state  $\rho_E = e^{-\beta H}/\text{tr}[e^{-\beta H}]$ , with  $H$  as the corresponding Hamiltonian and  $\beta = 1/k_B T$  the inverse temperature. Then one can rewrite Eq. (B.17) as

$$I(\rho'_{SE}) - \Delta S_S = \Delta S_E = S(\rho'_E) - S(\rho_E) = -\text{tr}[\rho'_E \ln(\rho'_E)] + \text{tr}\left[\rho_E \ln\left(\frac{e^{-\beta H}}{\text{tr}[e^{-\beta H}]}\right)\right] \quad (\text{B.18})$$

$$= -\text{tr}[\rho'_E \ln(\rho'_E)] + \text{tr}\left[\rho_E \left(-\beta H - \mathbb{1} \ln\left(\text{tr}[e^{-\beta H}]\right)\right)\right] \quad (\text{B.19})$$

$$= -\text{tr}[\rho'_E \ln(\rho'_E)] - \beta \text{tr}[\rho_E H] - \ln\left(\text{tr}[e^{-\beta H}]\right) + \beta \text{tr}[H\rho'_E] - \beta \text{tr}[H\rho'_E] \quad (\text{B.20})$$

$$= \beta \text{tr}[H(\rho'_E - \rho_E)] - \text{tr}[\rho'_E \ln(\rho'_E)] + \text{tr}\left[\rho'_E \ln\left(\frac{e^{-\beta H}}{\text{tr}[e^{-\beta H}]}\right)\right] \quad (\text{B.21})$$

$$= \beta Q_E - S(\rho'_E \| \rho_E), \quad (\text{B.22})$$

where we identified the change in energy of the reservoir as the amount of exchanged heat  $Q_E = (\text{tr}[H\rho'_E] - \text{tr}[H\rho_E])$  during the process, and  $S(\rho \| \sigma)$  denotes the quantum relative entropy. By reordering Eq. (B.22), one obtains the desired result

$$\Delta S_S + \beta Q_E = I(\rho'_{SE}) + S(\rho'_E \| \rho_E) \geq 0. \quad (\text{B.23})$$

**Global fixed point:** We start from Eq. (II.26) which states

$$\Sigma = I(\rho'_{SE}) + S(\rho'_E \| \rho_E) = \Delta S_S + \beta Q_E. \quad (\text{B.24})$$

We consider the special case where the unitary map has a global fixed point  $\rho_S^*$  that satisfies

$$U(\rho_S^* \otimes \rho_E) U^\dagger = \rho_S^* \otimes \rho_E. \quad (\text{B.25})$$

Let us rewrite the expression for the entropy production in Eq. (B.24) as

$$\Sigma = I(\rho'_{SE}) + S(\rho'_E \| \rho_E) = \Delta S_S + \Delta S_E - \text{tr}[\rho'_E \ln(\rho_E)] - S(\rho'_E) = \Delta S_S + \text{tr}[(\rho_E - \rho'_E) \ln(\rho_E)], \quad (\text{B.26})$$

where we can write the second term as

$$\text{tr}[(\rho_E - \rho'_E) \ln(\rho_E)] = \text{tr}_{SE}[(\rho_S \otimes \rho_E - \rho'_{SE}) \mathbb{1}_S \otimes \ln(\rho_E)]. \quad (\text{B.27})$$

Taking the logarithm on both sides of Eq. (B.25) we obtain

$$\mathbb{1}_S \otimes \ln(\rho_E) = U^\dagger \mathbb{1}_S \otimes \ln(\rho_E) U + U^\dagger \ln(\rho_S^*) \otimes \mathbb{1}_E U - \ln(\rho_S^*) \otimes \mathbb{1}_E. \quad (\text{B.28})$$

Plugging the expression in Eq. (B.28) into Eq. (B.27) and tracing out the environment E we obtain

$$\text{tr}[(\rho_E - \rho'_E) \ln(\rho_E)] = \text{tr}_S[(\rho_S - \rho_S^*) \ln(\rho_S^*)]. \quad (\text{B.29})$$

Then, plugging Eq. (B.29) into Eq. (B.26) we obtain

$$\Sigma = \Delta S_S + \text{tr}[(\rho_S - \rho_S^*) \ln(\rho_S^*)], \quad (\text{B.30})$$

which can be rewritten as

$$\Sigma = S(\rho_S \| \rho_S^*) - S(\rho_S' \| \rho_S^*). \quad (\text{B.31})$$

Equation (B.31) is the desired expression given in Eq. (II.30).

### B.3 Distinct approaches to calculate observer-dependent clockwork states

Here, we provide additional results on the three distinct approaches to calculate observer-dependent clockwork states discussed in Section II.3. Figure B.1 shows that when  $\rho_C^{(b,k-1)}$  is calculated using approach 2 (Eq. (II.54)), it is still dependent on  $k$  for ladder ticking clocks. This is in contrast to approach 1 (Eq. (II.47)).

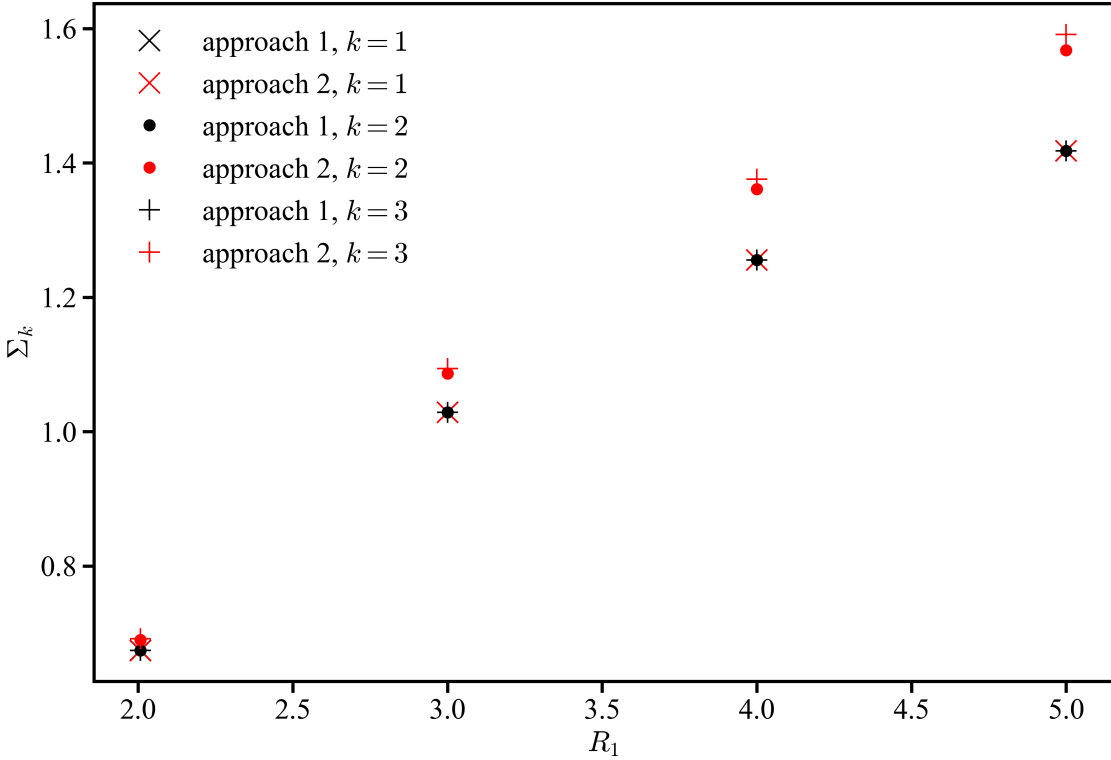


Figure B.1: Entropy production per tick  $\Sigma_k = S(\rho_{CP}^{(b,k-1)})$  for  $k = 1, 2, 3$  of ladder ticking clocks with clockworks of various dimensions  $d = R_1$  based on the state of the clockwork at an instance before the  $k$ th tick  $\rho_{CP}^{(b,k-1)}$  obtained using approach 1 (black, Eq. (II.47)) or approach 2 (red, Eq. (II.54)), see Section II.3. Here, the ladder ticking clock serves as an example of a reset clock for which we expect the entropy production to be the same for all ticks. Because the ladder clock resets to a pure clockwork state, we have  $\Sigma_k = S(\rho_{CP}^{(b,k-1)}) = S(\rho_C^{(b,k-1)})$ . Note that the entropy production per tick obtained in approach 1 is independent of the tick under consideration, whereas the entropy production per tick obtained in approach 2 depends on  $k$ .

Next, we contrast the expressions for the observer-dependent clockwork states  $\rho_C^{(b,k)}$  and

$\rho_C^{(a,k)}$  obtained by following approach 1 and 3. Starting with the first tick where both approaches agree, we have

$$\rho_C^{(a,1)} = \int_0^\infty \sum_j J_j \tilde{\rho}_C^{(0)}(t) J_j^\dagger dt, \quad (\text{B.32})$$

where

$$\tilde{\rho}_C^{(0)}(t) = \text{tr} \left[ \mathbb{1}_C \otimes |0\rangle\langle 0|_R \mathcal{M}_{C \rightarrow CR}^{t,0}(\rho_C^0) \right]. \quad (\text{B.33})$$

Then, for the second tick following approach 1 we have

$$\rho_C^{(b,1)} = \int_0^\infty P^{(1 \rightarrow 2)}(t') \rho_C^{(1)}(t') dt' \quad (\text{B.34})$$

as the state of the clockwork an instance before the second tick. The state an instance after the second tick is given by

$$\rho_C^{(a,2)} = \int_0^\infty \sum_j J_j \text{tr}_R \left[ \mathbb{1}_C \otimes |1\rangle\langle 1|_R \mathcal{M}_{C \rightarrow CR}^{t',1} \left( \rho_C^{(a,1)} \right) \right] J_j^\dagger dt'. \quad (\text{B.35})$$

Plugging the expression for  $\rho_C^{(a,1)}$  given in Eq. (B.32) into Eq. (B.35), we obtain

$$\rho_C^{(a,2)} = \int_0^\infty \sum_j J_j \text{tr}_R \left[ \mathbb{1}_C \otimes |1\rangle\langle 1|_R \mathcal{M}_{C \rightarrow CR}^{t',1} \left( \int_0^\infty \sum_j J_j \tilde{\rho}_C^{(0)}(t) J_j^\dagger dt \right) \right] J_j^\dagger dt' \quad (\text{B.36})$$

$$= \int_0^\infty \int_0^\infty \text{tr} \left[ \sum_j J_j \tilde{\rho}_C^{(0)}(t) J_j^\dagger \right] \sum_j J_j \text{tr}_R \left[ \mathbb{1}_C \otimes |1\rangle\langle 1|_R \mathcal{M}_{C \rightarrow CR}^{t',1} \left( \rho_C^{(1)}(t) \right) \right] J_j^\dagger dt dt', \quad (\text{B.37})$$

where  $\tilde{\rho}_C^{(1)}(t) = \sum_j J_j \tilde{\rho}_C^{(0)}(t) J_j^\dagger$ . Here, we used

$$\tilde{\rho}_{CR}^{(1)}(t') = \text{tr}_R \left[ \mathbb{1}_C \otimes |1\rangle\langle 1|_R \mathcal{M}_{C \rightarrow CR}^{t',1}(\rho_C^{(a,1)}) \right], \quad (\text{B.38})$$

and

$$P^{(1 \rightarrow 2)}(t') = \text{tr} \left[ \sum_j J_j \tilde{\rho}_C^{(1)}(t') J_j^\dagger \right]. \quad (\text{B.39})$$

Similarly, following approach 3 the state of the clockwork an instance before the second tick is calculated as

$$\rho_C^{(b,1)} = \int_0^\infty \int_0^\infty \text{tr} \left[ \sum_j J_j \tilde{\rho}_C^{(1)}(t, t') J_j^\dagger \right] \text{tr} \left[ \sum_j J_j \tilde{\rho}_C^{(0)}(t) J_j^\dagger \right] \rho_C^{(1)}(t, t') dt dt', \quad (\text{B.40})$$

where  $P^{(0 \rightarrow 1)}(t) = \text{tr} \left[ \sum_j J_j \tilde{\rho}_C^{(0)}(t) J_j^\dagger \right]$  and  $P^{(1 \rightarrow 2)}(t, t') = \text{tr} \left[ \sum_j J_j \tilde{\rho}_C^{(1)}(t, t') J_j^\dagger \right]$ . With that, we can rewrite Eq. (B.40) as

$$\rho_C^{(b,1)} = \int_0^\infty \int_0^\infty P^{(0 \rightarrow 1)}(t) P^{(1 \rightarrow 2)}(t, t') \rho_C^{(1)}(t, t') dt dt'. \quad (\text{B.41})$$

The state an instance after the second tick is given by

$$\begin{aligned} \rho_C^{(a,2)} &= \int_0^\infty \int_0^\infty \text{tr} \left[ \sum_j J_j \tilde{\rho}_C^{(1)}(t, t') J_j^\dagger \right] \text{tr} \left[ \sum_j J_j \tilde{\rho}_C^{(0)}(t) J_j^\dagger \right] \frac{\sum_j J_j \tilde{\rho}_C^{(1)}(t, t') J_j^\dagger}{\text{tr} \left[ \sum_j J_j \tilde{\rho}_C^{(1)}(t, t') J_j^\dagger \right]} dt dt' \\ &\quad (\text{B.42}) \end{aligned}$$

$$= \int_0^\infty \int_0^\infty \text{tr} \left[ \sum_j J_j \tilde{\rho}_C^{(0)}(t) J_j^\dagger \right] \sum_j J_j \tilde{\rho}_C^{(1)}(t, t') J_j^\dagger dt dt' \quad (\text{B.43})$$

$$= \int_0^\infty \int_0^\infty \text{tr} \left[ \sum_j J_j \tilde{\rho}_C^{(0)}(t) J_j^\dagger \right] \sum_j J_j \text{tr}_R \left[ \mathbb{1}_C \otimes |1\rangle\langle 1|_R \mathcal{M}_{C \rightarrow CR}^{t',1} \left( \rho_C^{(1)}(t) \right) \right] J_j^\dagger dt dt'. \quad (\text{B.44})$$

Here, we used

$$\tilde{\rho}_C^{(1)}(t, t') = \text{tr}_R \left[ \mathbb{1}_C \otimes |1\rangle\langle 1|_R \mathcal{M}_{C \rightarrow CR}^{t',1} \left( \rho_C^{(1)}(t) \right) \right], \quad (\text{B.45})$$

and  $\tilde{\rho}_C^{(1)}(t) = \sum_j J_j \tilde{\rho}_C^{(0)}(t) J_j^\dagger$ . Thus, we can verify that both approaches yield the same state  $\rho_C^{(a,2)}$  (compare Eq. (B.36) and (B.44)). Similarly, one can then show that both approaches yield the same states  $\rho_C^{(a,k)}$   $\forall k > 2$ .

Now, let us compare the expressions for the state of the clockwork an instance before the second tick  $\rho_C^{(b,1)}$ . We start by rewriting the expression obtained using approach 1 given in Eq. (B.34) as

$$\rho_C^{(b,1)} = \int_0^\infty P^{(1 \rightarrow 2)}(t') \rho_C^{(1)}(t') dt' = \int_0^\infty \text{tr} \left[ \sum_j J_j \tilde{\rho}_C^{(1)}(t') J_j^\dagger \right] \rho_C^{(1)}(t') dt', \quad (\text{B.46})$$

with

$$P^{(1 \rightarrow 2)}(t') = \lim_{\delta t \rightarrow 0^+} \frac{\text{tr} \left[ \mathbb{1}_C \otimes |2\rangle\langle 2|_R \left( \mathcal{M}_{C \rightarrow CR}^{\delta t,1} \left( \tilde{\rho}_C^{(1)}(t') \right) - \tilde{\rho}_C^{(1)}(t') \right) \right]}{\delta t}. \quad (\text{B.47})$$

This yields

$$\rho_C^{(b,1)} = \int_0^\infty \lim_{\delta t \rightarrow 0^+} \frac{\text{tr} \left[ \mathbb{1}_C \otimes |2\rangle\langle 2|_R \mathcal{M}_{C \rightarrow CR}^{\delta t,1} \left( \rho_C^{(1)}(t') \right) \right]}{\delta t} \tilde{\rho}_C^{(1)}(t') dt'. \quad (\text{B.48})$$

We rewrite  $\tilde{\rho}_C^{(1)}(t')$  as

$$\tilde{\rho}_C^{(1)}(t') = \text{tr}_R \left[ \mathbb{1}_C \otimes |1\rangle\langle 1|_R \mathcal{M}_{CR \rightarrow CR}^{t',1} \left( \rho_C^{(a,1)} \right) \right] \quad (\text{B.49})$$

$$= \int_0^\infty P^{(0 \rightarrow 1)}(t) \text{tr}_R \left[ \mathbb{1}_C \otimes |1\rangle\langle 1|_R \mathcal{M}_{CR \rightarrow CR}^{t',1} \left( \frac{\sum_j J_j \rho_C^{(0)}(t) J_j^\dagger}{\text{tr} \left[ \sum_j J_j \rho_C^{(0)}(t) J_j^\dagger \right]} \right) \right] dt \quad (\text{B.50})$$

$$= \int_0^\infty P^{(0 \rightarrow 1)}(t) \tilde{\rho}_C^{(1)}(t, t') dt. \quad (\text{B.51})$$

Plugging Eq. (B.51) into Eq. (B.48) we have

$$\rho_C^{(b,1)} = \int_0^\infty \int_0^\infty P^{(0 \rightarrow 1)} \lim_{\delta \rightarrow 0^+} \frac{\text{tr} \left[ \mathbb{1}_C \otimes |2\rangle\langle 2|_R \mathcal{M}_{CR \rightarrow CR}^{\delta t,1} \left( \rho_C^{(1)}(t') \right) \right]}{\delta t} \tilde{\rho}_C^{(1)}(t, t') dt dt'. \quad (\text{B.52})$$

We write

$$\lim_{\delta t \rightarrow 0^+} \frac{\text{tr} \left[ \mathbb{1}_C \otimes |2\rangle\langle 2|_R \mathcal{M}_{CR \rightarrow CR}^{\delta t,1} \left( \rho_C^{(1)}(t') \right) \right]}{\delta t} = \frac{\text{tr} \left[ \sum_j J_j^\dagger J_j \int_0^\infty P^{(0 \rightarrow 1)}(t) \tilde{\rho}_C^{(1)}(t, t') dt \right]}{\text{tr} \left[ \int_0^\infty P^{(0 \rightarrow 1)}(t) \tilde{\rho}_C^{(1)}(t, t') dt \right]}, \quad (\text{B.53})$$

to obtain

$$\rho_C^{(b,1)} = \int_0^\infty \int_0^\infty P^{(0 \rightarrow 1)} \frac{\text{tr} \left[ \sum_j J_j^\dagger J_j \int_0^\infty P^{(0 \rightarrow 1)}(t) \tilde{\rho}_C^{(1)}(t, t') dt \right]}{\text{tr} \left[ \int_0^\infty P^{(0 \rightarrow 1)}(t) \tilde{\rho}_C^{(1)}(t, t') dt \right]} \tilde{\rho}_C^{(1)}(t, t') dt dt'. \quad (\text{B.54})$$

We identify  $P^{(1 \rightarrow 2)}(t, t') = \text{tr} \left[ \sum_j J_j^\dagger J_j \int_0^\infty P^{(0 \rightarrow 1)}(t) \tilde{\rho}_C^{(1)}(t, t') dt \right]$  and rewrite Eq. (B.54) as

$$\rho_C^{(b,1)} = \int_0^\infty \left( \int_0^\infty P^{(0 \rightarrow 1)}(t) P^{1 \rightarrow 2}(t, t') dt \right) \frac{\left( \int_0^\infty P^{(0 \rightarrow 1)}(t) \tilde{\rho}_C^{(1)}(t, t') dt \right)}{\left( \int_0^\infty P^{(0 \rightarrow 1)}(t) \text{tr} \left[ \tilde{\rho}_C^{(1)}(t, t') \right] dt \right)} dt'. \quad (\text{B.55})$$

Defining  $P_{\text{eff}}^{(1 \rightarrow 2)}(t') = \int_0^\infty P^{(0 \rightarrow 1)}(t) P^{1 \rightarrow 2}(t, t') dt$ , and  $\rho_{C,\text{eff}}^{(1)}(t') = \frac{\left( \int_0^\infty P^{(0 \rightarrow 1)}(t) \tilde{\rho}_C^{(1)}(t, t') dt \right)}{\left( \int_0^\infty P^{(0 \rightarrow 1)}(t) \text{tr} \left[ \tilde{\rho}_C^{(1)}(t, t') \right] dt \right)}$ , we have

$$\rho_C^{(b,1)} = \int_0^\infty P_{\text{eff}}^{(1 \rightarrow 2)}(t') \rho_{C,\text{eff}}^{(1)}(t') dt'. \quad (\text{B.56})$$

Compare Eq. (B.56), the expression for  $\rho_C^{(b,1)}$  obtained using approach 1, to the expression for  $\rho_C^{(b,1)}$  obtained with approach 3 (see Eq. (B.41)) given by

$$\rho_C^{(b,1)} = \int_0^\infty \int_0^\infty P^{(0 \rightarrow 1)}(t) P^{(1 \rightarrow 2)}(t, t') \rho_C^{(1)}(t, t') dt dt'. \quad (\text{B.57})$$

Clearly, the two expressions for  $\rho_C^{(b,1)}$  (and equally for  $\rho_C^{(b,k)}$ ,  $k > 1$ ) obtained via approach 1 and 3 will generally differ. Approach 1 yields an expression (Eq. (B.56)) which can be obtained by “coarse-graining” of the expression obtained by approach 3 (Eq. (B.57)). That is, given the expression in Eq. (B.57) we can cast it into an expression that only depends on  $t'$  by replacing the weight  $P^{(0 \rightarrow 1)}(t)P^{(1 \rightarrow 2)}(t', t)$  with  $P_{\text{eff}}^{(1 \rightarrow 2)}(t')$  by integrating out the coordinate time  $t$ . Similarly, we replace the corresponding state  $\rho_C^{(1)}(t, t')$  by integration out the coordinate time  $t$ . That is, we integrate over all possible times  $t$  at which the first tick occurred.

## B.4 Kraus operator representation of ticking channels

Here, we provide explicit Kraus operator representations of the ticking channels discussed in Section II.5.2. In particular we consider the CPTP map  $\mathcal{E}_{k-1}^{(A)}$  specified by

$$\rho_C^{(a,k)} = \mathcal{E}_{k-1}^{(A)}(\rho_C^{(a,k-1)}). \quad (\text{B.58})$$

To start, we can rewrite the state  $\rho_C^{(a,k)}$  as follows

$$\rho_C^{(a,k)} = \int_0^\infty P^{(k-1 \rightarrow k)}(t) \frac{\sum_j J_j \tilde{\rho}_C^{(k-1)}(t) J_j^\dagger}{\text{tr} \left[ \sum_j J_j^\dagger J_j \tilde{\rho}_C^{(k-1)}(t) \right]} dt \quad (\text{B.59})$$

$$= \int_0^\infty \sum_j J_j \text{tr}_R \left[ \mathbb{1} \otimes |k-1\rangle\langle k-1|_R \mathcal{M}_{C \rightarrow CR}^{t,k-1} \left( \rho_C^{(a,k-1)} \right) \right] J_j^\dagger dt. \quad (\text{B.60})$$

Using the Kraus representation theorem [25, 69, 70], for every quantum channel  $\mathcal{M}_{C \rightarrow CR}^{t,k}$  there exists a Kraus operator representation of the form

$$\mathcal{M}_{C \rightarrow CR}^{t,k}(\rho_C) = \sum_{l=0}^{N_T} \sum_{x=1}^{N_O} K_x^{(k)}(l, t) \rho_C K_x^{(k)\dagger}(l, t) \otimes |l\rangle\langle l|_R, \quad (\text{B.61})$$

where  $1 \leq N_O \leq d^2$  with  $d = \dim(\mathcal{H}_C)$ . Here,  $\{K_x^{(k)}(l, t)\}_{x=1}^{N_O}$  is a set of operators satisfying  $\sum_{x=1}^{N_O} K_x^{(k)\dagger}(l, t) K_x^{(k)}(l, t) = \mathbb{1}$ , i.e., a valid set of Kraus operators. The Kraus operators depend on the input and output state of the register,  $k$  and  $l$ , respectively, as well as the coordinate time  $t$ . Note that to obtain Eq. (B.61), we invoked the fact that the register is classical (Def. 3) and remains incoherent at all times in the chosen basis. Plugging Eq. (B.61) into Eq. (B.60), we obtain

$$\rho_C^{(a,k)} = \int_0^\infty \sum_{jx} J_j K_x^{(k-1)}(k, t) \rho_C^{(a,k-1)} K_x^{(k-1)\dagger}(k, t) J_j^\dagger dt. \quad (\text{B.62})$$

We can use Axiom 4 to see that the Kraus operators must only depend on the difference between the input and output state of the register. This allows us to write

$$\rho_C^{(a,k)} = \int_0^\infty \sum_{jx} J_i K_x^{(0)}(1,t) \rho_C^{(a,k-1)} K_x^{(0)\dagger}(1,t) J_i^\dagger dt = \mathcal{E}_{k-1}^{(A)}(\rho_C^{(a,k-1)}). \quad (\text{B.63})$$

We see that  $\rho_C^{(a,k)}$  can be obtained from  $\rho_C^{(a,k-1)}$  via application of a quantum channel  $\mathcal{E}_{k-1}^{(A)}$ , i.e., a CPTP map, whose Kraus operator representation is given in Eq. (B.63). Complete positivity of the map is guaranteed by the fact that the map admits a Kraus operator representation. Thus, it remains to be shown that the map is indeed trace-preserving. This follows from the fact that  $\rho_C^{(a,k)}$  is properly normalized for any arbitrary normalized input state  $\rho_C^{(a,k-1)}$  by construction.

## B.5 Observer-dependent clockwork states for ticking clocks with vanishing no-tick operators

Here, we discuss the form of the relevant observer-dependent clockwork states for ticking clocks with vanishing no-tick operators  $L_j = 0 \forall j \in (1, N_L)$ . We have

$$\rho_C^{(b,k-1)} = \int_0^\infty P^{(k-1 \rightarrow k)}(t) \rho_C^{(k-1)}(t) dt, \quad (\text{B.64})$$

and

$$\rho_C^{(a,k)} = \int_0^\infty P^{(k-1 \rightarrow k)}(t) \frac{\sum_j J_j \tilde{\rho}_C^{(k-1)}(t) J_j^\dagger}{\text{tr} \left[ \sum_j J_j \tilde{\rho}_C^{(k-1)}(t) J_j^\dagger \right]} dt, \quad (\text{B.65})$$

where

$$P^{(k-1 \rightarrow k)}(t) = \text{tr} \left[ \sum_j J_j \tilde{\rho}_C^{(k-1)}(t) J_j^\dagger \right], \quad (\text{B.66})$$

with

$$\tilde{\rho}_C^{(k-1)}(t) = \text{tr}_R \left[ \mathbb{1}_C \otimes |k-1\rangle\langle k-1|_R \mathcal{M}_{C \rightarrow CR}^{t,k-1} \left( \rho_C^{(a,k-1)} \right) \right]. \quad (\text{B.67})$$

Using Axiom 4, we can rewrite Eq. (B.67) as

$$\tilde{\rho}_C^{(k-1)}(t) = \text{tr}_R \left[ \mathbb{1}_C \otimes |0\rangle\langle 0|_R \mathcal{M}_{C \rightarrow CR}^{t,0} \left( \rho_C^{(a,k-1)} \right) \right], \quad (\text{B.68})$$

which simply corresponds to the state  $\tilde{\rho}_C^{(0)}(t)$  for a ticking clock initialized in the state  $\rho_C^0 = \rho_C^{(a,k-1)}$ . Thus, we can use Eq. (B.3) from Appendix B.1 to write

$$\tilde{\rho}_C^{(k-1)}(t) = e^{t\mathcal{C}_{(1,0)}}(\rho_C^{(a,k-1)}). \quad (\text{B.69})$$

Recall that the map  $\mathcal{C}_{(1,0)}$  given in Lemma 1 has the following form

$$\mathcal{C}_{(1,0)}(\cdot) = -i[H,(\cdot)] - \sum_j \frac{1}{2}\{L_j^\dagger L_j + J_j^\dagger J_j, (\cdot)\} + L_j(\cdot)L_j^\dagger. \quad (\text{B.70})$$

If all no-tick operators vanish,  $\mathcal{C}_{(1,0)}$  reduces to

$$\mathcal{C}_{(1,0)}(\cdot) = -i[H,(\cdot)] - \sum_i \frac{1}{2}\{J_i^\dagger J_i, (\cdot)\}. \quad (\text{B.71})$$

Let us propose the following ansatz for the form of  $\tilde{\rho}_C^{(k-1)}(t)$ :

$$\tilde{\rho}_C^{(k-1)}(t) = e^{t\mathcal{C}_{(1,0)}}(\rho_C^{(a,k-1)}) = e^{-iHt-t/2\sum_j J_j^\dagger J_j} \rho_C^{(a,k-1)} e^{iHt-t/2\sum_j J_j^\dagger J_j}. \quad (\text{B.72})$$

Taking the derivative of Eq. (B.72) with respect to coordinate time  $t$  we have

$$\frac{d}{dt}\tilde{\rho}_C^{(k-1)}(t) = -i[H, \tilde{\rho}_C^{(k-1)}(t)] - \sum_i \frac{1}{2}\{J_i^\dagger J_i, \tilde{\rho}_C^{(k-1)}(t)\} = \mathcal{C}_{(1,0)}(\tilde{\rho}_C^{(k-1)}(t)). \quad (\text{B.73})$$

Moreover, evaluating Eq. (B.72) at  $t = 0$  yields  $\tilde{\rho}_C^{(k-1)}(0) = \mathbb{1}\rho_C^{(a,k-1)}\mathbb{1} = \rho_C^{(a,k-1)}$ . Thus, we recover the appropriate derivative and initial conditions as specified in Eq. (B.1) and (B.2) in Appendix B.1, respectively. Therefore, for ticking clocks with vanishing no-tick operators we can write

$$\tilde{\rho}_C^{(k)}(t) = e^{-iHt-t/2\sum_j J_j^\dagger J_j} \rho_C^{(a,k)} e^{iHt-t/2\sum_j J_j^\dagger J_j} \quad \forall k \in \mathbb{N}. \quad (\text{B.74})$$

## B.6 Accuracy of classical ticking clocks with a diagonal no-tick generator

Here, we discuss the accuracy of classical ticking clocks whose no-tick generator  $\mathcal{N}$  is diagonal. The delay function of the first tick is then given by

$$\tau^{(1)}(t) = \|\mathcal{T}e^{\mathcal{N}t}\vec{v}_C^0\| = \sum_i v_{C,i}^0 e^{-\mathcal{N}_{ii}t} \|\mathcal{T}\vec{e}_i\| = \sum_i v_{C,i}^0 (-\mathcal{N}_{ii}) e^{\mathcal{N}_{ii}t}, \quad (\text{B.75})$$

where the diagonal elements are non-positive  $\mathcal{N}_{ii} \leq 0$ . Denoting  $\tau_i^{(1)}(t) = (-\mathcal{N}_{ii}) e^{\mathcal{N}_{ii}t}$  as individual delay functions, we have

$$\tau^{(1)}(t) = \sum_i v_{C,i}^0 \tau_i^{(1)}(t). \quad (\text{B.76})$$

Lemma 4 in Ref. [14] on the accuracy of delay functions which are themselves given as a linear combination of delay functions states that  $R(\tau^{(1)}(t)) \leq \max_i R(\tau_i^{(1)}(t))$ . Equality

can be achieved by choosing an appropriate pure state of the clockwork as an initial state. By direct integration we have  $\mu(\tau_i^{(1)}(t)) = 1/(-\mathcal{N}_{ii})$  and  $\sigma^2(\tau_i^{(1)}(t)) = 1/\mathcal{N}_{ii}^2$ . Therefore  $R(\tau_i^{(1)}(t)) = 1 \forall i$ . So the maximal achievable accuracy for the first tick of these clocks is given by  $R_1 = 1$ . Using Theorem 1, we have  $R_k \leq kR_1 = k$ . This is because any pure state reset clock with a diagonal no-tick generator can still only achieve a maximal accuracy of the first tick of  $R_1 = 1$ , and thus  $R_k = kR_1 = k$ .

## B.7 Observer-dependent clockwork states for classical ticking clocks

Here, we discuss how to express the observer-dependent clockwork states for classical ticking clocks in “classical” notation. For general quantum ticking clocks we have

$$\rho_C^{(b,k-1)} = \int_0^\infty P^{(k-1 \rightarrow k)}(t) \rho_C^{(k-1)}(t) dt, \quad (\text{B.77})$$

and

$$\rho_C^{(a,k)} = \int_0^\infty P^{(k-1 \rightarrow k)}(t) \frac{\sum_j J_j \tilde{\rho}_C^{(k-1)}(t) J_j^\dagger}{\text{tr} \left[ \sum_j J_j \tilde{\rho}_C^{(k-1)}(t) J_j^\dagger \right]} dt, \quad (\text{B.78})$$

where

$$P^{(k-1 \rightarrow k)}(t) = \text{tr} \left[ \sum_j J_j \tilde{\rho}_C^{(k-1)}(t) J_j^\dagger \right], \quad (\text{B.79})$$

with

$$\tilde{\rho}_C^{(k-1)}(t) = \text{tr}_R \left[ \mathbb{1}_C \otimes |k-1\rangle\langle k-1| R \mathcal{M}_{C \rightarrow CR}^{t,k-1} \left( \rho_C^{(a,k-1)} \right) \right]. \quad (\text{B.80})$$

Using Axiom 4, we can rewrite Eq. (B.80) as

$$\tilde{\rho}_C^{(k-1)}(t) = \text{tr}_R \left[ \mathbb{1}_C \otimes |0\rangle\langle 0| R \mathcal{M}_{C \rightarrow CR}^{t,0} \left( \rho_C^{(a,k-1)} \right) \right], \quad (\text{B.81})$$

which simply corresponds to the state  $\tilde{\rho}_C^{(0)}(t)$  for a ticking clock initialized in the state  $\rho_C^0 = \rho_C^{(a,k-1)}$ . Thus, we can use Eq. (B.3) from Appendix B.1 to write

$$\tilde{\rho}_C^{(k-1)}(t) = e^{t\mathcal{C}_{(1,0)}}(\rho_C^{(a,k-1)}). \quad (\text{B.82})$$

From Corollary 1, we have that the state  $\tilde{v}_C^{(0)}(t)$  evolves according to

$$\frac{d}{dt} \tilde{v}_C^{(0)}(t) = \mathcal{N} \tilde{v}_C^{(0)}(t), \quad (\text{B.83})$$

where  $\tilde{v}_C^{(0)}(0) = \bar{v}_C^0$ . Solving this first-order differential equation, we obtain

$$\tilde{v}_C^{(0)}(t) = e^{\mathcal{N}t}\bar{v}_C^0. \quad (\text{B.84})$$

So the classical analogue of  $\tilde{\rho}_C^{(k-1)}(t)$  is given by

$$\tilde{v}_C^{(k-1)}(t) = e^{\mathcal{N}t}\bar{v}_C^{(a,k-1)}. \quad (\text{B.85})$$

The probability density  $P^{(k-1 \rightarrow k)}(t)$  simply corresponds to the delay function of the first tick of a ticking clock with the same dynamics whose clockwork initialized in the state  $\rho_C^0 = \rho_C^{(a,k-1)}$  instead. In classical notation, the delay function of the first tick can be computed as (see Section I.3)

$$\tau^{(1)}(t) = \|\mathcal{T}\tilde{v}_C^{(0)}(t)\| = \|\mathcal{T}e^{\mathcal{N}t}\bar{v}_C^0\|. \quad (\text{B.86})$$

Therefore, in classical notation we have

$$P^{(k-1 \rightarrow k)}(t) = \|\mathcal{T}e^{\mathcal{N}t}\bar{v}_C^{(a,k-1)}\|. \quad (\text{B.87})$$

Thus, the state just before the  $k$ th tick can be written as

$$\bar{v}_C^{(b,k-1)} = \int_0^\infty P^{(k-1 \rightarrow k)}(t) \tilde{v}_C^{(k-1)}(t) dt = \int_0^\infty \|\mathcal{T}e^{\mathcal{N}t}\bar{v}_C^{(a,k-1)}\| \frac{e^{\mathcal{N}t}\bar{v}_C^{(a,k-1)}}{\|\mathcal{T}e^{\mathcal{N}t}\bar{v}_C^{(a,k-1)}\|} dt. \quad (\text{B.88})$$

Similarly, the observer-dependent state after the  $k$ th tick is given by

$$\rho_C^{(a,k)} = \int_0^\infty P^{(k-1 \rightarrow k)}(t) \frac{\mathcal{T}\tilde{v}_C^{(k-1)}(t)}{\|\mathcal{T}\tilde{v}_C^{(k-1)}(t)\|} dt = \int_0^\infty \mathcal{T}\tilde{v}_C^{(k-1)}(t) dt = \int_0^\infty \mathcal{T}e^{\mathcal{N}t}\bar{v}_C^{(a,k-1)} dt, \quad (\text{B.89})$$

where  $\bar{v}_C^{(a,0)} = \bar{v}_C^0$  by definition.

## B.8 Accuracy and entropy production of ladder ticking clock

Here, we provide expressions for the accuracy and entropy production per tick of a ladder ticking clock (see Section I.1.1). Note that the ladder ticking clock is a reset clock that resets to a pure clockwork state. Therefore,  $R_k = kR_1$  and  $\Sigma_k = \Sigma_1 = S(\rho_C^{(b,0)})$  for all  $k \in \mathbb{N}_{>0}$ . Given the no-tick generator  $\mathcal{N}$  and tick generator  $\mathcal{T}$  of the ladder ticking clocks (Eq. (I.54)), we can write

$$e^{\mathcal{N}t}\bar{v}_C^0 = e^{\mathcal{N}t}\vec{e}_0 = e^{-t}(1, f_2(t), \dots, f_d(t))^\top, \quad (\text{B.90})$$

with  $f_k(t) = \frac{t^{k-1}}{(k-1)!}$  and  $\tau^{(1)}(t) = \|\mathcal{T}e^{\mathcal{N}t}\vec{e}_0\| = e^{-t}f_d(t)$ . A direct calculation then yields  $\mu_1 = d$ ,  $\sigma_1^2 = \sqrt{d}$ , and thus  $R_1 = d$ .

The entropy production of the first tick of ladder clocks is given by  $\Sigma_1 = S(\vec{v}_C^{(b,0)})$ , where

$$\vec{v}_C^{(b,0)} = \int_0^\infty \|\mathcal{T}e^{\mathcal{N}t}\vec{e}_0\| \frac{e^{\mathcal{N}t}\vec{e}_0}{\|e^{\mathcal{N}t}\vec{e}_0\|} dt. \quad (\text{B.91})$$

The individual elements of the state  $\vec{v}_C^{(b,0)}$  can thus be computed as

$$v_{C,k \in (1,d)}^{(b,0)} = \int_0^\infty e^{-2t} \frac{t^{d-1}}{\Gamma(d,t)} \frac{t^{k-1}}{(k-1)!} dt, \quad (\text{B.92})$$

where  $\Gamma(d,t) = \int_t^\infty x^{d-1}e^{-x}$  is the incomplete Gamma function. Because the dimension of the clockwork  $d$  is an integer, we can simplify this expression as  $\Gamma(d,t) = (d-1)!e^{-t} \sum_{n=0}^{d-1} \frac{t^n}{n!}$ . Figure B.2 shows the entropy production of the first tick  $\Sigma_1$  as a function of the accuracy of the first tick  $R_1 = d$  for ladder ticking clocks with clockworks of dimension  $d \in (2, 100)$ . Here, the entropy production is calculated based on Eq. (B.92).

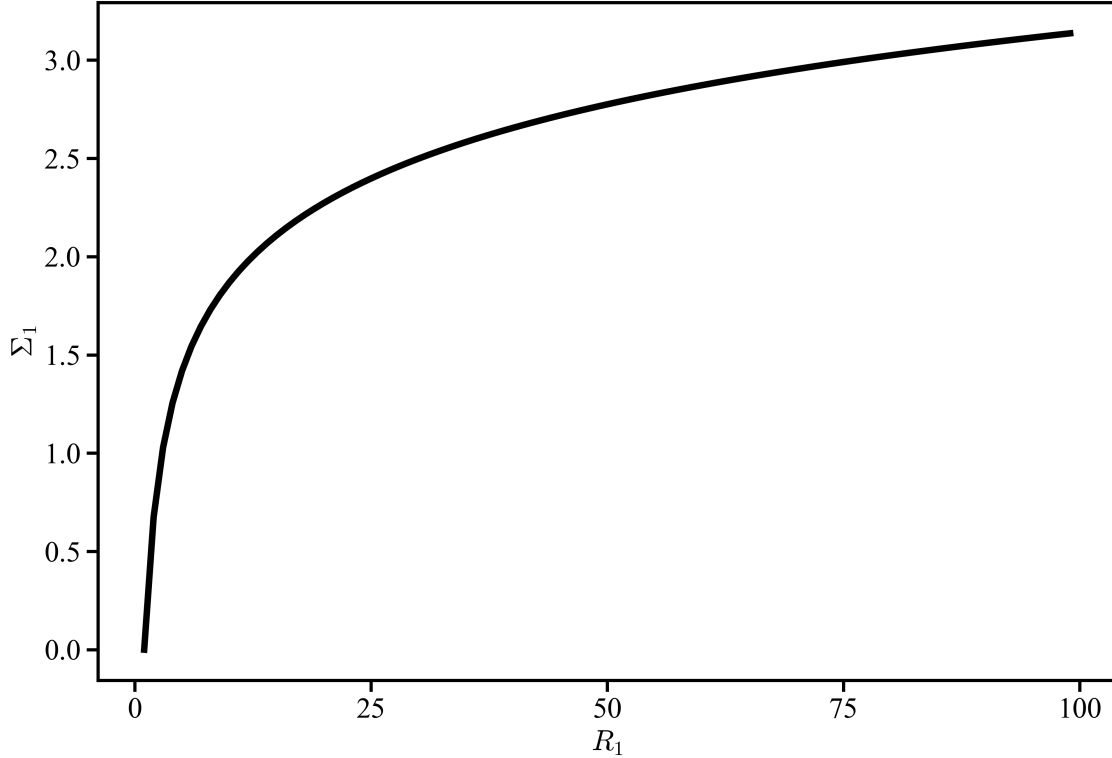


Figure B.2: Entropy production of the first tick  $\Sigma_1$  as a function of the accuracy of the first tick  $R_1$  for ladder ticking clocks (see Section I.1.1) with clockworks of varying dimension  $d = R_1$  ( $d \in (2, 100)$ ). Because ladder clocks are reset clocks, we additionally have that  $\Sigma_k = \Sigma_1$  and  $R_k = kR_1 = kd$  for all  $k \in \mathbb{N}_{>0}$ .

# Bibliography

- [1] W. McGrew, X. Zhang, R. Fasano, S. Schäffer, K. Beloy, D. Nicolodi, R. Brown, N. Hinkley, G. Milani, M. Schioppo, et al., *Nature* **564**, 87 (2018).
- [2] T. Nicholson, S. Campbell, R. Hutson, G. Marti, B. Bloom, R. McNally, W. Zhang, M. Barrett, M. Safronova, G. Strouse, et al., *Nat. Commun.* **6**, 1 (2015).
- [3] S. Brewer, J.-S. Chen, A. Hankin, E. Clements, C.-W. Chou, D. Wineland, D. Hume, and D. Leibrandt, *Phys. Rev. Lett.* **123**, 033201 (2019).
- [4] T. Rosenband, D. Hume, P. Schmidt, C.-W. Chou, A. Brusch, L. Lorini, W. Oskay, R. E. Drullinger, T. M. Fortier, J. E. Stalnaker, et al., *Science* **319**, 1808 (2008).
- [5] S. Kolkowitz, I. Pikovski, N. Langellier, M. D. Lukin, R. L. Walsworth, and J. Ye, *Phys. Rev. D* **94**, 124043 (2016).
- [6] W. Pauli, in *Quantentheorie* (Springer, 1933), pp. 83–272.
- [7] J. C. Garrison and J. Wong, *J. Math. Phys.* **11**, 2242 (1970).
- [8] S. L. Braunstein, C. M. Caves, and G. J. Milburn, *Ann. Phys. (N. Y.)* **247**, 135 (1996).
- [9] P. Erker, “The Quantum Hourglass: Approaching Time Measurement with Quantum Information Theory”, MA thesis (ETH Zürich, 2014).
- [10] A. C. Barato and U. Seifert, *Phys. Rev. X* **6**, 041053 (2016).
- [11] E. Schwarzhans, M. P. Lock, P. Erker, N. Friis, and M. Huber, arXiv:2007.01307 (2020).
- [12] S. Ranković, Y.-C. Liang, and R. Renner, arXiv:1506.01373 (2015).
- [13] S. Stupar, C. Klumpp, R. Renner, and N. Gisin, arXiv:1806.08812 (2018).
- [14] M. P. Woods, R. Silva, G. Piütz, S. Stupar, and R. Renner, arXiv:1806.00491 (2018).
- [15] M. P. Woods, R. Silva, and J. Oppenheim, in *Ann. Henri Poincaré*, Vol. 20, 1 (Springer, 2019), pp. 125–218.
- [16] M. P. Woods, *Quantum* **5**, 381 (2021).
- [17] Y. Yang and R. Renner, arXiv:2004.07857 (2020).

- [18] P. Erker, M. T. Mitchison, R. Silva, M. P. Woods, N. Brunner, and M. Huber, Phys. Rev. X **7**, 031022 (2017).
- [19] A. Pearson, Y. Guryanova, P. Erker, E. Laird, G. Briggs, M. Huber, and N. Ares, arXiv:2006.08670 (2020).
- [20] G. J. Milburn, arXiv:2007.02217 (2020).
- [21] A. C. Barato and U. Seifert, Phys. Rev. Lett. **114**, 158101 (2015).
- [22] J. M. Horowitz and T. R. Gingrich, Nat. Phys. **16**, 15 (2020).
- [23] Y. Hasegawa, Phys. Rev. Lett. **126**, 010602 (2021).
- [24] Y. Hasegawa, arXiv:2101.06831 (2021).
- [25] M. A. Nielsen and I. L. Chuang, *Quantum Computation and Quantum Information* (CUP, 2010).
- [26] H.-P. Breuer and F. Petruccione, *The Theory of Open Quantum Systems* (OUP, 2007).
- [27] M.-D. Choi, Linear Algebra Its Appl. **10**, 285 (1975).
- [28] A. Kossakowski, Rep. Math. Phys. **3**, 247 (1972).
- [29] E. Hille and R. S. Phillips, *Functional Analysis and Semi-Groups*, Vol. 31 (American Mathematical Soc., 1996).
- [30] G. Lindblad, Commun. Math. Phys. **48**, 119 (1976).
- [31] V. Gorini, A. Frigerio, M. Verri, A. Kossakowski, and E. Sudarshan, Rep. Math. Phys. **13**, 149 (1978).
- [32] P. Palmer, J. Math. Phys. **18**, 527 (1977).
- [33] A. Papoulis and U. Pillai, *Probability, Random Variables and Stochastic Processes* (McGraw-Hill, 2001).
- [34] D. W. Allan, Proc. IEEE **54**, 221 (1966).
- [35] D. Dasenbrook, P. P. Hofer, and C. Flindt, Phys. Rev. B **91**, 195420 (2015).
- [36] S. Dambach, B. Kubala, and J. Ankerhold, Fortschritte der Phys. **65**, 1600061 (2017).
- [37] R. Shankar, *Principles of Quantum Mechanics* (Springer, 1994).
- [38] R. Landauer, IBM J. Res. Dev. **5**, 183 (1961).
- [39] M. Esposito, K. Lindenberg, and C. V. den Broeck, New J. Phys. **12**, 013013 (2010).
- [40] C. E. Shannon, Bell Labs Tech. J. **27**, 379 (1948).
- [41] B. Schumacher, Phys. Rev. A **51**, 2738 (1995).
- [42] S. L. Braunstein and A. K. Pati, Phys. Rev. Lett. **98**, 080502 (2007).

- [43] F. Brandao, M. Horodecki, N. Ng, J. Oppenheim, and S. Wehner, PNAS **112**, 3275 (2015).
- [44] J. Goold, M. Huber, A. Riera, L. Del Rio, and P. Skrzypczyk, J. Phys. A **49**, 143001 (2016).
- [45] G. T. Landi and M. Paternostro, arXiv:2009.07668 (2020).
- [46] N. Brunner, N. Linden, S. Popescu, and P. Skrzypczyk, Phys. Rev. E **85**, 051117 (2012).
- [47] D. Reeb and M. M. Wolf, New J. Phys. **16**, 103011 (2014).
- [48] Y. Guryanova, N. Friis, and M. Huber, Quantum **4**, 222 (2020).
- [49] P. Faist, “Quantum Coarse-Graining: An Information-Theoretic Approach to Thermodynamics”, PhD thesis (ETH Zürich, 2016).
- [50] L. Del Rio, J. Åberg, R. Renner, O. Dahlsten, and V. Vedral, Nature **474**, 61 (2011).
- [51] E. T. Jaynes, in *Maximum Entropy and Bayesian Methods*, Vol. 50, edited by C. R. Smith, G. Erickson, and P. O. Neudorfer (Springer, 1992), pp. 1–21.
- [52] P. Faist and R. Renner, Phys. Rev. X **8**, 021011 (2018).
- [53] M. N. Bera, A. Riera, M. Lewenstein, and A. Winter, Nat. Commun. **8**, 1 (2017).
- [54] D. V. Schroeder, *An Introduction to Thermal Physics* (Addison Wesley Longman, 2000).
- [55] S. J. Blundell and K. M. Blundell, *Concepts in Thermal Physics* (OUP, 2009).
- [56] D. Jennings and T. Rudolph, Phys. Rev. E **81**, 061130 (2010).
- [57] K. Micadei, J. P. Peterson, A. M. Souza, R. S. Sarthour, I. S. Oliveira, G. T. Landi, T. B. Batalhão, R. M. Serra, and E. Lutz, Nat. Commun. **10**, 1 (2019).
- [58] H. Araki and E. H. Lieb, *Entropy Inequalities* (Springer, 2002).
- [59] H. Spohn, J. Math. Phys. **19**, 1227 (1978).
- [60] D. Janzing, P. Wocjan, R. Zeier, R. Geiss, and T. Beth, Int. J. Theor. Phys. **39**, 2717 (2000).
- [61] F. G. Brandao, M. Horodecki, J. Oppenheim, J. M. Renes, and R. W. Spekkens, Phys. Rev. Lett. **111**, 250404 (2013).
- [62] M. Horodecki and J. Oppenheim, Nat. Commun. **4**, 1 (2013).
- [63] K. Ptaszyński and M. Esposito, Phys. Rev. Lett. **123**, 200603 (2019).
- [64] M. Esposito and C. V. den Broeck, EPL **95**, 40004 (2011).
- [65] H. Leff and A. F. Rex, *Maxwell’s Demon 2 Entropy, Classical and Quantum Information, Computing* (CRC Press, 2002).
- [66] C. H. Bennett, Int. J. Theor. Phys. **21**, 905 (1982).

- [67] C. H. Bennett, Stud. Hist. Philos. Sci. A **34**, 501 (2003).
- [68] S. D. Bartlett, T. Rudolph, and R. W. Spekkens, Int. J. Quantum Inf. **4**, 17 (2006).
- [69] J. Preskill, *Lecture Notes for Physics 219/Computer Science 219: Quantum Information*, <http://theory.caltech.edu/~preskill/ph229/>, 2015.
- [70] J. M. Renes, *Quantum Information Theory - Lecture Notes*, [https://edu.itp.phys.ethz.ch/hs15/QIT/renes\\_lecture\\_notes14.pdf](https://edu.itp.phys.ethz.ch/hs15/QIT/renes_lecture_notes14.pdf), 2015.
- [71] B. Schumacher and M. A. Nielsen, Phys. Rev. A **54**, 2629 (1996).
- [72] B. Schumacher, Phys. Rev. A **54**, 2614 (1996).
- [73] B. Schumacher and M. D. Westmoreland, Phys. Rev. Lett. **80**, 5695 (1998).
- [74] H. Barnum, M. A. Nielsen, and B. Schumacher, Phys. Rev. A **57**, 4153 (1998).
- [75] B. Schumacher and M. Nielsen, arXiv:quant-ph/9604022 (1996).
- [76] R. Kubo, Rep. Prog. Phys. **29**, 255 (1966).
- [77] U. Weiss, *Quantum Dissipative Systems*, Vol. 13 (World Scientific, 2012).
- [78] W. H. Zurek, Los Alamos Science **27**, 86 (2002).
- [79] W. H. Zurek, Rev. Mod. Phys. **75**, 715 (2003).
- [80] M. A. Schlosshauer, *Decoherence and the Quantum-To-Classical Transition* (Springer, 2007).
- [81] W. H. Zurek, Nat. Phys. **5**, 181 (2009).
- [82] T. D. Ladd, F. Jelezko, R. Laflamme, Y. Nakamura, C. Monroe, and J. L. O'Brien, Nature **464**, 45 (2010).
- [83] H. Bateman, *Higher Transcendental Functions [Volumes i-iii]*, Vol. 1 (McGraw-Hill, 1953).
- [84] S. Boyd, S. P. Boyd, and L. Vandenberghe, *Convex Optimization* (CUP, 2004).
- [85] M. J. Kochenderfer and T. A. Wheeler, *Algorithms for Optimization* (MIT Press, 2019).
- [86] D. Kraft et al., Technical Report DFVLR-FB 88-28 (1988).
- [87] D. Kraft, ACM Trans. Math. Softw. **20**, 262 (1994).
- [88] S. G. Johnson, *The NLOpt Nonlinear-Optimization Package*, <http://github.com/stevengj/nlopt>.
- [89] J. Nocedal and S. J. Wright, *Numerical Optimization* (Springer, 2006), pp. 529–562.
- [90] J. A. Nelder and R. Mead, Comput. J. **7**, 308 (1965).
- [91] I. Wolfram Research, *Mathematica, Version 12.2*, Champaign, IL, 2020.

- [92] P. Virtanen, R. Gommers, T. E. Oliphant, M. Haberland, T. Reddy, D. Cournapeau, E. Burovski, P. Peterson, W. Weckesser, J. Bright, S. J. van der Walt, M. Brett, J. Wilson, K. J. Millman, N. Mayorov, A. R. J. Nelson, E. Jones, R. Kern, E. Larson, C. J. Carey, İ. Polat, Y. Feng, E. W. Moore, J. VanderPlas, D. Laxalde, J. Perktold, R. Cimrman, I. Henriksen, E. A. Quintero, C. R. Harris, A. M. Archibald, A. H. Ribeiro, F. Pedregosa, P. van Mulbregt, and SciPy 1.0 Contributors, *Nat. Methods* **17**, 261 (2020).
- [93] D. S. Arnon, G. E. Collins, and S. McCallum, *SIAM J. Comput.* **13**, 865 (1984).
- [94] G. E. Collins and H. Hong, *J. Symb. Comput.* **12**, 299 (1991).
- [95] B. F. Caviness and J. R. Johnson, *Quantifier Elimination and Cylindrical Algebraic Decomposition* (Springer, 2012).
- [96] H. A. Schwarz, *J. Reine Angew. Math.* **1873**, 292 (1873).
- [97] V. Čern, *J. Optimiz. Theory App.* **45**, 41 (1985).
- [98] C. Tsallis, *J. Stat. Phys.* **52**, 479 (1988).
- [99] C. Tsallis and D. A. Stariolo, *Physica A* **233**, 395 (1996).
- [100] Y. Xiang, D. Sun, W. Fan, and X. Gong, *Phys. Lett. A* **233**, 216 (1997).
- [101] S. Karlin and H. E. Taylor, *A Second Course in Stochastic Processes* (Elsevier, 1981).
- [102] F. Gebali, *Analysis of Computer and Communication Networks* (Springer, 2008).
- [103] N. Privault, *Understanding Markov Chains* (Springer, 2013).
- [104] J. P. Dowling and G. J. Milburn, *Philos. Trans. Royal Soc. A* **361**, 1655 (2003).
- [105] A. Acín, I. Bloch, H. Buhrman, T. Calarco, C. Eichler, J. Eisert, D. Esteve, N. Gisin, S. J. Glaser, F. Jelezko, et al., *New J. Phys.* **20**, 080201 (2018).
- [106] A. Wehrl, *Rev. Mod. Phys.* **50**, 221 (1978).